



Fakultät für Medizin

**Zentrum für Allergie und Umwelt (ZAUM)
Institut für Allergieforschung (IAF)**

Tissue-resident $\gamma\delta$ T cells as gatekeepers of psoriatic skin inflammation and dietary interventions

Stephanie Sarah Musiol

Vollständiger Abdruck der von der Fakultät für Medizin der Technischen Universität München zur Erlangung des akademischen Grades eines

Doktors der Naturwissenschaften (Dr. rer. nat)

genehmigte Dissertation.

Vorsitzender: Prof. Dr. Dirk Busch

Prüfer der Dissertation:

1. Prof. Dr. Carsten Schmidt-Weber
2. Prof. Dr. Bernhard Küster

Die Dissertation wurde am 23.08.2019 bei der Fakultät für Medizin der Technischen Universität München eingereicht und durch die Fakultät für Medizin am 11.02.2020 angenommen.

This Thesis is dedicated to my parents

Content

Content	<i>i</i>
List of Figures	<i>iv</i>
List of Tables	<i>vi</i>
Disclaimer	<i>vii</i>
Abbreviations	<i>viii</i>
1. Abstract	1
2. Zusammenfassung	3
3. Introduction	5
3.1 The skin immune system.....	5
3.1.1 Immune functions of non-hematopoietic stromal cells	6
3.1.2 Skin-resident immune compartment	7
3.1.3 Conventional T cells in the skin.....	8
3.2 Psoriasis vulgaris - chronic inflammation of the skin.....	10
3.2.1 Immunogenetics of psoriasis.....	10
3.2.2 Clinical manifestation of Psoriasis	11
3.2.3 Mouse models of psoriasis	11
3.2.3.1 The imiquimod-induced model of psoriatic plaque formation.....	12
3.2.4 Pathophysiology of psoriasis vulgaris	13
3.2.4.1 Psoriasis – a T _H 1 or T _H 17-mediated disease?	13
3.2.4.2 Immunomechanisms of Psoriasis.....	14
3.3 $\gamma\delta$ T cells – Innate immune players in psoriasis.....	16
3.3.1 Pathogenic role of murine $\gamma\delta$ T17 cells in psoriasis.....	17
3.3.2 Human $\gamma\delta$ T cells and their role in psoriasis	18
3.4 Current treatment options for psoriasis.....	19
3.5 Excess dietary salt intake – A risk factor for psoriasis?	21
4. Aims of the study	24
5. Materials	25
5.1 Chemicals and enzymes	25
5.2 Buffers and cell culture media composition	26
5.3 Material for animal experiments.....	27
5.4 Antibodies for flow cytometry.....	28
5.5 Material for histology of murine skin and histochemistry of human skin biopsies	28
5.6 General Material and equipment	29
5.7 Material and primers for genotyping of mice.....	31
5.8 Primers for qPCR	32
6. Methods	34

6.1	Animal procedures	34
6.1.1	Laboratory animals	34
6.1.2	Genotyping of genetically modified mice	35
6.1.3	Induction of psoriatic plaque formation in mice.....	36
6.1.3.1	Scoring severity of skin inflammation	37
6.1.3.2	TEWL measurement	37
6.1.3.3	Histology.....	38
6.1.4	Antibody treatment and application of IL-12Fc	38
6.1.5	Measurement of dehydration status in mice	39
6.2	Cell biology methods	39
6.2.1	Leukocyte isolation from mice	39
6.2.1.1	Isolation of leukocytes from lymph nodes	39
6.2.1.2	Isolation of leukocytes from murine skin	39
6.3	Molecular biology methods.....	40
6.3.1	Flow cytometry.....	40
6.3.1.1	Cell surface staining for Flow Cytometry.....	40
6.3.1.2	Staining procedure for V γ 5/V δ 1 ⁺ and V γ 6/V δ 1 ⁺ cells.....	41
6.3.1.3	Intracellular Staining for Flow Cytometry.....	41
6.3.2	Cell sorting	41
6.3.3	Enzyme-linked immunosorbent assay (ELISA)	42
6.3.4	Gene expression analysis.....	43
6.3.4.1	RNA extraction	43
6.3.4.2	cDNA-synthesis.....	43
6.3.4.3	Quantitative real-time PCR (qRT-PCR).....	43
6.4	Histochemistry of human skin biopsies.....	44
6.5	Data Analysis and Statistics	44
7.	Results.....	45
7.1	Divergent roles of IL-12 and IL-23 in psoriatic inflammation	45
7.1.1	Reduced skin inflammation in IL-12/23p40-deficient mice.....	45
7.1.2	Exacerbated clinical phenotype on IL-12-signaling deficiency.....	46
7.2	IL-12 controls accumulation and effector functions of $\gamma\delta$ T17 cells in the skin	52
7.2.1	Characterization of accumulating V γ 6V δ 1 ⁺ $\gamma\delta$ T17 cells in psoriatic skin.....	52
7.2.2	Effect of IL-17A neutralization in IMQ-treated <i>Il12rb2</i> ^{-/-} mice.....	56
7.2.3	Reduced skin inflammation in mice functionally lacking V γ 6 ⁺ $\gamma\delta$ T cells	57
7.2.4	IL-12 limits psoriasiform skin inflammation.....	59
7.3	Screening for IL-12 responders in the skin	61
7.4	Effect of nutritional salt on psoriatic plaque formation in mice.....	64
7.4.1	High salt diet exacerbates psoriatic plaque formation in mice	65
7.5	$\gamma\delta$ T17 cells drive disease aggravation after high salt diet feeding	69
7.5.1	Effect of HSD on effector $\gamma\delta$ T17 cells in skin and skin-dLNs	69
7.5.2	V γ 6 ⁺ $\gamma\delta$ T cells highly respond to high salt conditions	71
7.6	Effect of a minimal salt diet on psoriatic plaque formation	72
7.7	Molecular pathways induced by HSD	73
8.	Discussion.....	77
8.1	Targeting IL-12 by anti-p40 therapy is counterproductive in psoriasis treatment.....	77
8.1.1	Long-term consequences of IL-12 neutralization in psoriasis treatment	78
8.1.2	Future perspectives in psoriasis treatment.....	79
8.2	IL-12 limits skin inflammation in mice by regulating pathogenic V γ 6 ⁺ $\gamma\delta$ T17 cells...81	
8.2.1	Significance of the murine findings for humans.....	82

8.3	IL-12 initiates a tissue-protective response in keratinocytes	83
8.4	Nutritional salt shapes the psoriatic skin microenvironment through induction of pathogenic $\gamma\delta$ T17 cells	84
8.4.1	Molecular mechanism of the high salt induced effect on $\gamma\delta$ T17 cells	86
8.4.2	Impact of high salt diet on the skin microbiome.....	88
8.5	Conclusion	89
	Literature.....	91
	Publications.....	105
	Acknowledgement.....	106

List of Figures

Figure 1: Overview of the skin structure and skin-resident cellular effector cells.....	6
Figure 2: Summary of current concepts of psoriasis pathogenesis.	15
Figure 3: Functional development and intrinsic peripheral migration pattern of $\gamma\delta$ T cells.....	16
Figure 4: Discovery of the immune pathway in psoriasis and development of therapeutic approaches.	21
Figure 5: Protocol for the induction of psoriatic plaque formation in mice.....	36
Figure 6: Analysis of inflamed skin of WT and IL-12/23p40 deficient mice.....	46
Figure 7: Disease development in WT and <i>Ifnγ</i> ^{-/-} mice.....	47
Figure 8: Skin inflammation in IMQ-treated WT, <i>Il12a</i> ^{-/-} , <i>Il12b</i> ^{-/-} , <i>Il23a</i> ^{-/-} and <i>Il12rb2</i> ^{-/-} mice....	48
Figure 9: Appearance of skin lesions and TEWL in WT and IL-12-signaling deficient mice...	49
Figure 10: Histopathology of skin lesions of WT and IL-12-signaling deficient mice.....	50
Figure 11: Transcript analysis of lesional skin of WT and <i>Il12rb2</i> ^{-/-} mice.....	51
Figure 12: Analysis of $\gamma\delta$ T cell distribution in lesional skin of WT and <i>Il12rb2</i> ^{-/-} mice.	53
Figure 13: Identification of three subpopulations of $\gamma\delta$ T cells in the murine skin.	54
Figure 14: Ratio of skin effector $\gamma\delta$ T cells in IMQ-treated <i>Il23a</i> ^{-/-} , <i>Il12b</i> ^{-/-} and <i>Il12rb2</i> ^{-/-} mice.	54
Figure 15: IL-17A production in IMQ-treated WT and <i>Il12rb2</i> ^{-/-} mice.	55
Figure 16: Treatment protocol of IL-17A neutralization in IMQ-treated <i>Il12rb2</i> ^{-/-} mice.	56
Figure 17: Analysis of inflamed skin in WT and anti-IL-17A-treated <i>Il12rb2</i> ^{-/-} mice.....	57
Figure 18: Analysis of skin inflammation in mice functionally lacking V γ 6 ⁺ V δ 1 ⁺ T cells.....	58
Figure 19: Correlation analysis of V γ 6 ⁺ V δ 1 ⁺ $\gamma\delta$ T cells with skin thickness in WT mice.	58
Figure 20: Treatment protocol of loss- and gain-of-function experiments.....	59
Figure 21: Skin inflammation in IL-12Fc-treated mice deficient in IL-12-signaling.	60
Figure 22: Skin inflammation in WT mice after neutralization of IL-12.....	61
Figure 23: Expression of <i>Il12rb2</i> on murine $\gamma\delta$ T cell subsets.	62
Figure 24: IL-12R β 2 expression in healthy and psoriatic human skin.	63
Figure 25: Treatment protocol for HSD-experiments in WT mice.....	64
Figure 26: Measurement of the hematocrit in WT mice fed with chow or HSD.....	65
Figure 27: Analysis of skin inflammation in IMQ-treated WT mice fed with chow or HSD.	66
Figure 28: Histopathology and <i>Lcn2</i> -levels of IMQ-treated WT mice fed with chow or HSD..	67
Figure 29: Transcript analysis of lesional skin of WT mice fed with chow or HSD.....	68
Figure 30: $\gamma\delta$ T17 cell contribution in skin of IMQ-treated WT mice fed with chow or HSD. ...	69
Figure 31: Expression levels of CD44 in $\gamma\delta$ T cells in skin-dLN in mice on chow or HSD.....	70
Figure 32: Skin inflammation in HSD-fed mice functionally lacking V γ 6 ⁺ V δ 1 ⁺ T cells.....	71
Figure 33: Analysis of skin inflammation in IMQ-treated WT mice fed with HSD or LSD.....	73

Figure 34: Transcript analysis of the NFAT5-induced osmoadaptive response.....	74
Figure 35: Transcript analysis of sodium channels in the skin.	75
Figure 36: Transcript analysis of selected expression markers of macrophages in the skin..	76
Figure 37: Protective function of IL-12 in the skin and the effect of high dietary salt intake on the development of psoriatic plaque formation.	90

List of Tables

Table 1: Chemicals, substances and solutions	25
Table 2: Material and equipment for animal experiments.....	27
Table 3: Blocking antibodies and cytokines for <i>in vivo</i> experiments.....	27
Table 4: Antibodies for FACS analysis and sorting of $\gamma\delta$ T cells subsets	28
Table 5: Buffers and solutions for histology/histochemistry.....	28
Table 6: Antibodies for histochemistry of human skin biopsies	28
Table 7: Commercial kits	29
Table 8: Consumables.....	29
Table 9: Laboratory equipment.....	30
Table 10: Software	31
Table 11: Material for genotyping of mice	31
Table 12: Primers for genotyping of transgenic mice	31
Table 13: Primers for qPCR.....	33
Table 14: Composition of PCR reactions for genotyping of transgenic mice	35
Table 15: Conditions of PCR reactions and product lengths.	35
Table 16: Psoriasis Area and Severity Index in mice	37

Disclaimer

The first part of this thesis is based on and was partly adapted from the following publication:

Paulina Kulig¹, **Stephanie Musiol**², Sandra Nicole Freiburger³, Bettina Schreiner¹, Gabor Gyülveszi⁴, Giancarlo Russo⁵, Stanislav Pantelyushin¹, Kenji Kishihara⁶, Francesca Alessandrini², Thomas Kündig³, Federica Sallusto⁴, Günther FL Hofbauer³, Stefan Haak^{2#} and Burkhard Becher^{1#}. IL-12 protects from psoriasiform skin inflammation. *Nat Commun.* 2016 Nov 28;7:13466.

#these authors contributed equally

- ¹ Institute of Experimental Immunology, University of Zurich, 8057 Zurich, Switzerland
- ² Experimental Immunology Unit, Centre of Allergy and Environment (ZAUM), Technical University of Munich and Helmholtz Centre Munich, 80802 Munich, Germany
- ³ Department of Dermatology, University Hospital Zurich, 8091 Zurich, Switzerland
- ⁴ Institute for Research in Biomedicine, Cellular Immunology, 6500 Bellinzona, Switzerland
- ⁵ Functional Genomics Center Zurich, University of Zurich and ETH Zurich, 8057 Zurich, Switzerland
- ⁶ Department of Immunology, Faculty of Pharmaceutical Sciences, Nagasaki International University, 859-3298 Nagasaki, Japan

The Figures 8A und C, 13, 14, 15, 17, 18, 19, 22 and their corresponding data used in this thesis were collected during the framework of the PhD thesis and contributed to the published paper by *Kulig P. et al., 2016*.

The results of Figure 9, 10, 11, 12 were equally collected.

The data in the Figures 6, 7, 8B, 21, 23, 24 were collected and provided by Paulina Kulig and the other co-authors of this paper.

Abbreviations

Ab	Antibody
Ag	Antigen
APC	Antigen-presenting cell
AKR1B1	Aldo-keto reductase family 1, member B1
BGT1	Betaine transporter
BM	Bone marrow
BMDM	Bone-marrow-derived macrophages
CCL	C-C chemokine ligand
CCR	C-C chemokine receptor
CD	Cluster of differentiation
cDNA	Complementary DNA
CIA	Collagen-induced arthritis
CLA	Cutaneous lymphocyte-associated antigen
DC	Dendritic cell
DETC	Dendritic epidermal T cell
DNA	Deoxyribonucleic acid
EAE	Experimental autoimmune encephalomyelitis
EDTA	Ethylenediaminetetraacetic acid
EGF	Epidermal growth factor
ELISA	Enzyme-linked immunosorbent assay
FACS	Fluorescence-activated cell sorting
FCS	Fetal calf serum
FDA	Food and Drug Administration
FoxP3	Forkhead box P3
FOXO1	Forkhead box protein O1
g	Gram
G	G force
GAG	Glycosaminoglycan
GAPDH	Glyceraldehyde 3-phosphate dehydrogenase
GM-CSF	Granulocyte macrophage colony-stimulating factor
H&E	Hematoxylin and eosin stain
HEPES	4-(2-hydroxyethyl)-1-piperazineethanesulfonic acid

HSPA1B	Heat shock 70kDa protein 1B
IBD	Inflammatory bowel disease
IEL	Intraepithelial lymphocytes
IFN	Interferon
Ig	Immunoglobulin
IL	Interleukin
ILC	Innate lymphoid cells
IL-23R	IL-23 receptor
IMQ	Imiquimod
i.p.	Intraperitoneal(ly)
i.v.	Intravenous(ly)
KC	Keratinocyte
KGF	Keratinocyte growth factor
KO	Knock-out
L	Liter
LN	Lymph node
m	Milli
M Φ	Macrophages
mAb	Monoclonal antibody
mDC	Myeloid dendritic cell
MHC	Major histocompatibility complex
MS	Multiple sclerosis
n	Nano
NaCl	Sodium chloride
NFAT5	Nuclear factor of activated T cells-5
NK	Natural killer cell
NKT	Natural killer T cell
NO	Nitric oxide
NOS2	Type-2 nitric oxide synthase
p	p-value, significance level is 0.5
p38/MAPK	p38/mitogen-activated protein kinase
PAMP	Pathogen-associated molecular pattern
PASI	Psoriasis Activity and Severity Index
PBS	Phosphate buffered saline
PCR	Polymerase chain reaction
pDC	Plasmacytoid dendritic cell
PTGS2	Prostaglandin 2

PRR	Pattern recognition receptors
RNA	Ribonucleic acid
ROR	Retinoid-related orphan receptor
RPMI	Roswell Park Memorial Institute medium
RT	Room temperature
RT-qPCR	Real-time quantitative PCR
s.c.	Subcutaneous(ly)
SGK1	Serum-and glucocorticoid-inducible kinase 1
SLC5A3	Sodium/myo-inositol cotransporters
SMIT	Sodium/myo-inositol cotransporters
T _c	Cytotoxic T cell
TCR	T cell receptor
TEWL	Transepidermal water loss
TF	Transcription factor
T _{fh}	Follicular helper T cells
TGF	Transforming growth factor
T _H	T-helper cells
TLR	Toll-like receptor
TNF	Tumor necrosis factor
Treg	Regulatory T cell
T _{rm}	Tissue-resident memory T cell
VEGF-C	Vascular endothelial growth factor C
WHO	World Health Organization
WT	Wildtype
°C	Degree Celsius
μ	Micro

1. Abstract

Psoriasis is a chronic inflammatory, not curable skin disease that is accompanied by an extensive impact on the patient's quality of life. Currently, a genetic predisposition in combination with unknown initial triggers, including stress, infections and lifestyle factors, is thought to contribute to its development. Biologicals have proven their efficiency in psoriasis treatment as they target specific molecules involved in its pathogenesis. Among those, neutralization of the common p40 subunit of IL-12/23 is considered as one of the first-line biologics in moderate to severe psoriasis vulgaris. So far, all available data point towards the IL-23/17A effector axis to be the dominant pathway in disease pathogenesis. Hence, the curative effect of anti-p40 therapy might be due to the inhibition of IL-23 signaling alone, especially as information on a causal relationship of either IL-12 or IFN- γ and psoriasis is still missing.

This study addressed the contribution of IL-12 to the formation of psoriatic lesions. For this reason, psoriasiform inflammation was induced in mice by use of the IMQ-model. Whereas p40^{-/-} mice recapitulated the efficiency of anti-p40 therapy, mice deficient in IL-12 signaling alone developed an aggravated disease phenotype leading to the assumption of a protective role of IL-12 in the skin. This function was shown to be independent of IFN- γ , which in the lesion serves the expected pro-inflammatory effect. The use of loss- and gain-of-function in the IMQ-model revealed that IL-12, in contrast to IL-23, has a regulatory function in the skin by restraining the invasion of pathogenic V γ 6⁺ $\gamma\delta$ T17 cells, which were further shown to be causative for disease aggravation in IL-12-deficient mice. To investigate the underlying mechanism, transcriptomic analyses of murine skin and primary human keratinocytes were performed, demonstrating that IL-12 directly communicates with the local stroma and initiates a tissue-protective transcriptional program, which limits psoriasiform skin inflammation.

One of the lifestyle factors in the focus as critical triggers in psoriasis development are certain diets. In particular, high dietary salt intake, as part of the "western diet", is currently under discussion to be an environmental trigger for autoimmune diseases by increasing the differentiation of naive $\alpha\beta$ T cells into pro-inflammatory T_H17 cells. Skin tissue resident immune cells, like $\gamma\delta$ T cells, are sentinels of external triggers and tissue stress. Thus, the effect of high salt diet on these cell populations and its impact on the development of psoriasiform inflammation was additionally

investigated in WT mice. Flow cytometric analyses revealed that excessive salt intake primes the skin-resident immune system towards an inflammatory type 17 response with $V\gamma 6^+ \gamma\delta T17$ cells being the most affected cell population that is highly contributing to aggravated disease pathology.

This thesis considers two different aspects in psoriasis therapy. It reveals interference in efficacy of the biological pharmacotherapy of anti-p40 antibodies in psoriasis by parallel targeting of IL-23 and IL-12, which mediates a protective, autonomous regulatory programme in the skin. The study also presents high dietary salt intake as a dietary trigger for psoriasis development, thus offering dietary treatment as a lifestyle-based intervention in psoriasis patients. Both findings emphasize the importance of a deep knowledge on the specific mode of action of biologicals and dietary factors for an effective and safe therapeutic intervention.

2. Zusammenfassung

Psoriasis ist eine chronisch-entzündliche, bisher nicht heilbare, Hauterkrankung, die mit einer starken Einschränkung der Lebensqualität des Patienten einhergeht. Derzeit wird eine Kombination aus genetischer Prädisposition und unbekanntem, initialen Faktoren, wie Stress, Infektionen und Umweltfaktoren, als Entstehungsursache diskutiert. Biologika haben sich in der Behandlung von Psoriasis als sehr effizient erwiesen, da sie gezielt die an der Immunpathogenese beteiligten Moleküle und deren Signalwege beeinflussen. Die Hemmung der gemeinsamen p40-Untereinheit von IL-12/23 gilt als eine der Standardtherapien bei mittel-schwerer bis schwerer Psoriasis vulgaris. Doch bisher weisen alle wissenschaftlichen Erkenntnisse darauf hin, dass die IL-23/IL-17-Effektor-Achse den entscheidenden Beitrag zur Krankheitspathogenese leistet. Es stellt sich daher die Frage, ob der positive Effekt der Anti-p40 Therapie einzig auf die Hemmung des IL-23 Signalweges zurückzuführen ist, insbesondere da ein kausaler Zusammenhang von IL-12 oder IFN- γ und Psoriasis immer noch fehlt.

In dieser Studie wurde der Beitrag von IL-12 zur Entstehung psoriatischer Läsionen untersucht. Dazu wurde, unter Anwendung des IMQ-Modells, eine Psoriasis-ähnliche Hautentzündung in Mäusen induziert. Während p40^{-/-}-Mäuse die Wirksamkeit der Anti-p40-Therapie bestätigten, wiesen Mäuse mit Verlust des IL-12-Signalweges einen verstärkten Krankheitsverlauf auf, was auf eine schützende Funktion von IL-12 in der Psoriasis-belasteten Haut hindeutet. Diese Funktion zeigte sich unabhängig von IFN- γ , welches in den Läsionen selbst einen proinflammatorischen Effekt hat. Zudem machte die Anwendung von loss- und gain-of-function Experimenten im IMQ-Modell deutlich, dass IL-12, im Gegensatz zu IL-23, eine regulatorische Funktion in der Haut ausübt, indem es das Einwandern pathogener V γ 6⁺ γ δ T17 Immunzellen unterbindet, welche sich unter Verlust des IL-12 Signalweges als ursächlich für den verstärkten Krankheitsverlauf erwiesen. Um den zugrunde liegenden Mechanismus näher zu untersuchen, wurden Transkriptomanalysen von muriner Haut und primären human Keratinozyten durchgeführt. Diese ergaben, dass IL-12 direkt mit dem lokalen Stroma kommuniziert und dabei ein schützendes Programm in den Hautzellen aktiviert, welches die Entzündung in der Haut begrenzt.

Einer der Umweltfaktoren, der als kritischer Auslöser für die Entstehung von Psoriasis gehandelt wird, ist die Ernährungsweise. Insbesondere die Einnahme

höherer Mengen an Kochsalz, im Zuge der westlichen Ernährungsweise, wird momentan als umweltbedingter Auslöser für die Entstehung autoimmuner Erkrankungen diskutiert, da es die Entwicklung naiver $\alpha\beta$ T Zellen in entzündungsfördernde T_H17 Zellen fördert. In der Haut ansässige Immunzellen wie $\gamma\delta$ T Zellen, üben eine „Wächterfunktion“ aus, mit der sie externe Einflüsse und Stress detektieren können. Daher wurde zusätzlich die Wirkung einer salzreichen Ernährung auf diese Zellpopulation und die Entwicklung psoriatischer Entzündungen in WT-Mäusen untersucht. Durchflusszytometrische Analysen ergaben, dass übermäßiger Salzkonsum das Immunsystems in der Haut in Richtung einer entzündlichen T_H17 -Immunantwort polarisiert, wobei $V\gamma6^+$ $\gamma\delta T17$ Zellen, welche beträchtlich zur Verschlechterung des Krankheitsbildes beitragen, die am stärksten betroffene Zellpopulation darstellten.

Diese Thesis betrachtet zwei verschiedene Aspekte in der Psoriasis-Therapie. Sie zeigt zum einen die Beeinträchtigung in der Wirksamkeit der Pharmakotherapie mit anti-p40-Antikörpern in Psoriasis aufgrund der parallelen Hemmung von IL-23 und IL-12, welches ein schützendes, autonomes Programm in der Haut induziert. Außerdem präsentiert die Studie eine hohe Salzaufnahme als möglichen Umweltfaktor für die Entwicklung von Psoriasis und stellt damit eine lebensmittelorientierte Behandlung als Maßnahme für Psoriasis Patienten dar. Die Ergebnisse in dieser Arbeit verdeutlichen, wie wichtig es ist, die spezifischen Wirkungsweisen von Biologika und den Einfluss der Ernährung zu verstehen, um mit den gewonnenen Erkenntnissen den Erfolg und die Sicherheit therapeutischer Anwendungen zu garantieren.

3. Introduction

3.1 The skin immune system

The immune system is a complex network of specialized cells, tissues and organs that preserves the integrity of the body and protects the organism from a multitude of infectious microorganisms (bacteria, viruses, parasites or fungi), harmful substances from the environment and neoplastic cellular transformations (e.g. cancer) [1, 2].

The skin represents the body's largest organ, which is constantly exposed to the outer environment. Therefore, it not only provides a passive physical barrier, but in particular represents an active immune organ, which protects the body from invading pathogens by activation of the innate and adaptive immune system. At the same time, it provides tolerance to self-antigens and commensal bacteria [3, 4].

Separated by the basement membrane, the skin is divided into two major compartments, the epidermis and the dermis with an underlying hypodermis consisting of loose connective and fatty tissue and multiple leukocyte subsets residing inside. The epidermis presents the outer layer of the skin that is composed of a multi-cell layer of differentiating keratinocytes, and an integral population of antigen-presenting cells (**APCs**), dendritic epidermal $\gamma\delta$ T cells (**DETCs**, mouse) and tissue-resident memory T cells (T_{RM}). The dermis is composed of collagenous connective tissue that gives the skin its flexibility and strength. Besides a network of blood and lymphatic vessels, through which migrating cells can traffic, it also contains nerve endings, hair follicles as well as sweat and sebaceous glands. It is populated by a variety of immune cells, including macrophages (**M Φ**), dendritic cells (**DCs**), mast cells, natural killer (**NK**) cells, natural killer T (**NKT**) cells as well as innate lymphoid cells (**ILCs**), dermal $\gamma\delta$ T cells and $\alpha\beta$ T cells [4, 5].

The close interaction between the skin environment with stromal cells and skin-resident and -infiltrating immune cells is the basis for the effectiveness of the skin immune system.

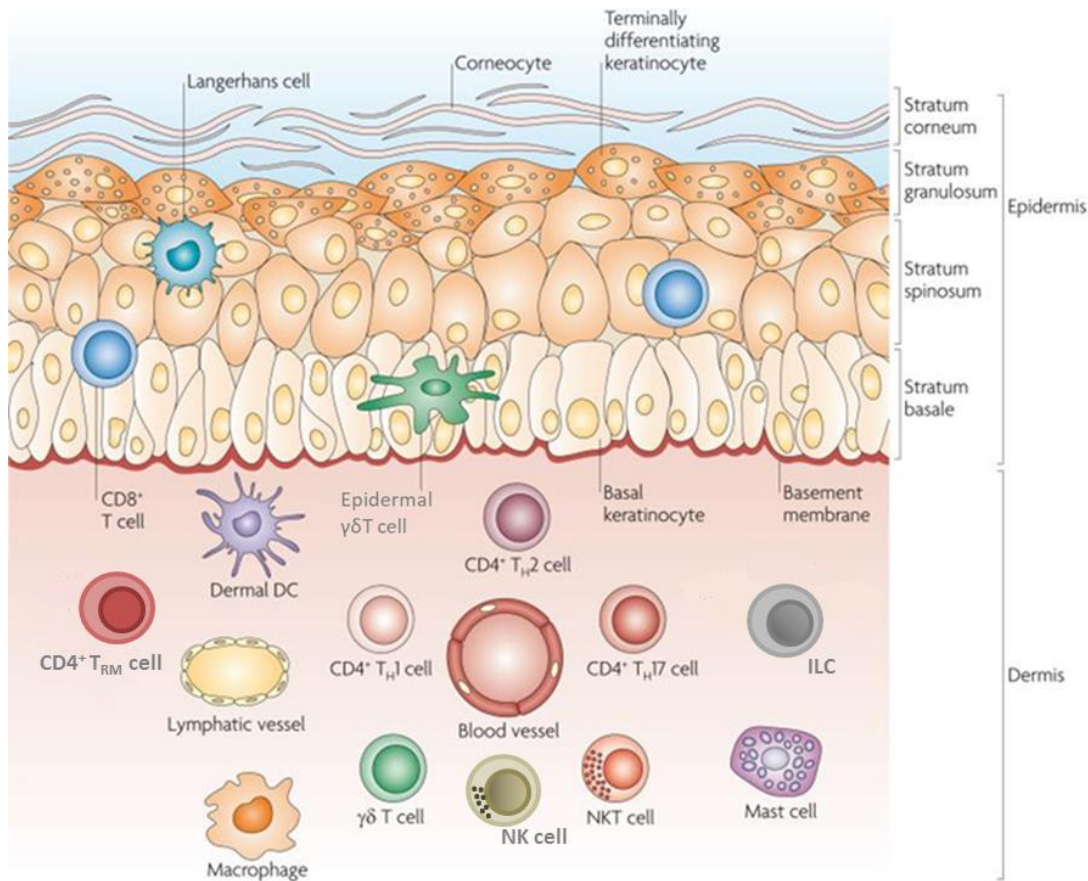


Figure 1: Overview of the skin structure and skin-resident cellular effector cells.
(adapted and modified from Nestle FO. *et al.*, 2009 [5])

3.1.1 Immune functions of non-hematopoietic stromal cells

Keratinocytes (**KCs**) are the major cell type of the epidermis and represent the outermost layer of the skin. They originate from stem cells in the deepest layer of the epidermis (stratum basale) and undergo a progressive differentiation program from spinous to granular KCs when they slowly migrate up towards the surface of the epidermis. In their terminal differentiation step they undergo keratinization, lack a nucleus and organelles and thus become metabolically inactive. The resulting dead corneocytes form the stratum corneum, a tight but not impermeable physical and chemical barrier, which provides protection against water loss, physical damage, as well as invasion of bacteria, viruses, and other foreign substances. Corneocytes are continuously shed of through desquamation and are replaced by cells derived from the stratum basale. In addition, KCs mediate cutaneous immune responses against environmental or pathogenic stimuli [5, 6]. To take over this role, KCs are equipped with a variety of toll like receptors (**TLRs**), by which they are able to recognize a wide range of pathogen-associated molecular-patterns (**PAMPs**) as well as danger-

associated molecular patterns (**DAMPs**) found on viruses, bacteria, fungi and other microbes [7]. Once being activated, they release antimicrobial peptides (**AMPs**; e.g. S100A proteins, β -defensins, cathelicidins), pro-inflammatory cytokines (e.g. IL-1, IL-6, and TNF- α), and chemokines (e.g. CXCL1, CXCL8- CXCL11, and CCL20) [8, 9]. Therefore, KCs are critical pro-inflammatory effector cells, which recruit various immune cells to the site of infection or injury making them important inducers of cutaneous innate and adaptive immunity [5, 8].

3.1.2 Skin-resident immune compartment

Like KCs, cells of the innate immune system in the skin express a variety of pattern-recognition receptors (**PRRs**) to detect damage and danger, which generate an initial and immediate immune response that is not directed against a specific antigen [10].

The most abundant haematopoietic population under steady-state conditions in the skin is represented by tissue-resident M Φ [11]. Once they are activated they attract other immune cells from the circulation to site of infection/injury by production of pro-inflammatory cytokines and chemokines [12]. These include granulocytes, which migrate from the bone marrow to the site of affected skin during an immune response. Whereas neutrophils are important in phagocytosis of a variety of microorganisms, basophils and eosinophils are more important in defense against parasites by releasing toxic proteins and enzymes [1].

Skin-specific APCs are dermal dendritic cells (**DDCs**) and Langerhans cells (**LCs**) residing in the epidermis. While LCs remain sessile during steady-state, forming a dense network between keratinocytes, DDCs are a more heterogeneous population that continuously migrates throughout the dermis [13]. Once they get in contact with a foreign antigen, they rapidly migrate to the draining LNs initiating a specific T cell immune response in order to neutralize or eliminate the antigen [14]. Mast cells are mainly found around blood vessels and are activated by PAMPs, cross-linked IgE molecules or unspecific triggers. Beneath their role in wound healing and pathogen defense, they are critical effectors of T_{H2} immune responses, like contact hypersensitivity, by release of inflammatory mediators [15].

In contrast to M Φ , DCs and mast cells, which arise from a common myeloid precursor, NK cells, NKT cells, $\gamma\delta$ T cells, ILCs and tissue-resident memory (T_{rm}) cells originate from the lymphoid lineage [2].

Residing in the dermis, NK cells are antigen non-specific, providing a rapid response in killing viral-infected cells and tumor cells [16], while NKT cells carry an invariant T

cell receptor (**TCR**), which can recognize lipids and glycolipids presented by non-polymorphic CD1d molecules [17].

ILCs, lacking common lineage marker expression, have been described in the dermis of both mice and humans and are characterized by their developmental requirements and cytokine production (ILC1-3), analogue to adaptive T_H cells [18].

The murine epidermis contains dendritic epidermal $\gamma\delta$ T cells (**DETCs**) that remain largely immobile, forming tight immunological synapses with keratinocytes [19] and are important in epidermal homeostasis and repair [20, 21]. In contrast, dermal $\gamma\delta$ T cells can form a long-lived population and thus provide an innate defense against pathogens by facilitating neutrophil recruitment via production of IL-17 [22]. Human and murine $\gamma\delta$ T cells are discussed later in this thesis in more detail.

Beneath cells of the innate immune system, the skin is also populated by cells of the adaptive immune system, which is characterized by its flexibility and immunological memory and mediated by B cells and $\alpha\beta$ T cells. Whereas B cells mature in the bone marrow, precursors of T cells migrate into the thymus, where their maturation takes place in a series of positive and negative selections under the guidance of the local stroma. Each clone of these cell types carries a highly specific receptor, generated by somatic recombination, which enables it to proliferate and differentiate once it encounters its specific antigen. B cells differentiate into plasma cells providing humoral immunity via production of antigen-specific antibodies. T cells are classified into CD8⁺ and CD4⁺ T cells. CD8⁺ cytotoxic T cells kill virus-infected cells as well as tumor cells directly and recognize antigens presented on major histocompatibility complex (**MHC**) class I molecules. Naive CD4⁺ T cells can be polarized into various T helper (**T_H**) effector subsets depending on the local cytokine milieu and recognize antigens presented on MHC class II molecules [1, 2]. Both CD4⁺ and CD8⁺ T cells can become long-lived tissue-resident memory cells after they have been recruited to the site of skin infection or inflammation, providing a fast and efficient immune response against local re-infection [23, 24]

3.1.3 Conventional T cells in the skin

During inflammation, naïve CD4⁺ T cells are polarized into different effector types mediating an immune response. T_H1 cells, which differentiate in the presence of interleukin (**IL**)-12, are defined by their primarily production of interferon gamma (**IFN γ**) and expression of the transcription factor (**TF**) T-bet [25, 26]. They participate in the generation of cytotoxic T cells and strongly activate M Φ , promoting the

elimination of intracellular bacteria and viruses via a cell-mediated immune response. Otherwise, T_H2 cells develop in the presence of IL-4 with GATA-3 being their master TF and produce IL-4, IL-5 and IL-13 [27]. They mainly mediate humoral immunity against extracellular parasites and are linked with allergic diseases and atopic eczema [1, 2, 28].

A distinct lineage from T_H1 and T_H2 cells is represented by T_H17 cells [29, 30]. They are characterized by their expression of the retinoid-related orphan receptor isoform γ t (**ROR γ t**) [31] and production of their signature cytokines IL-17A, IL-17F and IL-22. Additionally, they are also a source of tumor necrosis factor alpha (**TNF α**) and granulocyte-macrophage colony-stimulating factor (**GM-CSF**) [32]. Further lineage markers of mature T_H17 cells are IL-23R and IL-1R1 as well as the chemokine receptors (**CCR**) 6 and 4, which enable their migration to the site of acute inflammation [33]. They are induced by TGF- β , IL-1 β and IL-6 [34]. Although, IL-23 is not required for their initial differentiation, as IL-23R is not expressed on naive T cells, it is essential for their expansion and maintenance of IL-17A production [35]. With at least six IL-17 family members (IL-17A to IL17F), T_H17 cells mediate their effects through interaction with IL-17 receptor family proteins (IL-17RA to IL-17RE) [36]. Their main function lies in host defense against extracellular bacteria and fungi by means of activating the infected stroma and recruitment of neutrophils to the tissue [37]. Beneath their function in host defence, T_H17 cells as well as T_H1 are associated with the development of autoimmune diseases, like psoriasis [36, 38, 39].

Characterized by their production of IL-22 but not IL-17, T_H22 cells contribute to local skin inflammation by mediating proliferation of keratinocytes and their release of AMPs and are found to accumulate in lesions of psoriasis patients [40].

Regulatory T cells (**Tregs**), on the other hand, suppress excessive activity of effector cells to control the immune response and maintain self-tolerance and thus prevent autoimmune reactions [41].

In healthy skin, tissue-resident as well as -infiltrating cells of the innate and adaptive immune system perform their specialized function and provide all factors that are necessary for an effective cutaneous immune response. Moreover, they maintain skin tissue homeostasis and repair. Any dysregulation in these mechanisms can cause an imbalance leading to inflammatory skin diseases, like psoriasis [42].

3.2 Psoriasis vulgaris - chronic inflammation of the skin

Psoriasis is a chronic, relapsing inflammatory skin disease which approximately affects 125 million people globally with plaque psoriasis (*psoriasis vulgaris*) being the most prominent form. The disease develops after an unknown initial pathogenic, environmental or internal trigger or stress mostly in individuals that are genetically predisposed to the disease. Depending on age, ethnic differences, and geographic location the prevalence of psoriasis can vary. Due to its high degree of complexity, which counts for most inflammatory diseases, and the occurrence of several comorbidities, psoriasis is more and more recognized as a systemic disease (global report on psoriasis, WHO 2016 [43]).

3.2.1 Immunogenetics of psoriasis

The use of genomewide association studies (**GWAS**) resulted in the identification of several loci and genes that are linked to a higher susceptibility for developing psoriasis. They further led to a deeper biological understanding of the disease and confirmed the complex and multifactorial immunogenetic component in psoriasis. Besides the susceptibility locus *PSORS1*, which can be found in up to 60% of all psoriatic patients [44, 45], single nucleotide polymorphisms (**SNPs**) in genes involved in inflammatory pathways as well as in tissue homeostasis have been identified.

Most important and relevant for this study, was the identification of SNPs in genes of the IL-23 pathway and T_H17 cell immune responses, including the interleukin-23 receptor (*IL23R*), the interleukin-12B (*IL12B*; *p40*) [46, 47] as well as variants of the *IL23A* gene, encoding for the IL-23p19 subunit [48]. All are associated with an increased psoriasis risk highlighting the pivotal role of the IL-23/IL-17 axis in psoriasis [39].

Moreover, it could be shown that different gene variants of the inducible transcription factor NF-κB pathway have a direct connection to the development of psoriasis. These include two gene variants (*TNFAIP3*, *TNIP1*), which encode for proteins downstream of TNF signaling [48] as well as gene variants of inhibitory proteins of NF-κB, including IκBα (*NFKBIA*) [49] and the signalling adaptor molecule ACT1 (*TRAF3IP2*), which is involved in IL-17-mediated NF-κB activation [50].

Furthermore, the absence of intact genes of the late cornified envelope (**LCE**) family is associated with psoriasis susceptibility as they are expressed during epithelial differentiation, and are therefore critical in skin barrier repair [51, 52].

3.2.2 Clinical manifestation of Psoriasis

Patients suffering from plaque psoriasis show the characteristic demarcated red colored skin lesions with silvery-white, scaly plaques and a thickened epidermis mainly located on elbows, knees, scalp and the lumbosacral area. The histopathologic features more clearly define the clinical picture, including diffuse epidermal hyperplasia (acanthosis) with elongated rete ridges, a thickened stratum corneum (hyperkeratosis) and a less discrete epidermal granular layer due to a hyperproliferation of KCs. Thus, the squamous KCs aberrantly retain intact nuclei in the upper layers and stratum corneum (parakeratosis). Their release of extracellular lipids leads to a poorly adherent stratum corneum that becomes visible as scales. Another hallmark in psoriasis is the extensive accumulation of inflammatory infiltrates in the skin, consisting mainly of T cells, neutrophils and DCs. Neutrophils that are present in the stratum corneum represent the early manifestation of Munro's microabscesses. Finally, the observed erythema is the result of an impressive growth and an increased vascularity of dermal blood vessels [42].

Patients suffering from psoriasis show an increased risk of numerous disease-related comorbidities that correlate with psoriasis severity including cardiovascular diseases [53, 54], type II diabetes [55], metabolic syndrome [56] and inflammatory bowel disease [57]. Additionally, severe psoriasis is associated with an increased mortality and a decreased life expectancy [58, 59]. Due to this extensive impact on virtually all aspects of life, the necessity for an effective disease control of psoriasis and a better understanding of its pathogenesis become indispensable.

3.2.3 Mouse models of psoriasis

Much of what has been learned about the pathogenesis of psoriasis was obtained from preclinical mouse models that serve as an important tool to elucidate the complex cellular interactions and underlying molecular pathways of the disease. The current revolution in effective immunotherapy of psoriatic plaque formation serves as a good example for the role and impact of conceptual mouse research in effective drug discovery. To mimic a complex and multigenic inflammatory disease like psoriasis in a murine model is challenging as it should ideally reproduce the major clinical symptoms and involve the same cellular and molecular pathways as found in the human disease. Therefore, numerous spontaneous (e.g. asebia mouse), genetically engineered (e.g. K5.Stat3C mouse), xenotransplantation (e.g. psoriatic SCID mouse model) and inducible mouse models (e.g. IL-23-injected model, imiquimod-induced model) have been established. Today, the IMQ-Model is

commonly used in preclinical psoriasis studies as a suitable model for psoriasiform skin inflammation, due to its ease of use, mode of action, short treatment duration and low costs. But also the limitations have to be taken into consideration as it is only an acute model of skin inflammation, which does not mimic the chronic state of the human disease and does not picture the comorbidities of psoriasis [60, 61].

3.2.3.1 The imiquimod-induced model of psoriatic plaque formation

The TLR 7 agonist imiquimod (**IMQ**) acts as a potent immune response modifier for M Φ , monocytes, and DCs, thus contributing to a strong activation of the immune system [62]. Aldara[®] cream containing 5% IMQ was initially developed for topical treatment of genital and perianal warts caused by human papillomavirus [63] and was also found to be effective in treating (pre)cancerous skin lesions [64, 65]. Unexpectedly, in some patients, continuous topical application of IMQ induced or exacerbated psoriatic lesions not only in the area of use but also at distant, unaffected sites [66, 67]. Based on the clinical observations van der Fits and colleagues developed a novel targeted, induced mouse model of psoriasis, the IMQ-model [61]. Daily topical application of IMQ onto mouse skin causes the formation of psoriatic skin lesions with a similar pathophysiology of acute plaque formation in human patients. Changes in the mouse skin are accompanied by erythema, skin thickening, scaling, acanthosis, an impaired KC differentiation, angiogenesis and infiltration of various immune cells into the skin. Moreover, the IMQ model has proven itself a valuable experimental system as it mirrors the early cellular and molecular events during psoriatic plaque formation with abundant dermal expression of IL-17A, IL-17F, and IL-23 and responsiveness to conventional anti-psoriatic therapies [61, 68]. The usage of this model in combination with genetically modified mouse strains demonstrated the involvement of type I interferons [69], IFN- γ and the IL-23/IL-17 axis [61] in disease pathology, presenting these molecules as potential therapeutic targets. Furthermore, the effector capacity and potential relevance of innate lymphoid cells in psoriatic plaque formation was demonstrated as IL-17 is primarily produced by dermal $\gamma\delta$ T cells and ILCs and mice deficient for these cell populations develop a drastically reduced psoriasiform inflammation [68, 70].

3.2.4 Pathophysiology of psoriasis vulgaris

In the last three decades, the immunopathogenesis of psoriasis was revised as *in vitro* experiments, functional studies in animal models as well as clinical experiences in treating psoriasis, provided a deeper understanding of the involved immune mechanisms. Originally psoriasis was explained by dysfunctional keratinocytes, which trigger an immune response. This changed with the successful application of agents (cyclosporine, DAB389IL-2), which selectively block the proliferation of T cells but not keratinocytes, thus providing the first clinical evidence that T cells are critical in psoriasis pathogenesis [71, 72].

3.2.4.1 Psoriasis – a T_H1 or T_H17-mediated disease?

The presence of large numbers of T_H1 cells as well as an elevated expression of both mRNA and protein levels of IFN- γ and IL-12 (p40 subunit detection) in plaques and blood of psoriatic patients [73-76] suggested the involvement of a type 1 immune response in disease pathology. Moreover, intradermal injection of IFN- γ into non-lesional skin of psoriasis patients was able to induce an infiltration of multiple dermal cell populations (e.g. T cells, DCs) accompanied with chemokine and cytokine production [77].

The prevailed role of T_H1/IL-12-IFN γ functions in psoriasis pathology was questioned with the discovery of the new distinct lineage of T_H17 cells. The APC-derived signal that triggers IL-17 production by T cells was identified in 2000 with the discovery of a novel cytokine chain p19, which associates with the already existing p40 chain of IL-12, forming a heterodimeric cytokine termed IL-23 [78]. Whereas IL-23 signals through a receptor complex consisting of IL-23 receptor (IL-23R) and IL-12R1 [79], IL-12 uses IL-12R1 in combination with IL-12R2 [80]. Despite the structural bond of sharing a subunit both cytokines mediate functionally distinct signaling pathways. While IL-12 is involved in the induction of T_H1 cells [25], IL-23 is an important survival factor for T_H17 cells and promotes their production of IL-17 [32].

Support for the notion of a dominant role of IL-23 in psoriasis came from transcript analysis of psoriatic lesions, which revealed an increase of the IL-23 subunits IL-23p19 and IL-23p40, but not of IL-12p35 [81]. Furthermore, induction of psoriasiform inflammation in mice deficient for either IL-23p19, IL-17 or its receptor led to a delayed onset and reduced disease severity accompanied by the absence of T_H17 cells [61, 68]. Besides increased mRNA of IFN- γ in human psoriatic lesions, high mRNA and protein levels of IL-23 as well as type 17 cytokines (e.g. IL-17A, IL-17F, IL-22, TNF- α) were detected correlating positively with disease activity [42].

The results of GWAS studies further supported the role of the IL-23/T_H17 axis as the main driver in the pathogenesis of psoriasis and other inflammatory diseases [46-48].

3.2.4.2 Immunomechanisms of Psoriasis

Currently, the exact initiation of the immune response observed in psoriasis is still enigmatic, but environmental and genetic factors, injury or trauma (Koebner effect), tissue stress, infections as well as medications are possible triggers of the disease [42].

The early steps of the pathogenic cascade are mainly characterized by the activation of immune cells, in particular dermal dendritic cells, but how exactly the cascade initially starts is still unclear [82]. Pathogens can disrupt or stress KCs in the epidermis leading to the release of self-deoxyribonucleic acid (**DNA**) and AMPs (e.g. cathelicidins (LL-37), β -defensins). Those can form complexes and bind to TLRs on plasmacytoid dendritic cells (**pDCs**) [83] or keratinocytes [84], which activates them to produce type 1 interferons (IFN α and $-\beta$) and thus promote psoriasis pathogenesis. Hence, myeloid dendritic cells (**mDCs**) and M Φ are also activated [85]. Once activated they begin to produce pro-inflammatory cytokines, including IL-6, IL-23, TNF α as well as IL-12, leading to the differentiation and expansion of T cell effector subtypes that bear skin-homing receptors (CCR4, CCR6, CCR10, CXCR3) to infiltrate the dermis and epidermis of the skin. Based on their release of signature cytokines, T_H1, T_H17, and T_H22 cells can be identified within the cellular infiltrates as well as their CD8⁺ T cell counterparts (Tc1, Tc17, and Tc22) [82]. More recently, tissue-resident innate immune cells, including $\gamma\delta$ T cells and ILC3s have been identified as high producers of IL-17 in psoriatic lesions [68, 70, 86]. Therefore, the production of IL-23 in psoriatic skin by DCs and M Φ does not only support the development and proliferation of T_H17 cells, but also and initially most directly augmented the production of IL-17A, IL-17F, and IL-22 by IL-23R⁺ CCR6⁺ dermal $\gamma\delta$ 17 T cells, which are highly increased in skin lesions [68, 70].

The “key responding” tissue cells in the inflammatory skin microenvironment are represented by KCs as they express receptors for the majority of psoriatic signature cytokines including high amounts of IL-17 and IL-22 receptors [87]. In response to IL-17, KCs proliferate and amplify skin inflammation by the production of even more pro-inflammatory cytokines (e.g. IL-1 β , TNF α , IL-6), chemokines (e.g. CXCL1, CXCL8, CXCL10, CCL20), and AMPs (e.g. LL37, β -defensins, LCN2, S100A proteins), which led to further recruitment of inflammatory cells from the circulation [87, 88]. Additionally, IL-22 contributes to epidermal hyperproliferation by impairing

KC terminal differentiation [89]. The infiltration of even more IL-17 producing T cell subtypes (T_{H17} , T_{c17} , $\gamma\delta T$ cells), T_{H1} as well as T_{H22} cells, inflammatory DCs as well as neutrophils in combination with an abnormal activation of KCs lead to the formation of a self-amplifying pathological loop, which maintains a cutaneous inflammatory response [42].

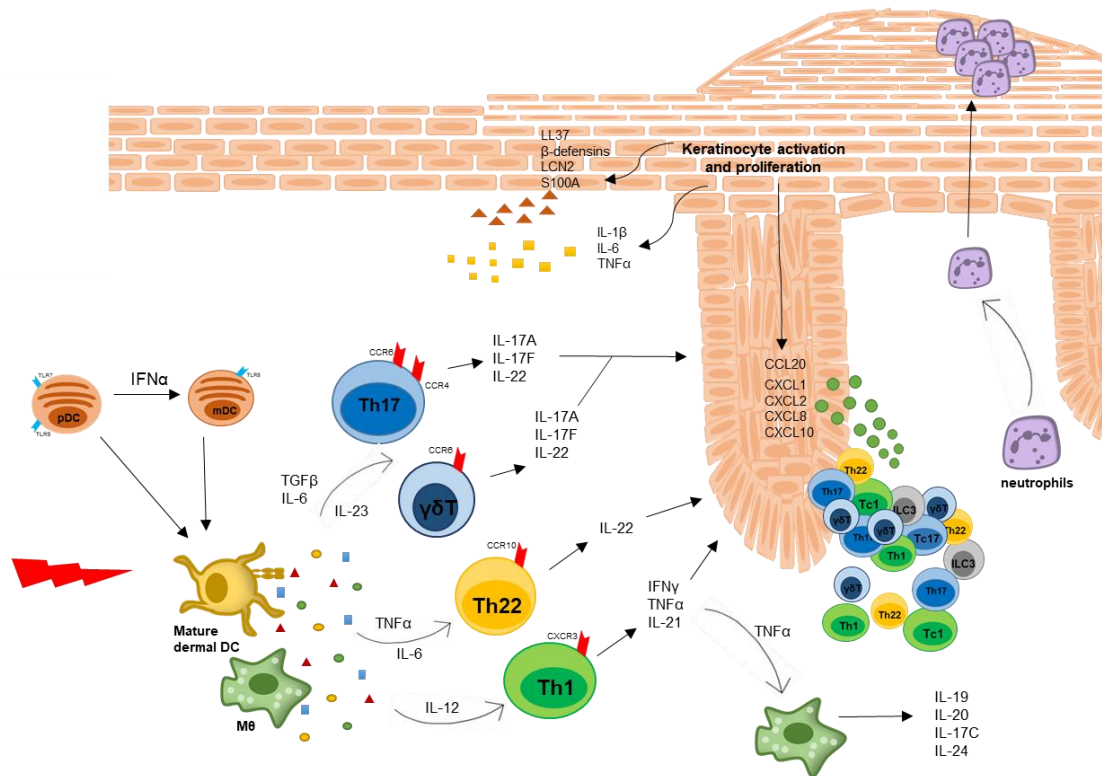


Figure 2: Summary of current concepts of psoriasis pathogenesis. (adapted from Nestle FO., Kaplan DH. and Barker J., 2009 [90]).

3.3 $\gamma\delta$ T cells – Innate immune players in psoriasis

In the mid 1980s $\gamma\delta$ T cells were discovered based on structural similarities to the $\alpha\beta$ TCR [91]. They share the same common progenitor cells with $\alpha\beta$ T cells, but are innate MHC-unrestricted lymphocytes with more unique antigen receptors [2]. In mice, five functional subsets of $\gamma\delta$ T cells develop in the thymus and migrate into the periphery in successive waves at defined periods of fetal, neonatal, and adult development (Figure 3). Depending on the tissue, antigen-receptor structure and local microenvironment they perform different functions [92, 93]. Throughout the thesis, the Tonegawa nomenclature is used for mouse V γ chains [94].

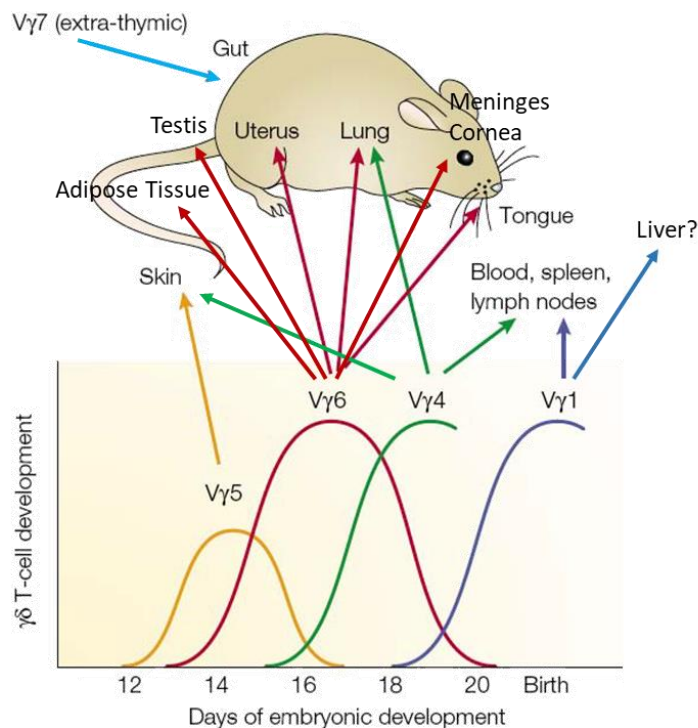


Figure 3: Functional development and intrinsic peripheral migration pattern of $\gamma\delta$ T cells. (adapted from Carding SR. and Egan PJ., 2002 [92])

Unlike, CD4⁺ $\alpha\beta$ T cells that mostly leave the thymus in a ‘naive’ state and differentiate in the periphery upon activation, murine $\gamma\delta$ T cells are developmentally imprinted to produce IFN- γ or IL-17 during thymic development. Thymic $\gamma\delta$ T cells that are antigen-naïve or bind antigen with low affinity mainly become IL-17 producers [95]. They share many features with T_H17 cells including the expression of the transcription factor ROR γ t, the signature cytokine receptor IL-23R, the chemokine receptor CCR6 [96, 97], and they also lack the tumor necrosis factor receptor family member CD27 [98]. In the periphery, they are able to directly

produce IL-17 induced by IL-1 β and IL-23 without further TCR stimulation [97]. In contrast, antigen-experienced $\gamma\delta$ T cells that bind antigen with high affinity produce IFN- γ and require CD27 for their development [95, 98].

Although, $\gamma\delta$ T cells only constitute a small fraction (about 1-5%) of circulating lymphocytes in adult mice, the specific subsets of $\gamma\delta$ T cells are present in much higher numbers e.g in epithelial tissues of the skin, the gastrointestinal tract and the reproductive tract, expressing their TCR with little to no diversity [93]. The TCR of $\gamma\delta$ T cells can directly recognize conserved phosphoantigens of bacterial metabolic pathways and products of cell damage. They can also be rapidly activated by inflammatory cytokines, produced by M Φ or DCs in response to PAMPs [2, 96]. Due to their early immune response in case of pathogen infection, $\gamma\delta$ T cells are the first line of defense prior to activation of the adaptive immune system [92]. Especially, with their rapid production of high amounts of IL-17 they are protective during bacterial and fungal infections as they recruit neutrophils as well as M Φ and natural killer cells to the site of infection, activate other effector T cells and induce AMPs [92, 99, 100].

3.3.1 Pathogenic role of murine $\gamma\delta$ T17 cells in psoriasis

Besides the role of $\gamma\delta$ T cells in tissue surveillance, they exert considerable impact in the pathogenesis of various inflammatory and autoimmune disease models, including IMQ-induced skin inflammation [68, 70] and experimental autoimmune encephalomyelitis (EAE) [97] as they are major providers of IL-17A. Using the IMQ-model of psoriatic plaque formation in mice their pathogenic role has been well described as disease induction in $TCR\delta^{-/-}$, but not in $TCR\beta^{-/-}$ mice, led to a much milder phenotype with significantly decreased epidermal hyperplasia and inflammation compared to WT mice, indicating that $\gamma\delta$ T cells are necessary and sufficient to drive psoriasiform plaque formation in these animals [68].

Mouse skin harbors distinct subsets of $\gamma\delta$ T cells. Exclusively generated during thymic development, DETCs migrate to the epidermis where they persist throughout life by limited peripheral expansion remaining in close contact with surrounding KCs. They produce IFN- γ and keratinocyte growth factors, participate in tissue surveillance and wound healing [20] and have been ruled out to be responsible for plaque formation [101].

Apart from that, two subsets have been described among murine dermal $\gamma\delta$ T17 cells: V γ 4⁺ and V γ 6⁺ [22, 102, 103]. They differ from DETCs in the amount of TCR expressed on their surface (DETC are TCR-bright, dermal $\gamma\delta$ T cells are TCR-intermediate), expression of CCR6, which is abundant on dermal $\gamma\delta$ T cells but

absent on DETCs [22], and they predominantly secrete IL-17A in response to IL-1 β and IL-23 [97]. Whereas V γ 4⁺ cells are heterogeneous and highly motile [102], V γ 6⁺ cells carry a canonical TCR, are *bona fide* resident in dermis and non-migratory [103].

As IMQ-treated *Sox4*^{-/-} or B6.SJL mice, in which V γ 4⁺ cells are nearly absent, developed only mild skin inflammation [104, 105], it was suggested that V γ 4⁺ T cells are the prominent dermal $\gamma\delta$ T17 cell subset that promotes psoriatic plaque formation. The pathogenic potential of V γ 6⁺ cells was later demonstrated by Cai and colleagues as *TCR δ* ^{-/-} mice reconstituted with V γ 6⁺ developed noticeable psoriasis-like skin inflammation after administration with IMQ [103].

Therefore, both murine dermal $\gamma\delta$ T cell subsets are functional competent in driving psoriatic skin inflammation by production of IL-17A, IL-17F, and IL-22 [68, 103].

3.3.2 Human $\gamma\delta$ T cells and their role in psoriasis

Compared to their murine counterparts, human $\gamma\delta$ T cells can be distinguished by their different V δ usage instead of V γ usage. Therefore, two major subsets of $\gamma\delta$ T cells, expressing either a V δ 1 or a V δ 2 chain have been identified in humans [106]. Human $\gamma\delta$ T cells mediate their effector functions early in infection and are potent cytolytic effector cells for killing a variety of tumor cells [107, 108].

In the skin, the composition of $\gamma\delta$ T cell subsets highly differs between mice and humans. In healthy human dermis, V δ 1⁺ cells, expressing skin-homing receptors like cutaneous lymphocyte-associated antigen (**CLA**) and producing TNF α and IFN- γ upon stimulation, predominate with an oligoclonal repertoire distinct from that of circulating V δ 2⁺ $\gamma\delta$ T cells, which are normally rare in the skin [109, 110]. As the number of naive V δ 1⁺ $\gamma\delta$ T cells in peripheral blood remains relatively constant into adulthood they may continuously be regenerated in the thymus [111]. With their varying γ chain pairing, these V δ 1⁺ $\gamma\delta$ T cells form an oligoclonal repertoire and are able to recognize a variety of stress-induced self-antigens or conserved foreign antigens [112]. One part of this heterogenic population shares certain characteristics with murine intraepithelial $\gamma\delta$ T cells (**IELs**), as they exert a cytotoxic, T_H1-like phenotype with frequent expression of CD8 [113]. By responding to various invading pathogens during lifetime, every individual carries a very diverse and unique TCR repertoire [114]. Furthermore, as well as DETCs, human V δ 1⁺ cells were shown to play a role in tissue homeostasis and repair [115].

Analyses of skin lesions of human psoriasis patients revealed elevated numbers of dermal $\gamma\delta$ T cells compared to normal control samples, which may suggest their potential involvement in pathogenesis [70]. Responsible for this increase is a skin

homing $V\gamma 9^+V\delta 2^+$ T cell subset, which expresses ROR γ t, CLA, and other skin homing chemokine receptors (e.g. CCR6) and is able to produce an array of pro-inflammatory cytokines, including IL-17 and TNF- α [116]. $V\gamma 9^+V\delta 2^+$ $\gamma\delta$ T cells constitute the majority of human peripheral blood $\gamma\delta$ T cells, which can present >50% of blood leucocytes during severe bacterial infections [117]. In skin lesions of psoriasis the elevation of $V\gamma 9^+V\delta 2^+$ T cells is accompanied by a substantial reduction of circulating $V\gamma 9^+V\delta 2^+$ cells in the blood of these patients that correlates well with disease severity. Thus, these cells might exit the blood to enter the skin where they selectively localize to areas of psoriasis development. During psoriasis-targeted therapy, the decreased number of circulating $V\gamma 9^+V\delta 2^+$ T cells normalises, presenting them as a potential biomarker [116].

3.4 Current treatment options for psoriasis

At current state, there is no treatment available to cure psoriasis, but a variety of treatment options exists that ameliorate the disease by controlling the symptoms and reducing inflammation.

The treatment of psoriasis rapidly changed with the clarification of the pathogenesis and discovery of major molecular targets leading to the development of cytokine-targeted therapies (biologics). As opposed to traditional systemic drugs that impact the entire immune system (e.g. cyclosporine, methotrexate), biologics specifically target different pathways in the inflammatory cascades of psoriasis. One of the first biologics in psoriasis treatment approved by the Food and Drug Administration (FDA) was Alefacept, which targets T cells [118], but was withdrawn in 2011 due to availability of better tolerated and more effective biologics for psoriasis treatment. Another group of biologicals, showing significant therapeutic efficacy in psoriasis, are TNF α inhibitors (Etanercept, Adalimumab and Infliximab) which neutralize the biological activity of TNF α by binding its soluble and membrane-bound form. Reported side effects are an increased risk for serious infections and development of cancer [119-121]. Surprisingly, in some cases TNF α inhibitors induced or exacerbated psoriatic skin lesions, caused by a dysbalance between TNF α and type 1 interferons [122].

As the former concept of psoriasis pathogenesis pointed towards an involvement of the IL-12/T_H1 axis, targeting IFN- γ or IL-12p40 became a possible treatment option. Whereas two small pilot studies were conducted with a neutralizing humanized anti-IFN- γ antibody (Fontolizumab), which was discontinued due to minimal clinical efficiency [123], targeting IL-12p40 successfully prevented murine psoriasis-like skin

disorder [124]. With the discovery of IL-23 sharing its p40 subunit with IL-12 [78], it became apparent that the therapeutic approach also inhibits the IL-23/IL-17 immune axis. With the increasing recognition of its relevance in psoriasis pathogenesis, it was hypothesized that targeting both IL-12 and IL-23 concomitantly would extend the drug's anti-inflammatory properties. This led to the development of new monoclonal antibodies (**mAbs**) against the p40 subunit, Ustekinumab and Briakinumab, for the treatment of psoriasis vulgaris. Whereas Briakinumab was withdrawn in 2011 [125] due to reports of a higher rate of adverse cardiovascular events [126], Ustekinumab was finally approved by the FDA in 2009. Due to its superior efficacy and safer profile compared to TNF α -inhibitors it is now applied as a standard therapy in psoriasis vulgaris [127, 128]. Studies in mice further confirmed the clinical data, as treatment with neutralizing p40 antibodies reduced disease development in IMQ-treated mice [68]. The most frequent reported adverse reactions to Ustekinumab treatment are infections (e.g. TB) and malignancies (mainly non-melanoma skin cancers) [127].

With the increasing importance of the IL-23/IL-17 axis in disease pathogenesis [39] the focus of psoriasis treatment is currently on targeting solely the IL-23/IL-17 axis by blockade of either IL-17, the IL-17 receptor or the IL-23p19 subunit. Therefore, three antibodies acting on IL-17 (Secukinumab, Ixekizumab and Brodalumab) were approved by the FDA. Whereas Secukinumab and Ixekizumab selectively bind and neutralize IL-17A and IL-17A/F directly [129, 130], Brodalumab blocks the action of IL-17RA, thus targeting all IL-17 cytokines that act via this receptor, including IL-17A, IL-17A/F, IL-17F, IL17-C and IL-17E (IL-25) [131]. All three exhibit superior efficacy to Ustekinumab [132-134]. Concerning their safety profile they are associated with an increased risk of mild infections (e.g. candida infections) and neutropenia. In the case of Brodalumab, patients have to undergo a Risk Evaluation and Mitigation Strategy (REMS) Program as events of suicidal ideation and behavior were registered in its clinical trials (FDA, 2016 [135]). Worth mentioning, as the T_H17 cytokine IL-22 was shown to be a critical cytokine for psoriatic plaque formation in mice [68, 136] its therapeutic potential was investigated in a clinical phase I study. Not meeting the primary endpoints, its development was discontinued (clinicaltrials.gov; Identifier: NCT01010542).

Moreover, several IL23p19 inhibitors are in development for psoriasis treatment, including Tildrakizumab [137], Guselkumab [138] and Risankizumab [139], with the last two showing striking efficacy over Ustekinumab [140, 141].

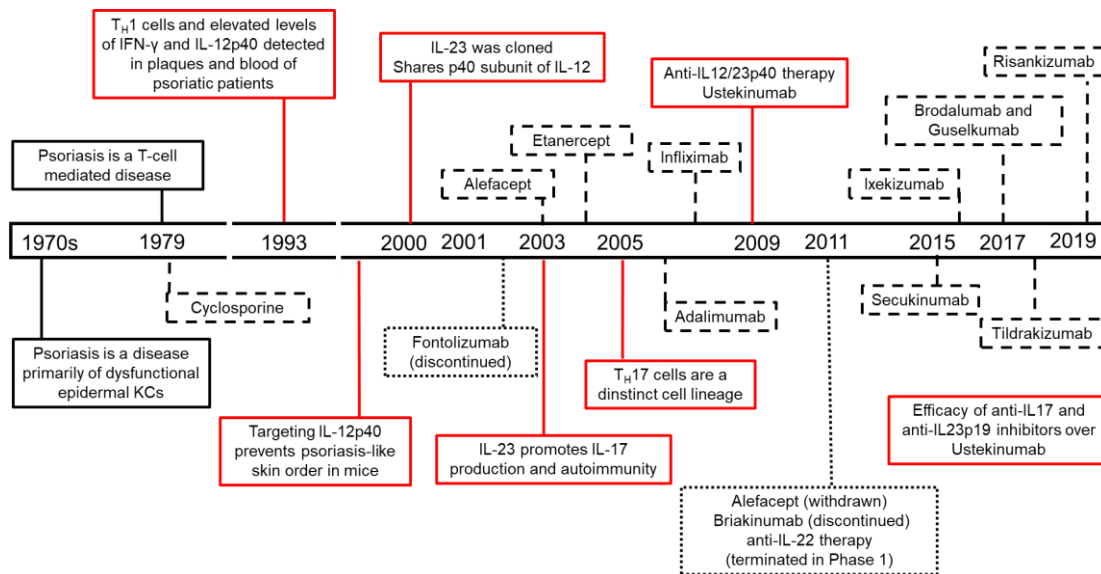


Figure 4: Discovery of the immune pathway in psoriasis and development of therapeutic approaches. (adapted and modified from *Gaffen SL. et al., 2014* [142])

3.5 Excess dietary salt intake – A risk factor for psoriasis?

Over the last decades, epidemiological data revealed a worldwide increase in the incidence of autoimmune diseases, including multiple sclerosis (**MS**), inflammatory bowel diseases (**IBD**), type 1 diabetes and psoriasis. Currently, an interplay of genetic, hormonal and environmental factors are discussed to contribute to the development of autoimmune diseases [143]. As the rising incidence can be observed in westernized societies, which underwent similar changes in lifestyle and food consumption, such dynamics in dietary patterns have received considerable attention with respect to their potential link to autoimmunity [144]. Particularly in IBD, dietary elements are already postulated as factors influencing the disease development, as fruit and vegetables seem to be protective, while red meat and saturated fatty acids have a negative effect [145]. Of note, fast and processed foods, which are characteristic for the “western diet” and which are frequently consumed, contain not only saturated fatty acids and refined sugar but also high amounts of salt [146]. The World Health Organization (**WHO**) recommends adults to consume not more than 5 g of salt per day (WHO, 2016 [147]). In fact, in some countries the daily consumption of salt is usually much higher as processed foods contain about 100 times more salt than comparable homemade meals [146].

The dynamic sodium homeostasis is critical for many biological processes in the body. It is involved in the maintenance of osmotic pressure and a normal pH, required for optimal nerve and muscle functioning. Furthermore, it is important for the distribution of body fluids and metabolic processes and plays a role in anti-microbial defence [148].

Under normal conditions, the extracellular fluid volume and Na^+ homeostasis are constantly regulated by the circulating volume and by osmotical active Na^+ excretion through the kidneys. This traditional view has been challenged as studies in healthy humans consuming larger amounts of salt for a period of time revealed that large amounts of Na^+ are able to accumulate in parts of the body without significant changes in body water content, [149, 150] presenting the interstitium as a third compartment, which is vital for electrolyte homeostasis and body fluid dynamics as well as blood pressure regulation [151]. These extra-renal regulatory mechanisms allow the presence of different osmolarities in different compartments of the body which are dynamic and can be actively induced [152]. Subsequent animal experiments in rats on high-salt diet supported this finding as Na^+ was not only present in the extracellular fluid where it exerts osmotic effects, but was highly accumulating in the skin without being osmotical active [153].

At present, two different ways are reported, how osmotical inactive Na^+ can be stored in the interstitium. One mechanism postulates an extracellular storage in the interstitial space, composed of a collagen-rich extracellular matrix and a gel phase of glycosaminoglycans (**GAGs**) with strong negative charge surrounded by a salt solution consisting of plasma proteins and electrolytes. Work of the Titze group showed that a high salt diet in rats increased the content and charge density of GAGs in the interstitium of the skin and cartilage [154]. Based on this dynamically regulated shift in the composition of GAGs, Na^+ can be released or captured and stored in an osmotic inactive form [155]. Another possibility is an intracellular storage of Na^+ (e.g. cell-rich muscle tissue) in exchange for another positive charged intracellular osmolyte (e.g. K^+) in occurrence of excess Na^+ [156]. Concerning the situation in the skin, keratinocytes may especially contribute to the generation of an osmotic gradient due to their ability to actively transport sodium via epithelial sodium channels (e.g. ENaCs) [157].

Under physiological conditions an immediate remarkable increase of the local sodium concentration can be observed in the skin of patients and mice with bacterial skin infection creating a hypertonic microenvironment. $\text{M}\Phi$ residing in this environment become activated and support immune-mediated host defence to ward off the infection [148]. Moreover, Na^+ accumulation in the skin is associated with increased release of nitric oxide (**NO**) and vascular endothelial growth factor C (**VEGF-C**) by activated $\text{M}\Phi$

that, together with lymphatics, act as systemic regulators of body fluid volume and blood pressure [158, 159]. Oppositely, constant intake of excess dietary salt (>5g/day), associated with increased storage of osmotic inactive Na⁺, can be a potential risk factor for the development of salt-sensitive hypertension and cardiovascular diseases [151, 160].

Murine bone-marrow-derived macrophages (**BMDM**) as well as human monocyte-derived macrophages cultured *in vitro* under high salt conditions showed a shift in their polarization pattern, promoting a pro-inflammatory M1-type (e.g. iNOS, IL-6, IL-8, TNF- α) while suppressing an anti-inflammatory M2-type (e.g. CD206, Fizz-1, Ym-1, Arg-1) [161, 162].

Recently, different groups revealed that naive $\alpha\beta$ T cells exposed to high-salt conditions polarize into a pro-inflammatory type 17 phenotype, characterized by enhanced production of IL-17, TNF α , GM-CSF and expression of the IL-23R [163, 164]. The same conditions promote the differentiation of follicular helper T cells (**Tfh**), which play a critical role in promoting autoimmunity by helping B cells [165]. Independently, FoxP3⁺ regulatory T cells seem to be affected as well, as increased salt concentrations reduce their suppressive capacity both in mice and humans [166].

The local inflammatory type 17 effector response is usually limited in time and space in its function as part of the bodies' barrier protection. However, in case of regular high salt diet consumption, the system is flooded with sodium from the outside, which can lead to a permanent dysregulation of sodium concentrations in sodium reservoir tissues and thus cause ongoing type 17 over-responsiveness. This altered immune response, especially in combination with an impaired Treg function, leads to more severe phenotypes in many experimental models of autoimmune diseases, like EAE [163], lupus nephritis [167], and colitis [168]. There are some slight hints from human patient studies indicating that a high salt intake might be associated with the development of immune-mediated diseases, such as MS [169] and rheumatoid arthritis [170].

4. Aims of the study

As all available data to date point towards the IL-23/17A effector axis to be the dominant pathway in psoriasis pathogenesis, it was hypothesized that the curative effect of anti-p40 therapy is due to the inhibition of the IL-23 and not IL-12 signaling pathway. Thus, one objective of this thesis was to analyze the impact of parallel inhibition of type 1 and type 17 immunity by anti-p40 blocking antibodies in a murine model of psoriatic plaque formation.

The intake of high amounts of salt in the “western diet” is currently discussed as a potential lifestyle factor for the development of autoimmune diseases. Thus, in the second part of this thesis, the impact of excessive salt intake on the skin-resident immune system and development of skin inflammation in IMQ-treated wildtype mice was analysed. Special focus was put on $\gamma\delta$ T cells, as they act as sentinels of external triggers and tissue stress and might be the most affected cell population during local changes in sodium concentration.

5. Materials

5.1 Chemicals and enzymes

Chemicals/enzymes	manufacturer
PBS, sterile	Invitrogen, Carlsbad, USA
RPMI-1640	Invitrogen
4-(2-hydroxyethyl)-1-piperazineethanesulfonic acid (HEPES)	Invitrogen
Non-essential amino acids (NEAA)	Invitrogen
Pen/Strep	Invitrogen
Glutamine	Invitrogen
sodium pyruvate	Invitrogen
β -mercaptoethanol (β -ME)	Sigma Aldrich, St. Louis, USA
Penicillin	Invitrogen
Streptomycin	Invitrogen
Ethylenediamine tetraacetic acid (EDTA)	Sigma-Aldrich
Phorbol 12-myristate 13-acetate (PMA)	AppliChem, Darmstadt, Germany
Ionomycin	Thermo Scientific, Carlsbad, USA
GolgiPlug	BD, Franklin Lakes, USA
Fetal calf serum (FCS)	PAA Laboratories, Pasching, Austria
Collagenase Type IV	Sigma-Aldrich
DNase I	Sigma-Aldrich
Tris	AppliChem
Potassium chloride (KCl)	Merck Millipore, Darmstadt, Germany
Ammonium chloride (NH_4Cl)	Sigma-Aldrich
Potassium hydrogen carbonate (KHCO_3)	Merck
Nonidet TM P 40 Substitute (NP-40)	Sigma-Aldrich
TWEEN [®] 20	Sigma-Aldrich
RNase Zap [®] Decontamination solution	Sigma-Aldrich

Table 1: Chemicals, substances and solutions

5.2 Buffers and cell culture media composition

RPMI 1640 Complete

RPMI1640, 10% FCS, 1% glutamine, 1% PenStrep, 0.1 mM NEAA, 1 mM sodium pyruvate, 50 μ M β -ME

Cell culture medium for 17D1 hybridoma cell line

RPMI 1640, 10% FCS, 10 mM HEPES, 1% penicillin, 1% streptomycin, 1% glutamine, 1 mM sodium pyruvate, 0.1 mM non-essential amino acids

Stimulation medium

RPMI 1640, 500 ng/ml ionomycin, 50 ng/ml PMA, 1 μ l/ml GolgiPlug

Digestion medium for murine skin

RPMI 1640, 1 mg/ml collagenase type IV, 25 mM HEPES, 0.1 mg/ml DNase I.

Red blood lysis buffer

1.5 M NH_4Cl , 10 mM KHCO_3 , 10 mM Na_2EDTA , ddH₂O, pH 7,4

Tail lysis buffer

10 mM Tris/HCl (pH 8.0), 50 mM KCl, 0.5 % NP40, 0.5% Tween, deionized water

TAE buffer (50x)

2 M Tris, 50 mM EDTA, ddH₂O, pH 8.5

FACS buffer

PBS (sterile), 2 % FCS

5.3 Material for animal experiments

material	type	manufacturer
Isoflurane		Baxter, Unterschleißheim, Germany
Aldara cream	5% Imiquimod	3M Pharmaceuticals, Maplewood, USA
Depilation cream	Veet Hair Removal Cream	Reckitt Benckiser, Heidelberg, Germany
TEWL meter	Aquaflux AF200	Biox System Ltd., London, UK
Razor	Contura	Wella, Darmstadt, Germany
Caliper	C1X078	Kroeplin, Schluechtern, Germany
Sodium chloride	NaCl	Sigma-Aldrich
High salt diet	4% NaCl	SSNIFF, Soest, Germany
minimal salt diet	0.03% NaCl	SSNIFF
hematology analyzer	scil Vet abc	scil animal care company, Viernheim, Germany

Table 2: Material and equipment for animal experiments

specifity	clone	concentration	manufacturer
IL-12Fc		200 ng	<i>Vom Berg J. et al. 2013 [171]</i>
anti-IL12p75	R2-9A5	200 µg	BioXcell, West Lebanon, USA
isotype control	LTF-2	200 µg	BioXcell
anti-IL-17A	17F3	200 µg	BioXcell
isotype control	MOPC-21	200 µg	BioXcell

Table 3: Blocking antibodies and cytokines for *in vivo* experiments

5.4 Antibodies for flow cytometry

Marker	clone	dilution	manufacturer
CD45	30-F11	1:800	BD
Ly6G	1A8	1:300	BD
CD3	17A2	1:100	eBioscience, San Diego, USA
$\gamma\delta$ TCR	GL3	1:400	eBioscience
CD11b	M1/70	1:400	BioLegend, San Diego, USA
V γ 4 TCR	UC3-10A6	1:400	BioLegend
V γ 5 TCR	536	1:400	BioLegend
CD27	LG.3A10	1:300	BioLegend
CD44	IM7	1:100	BioLegend
IL-17A	TC11-18H10	1:200	BioLegend
anti-rat IgM		1:200	Jackson ImmunoResearch, West Grove, USA
aCD16/CD32	2.4G2		eBioscience
17D1			Robert R. Tigelaar

Table 4: Antibodies for FACS analysis and sorting of $\gamma\delta$ T cells subsets

5.5 Material for histology of murine skin and histochemistry of human skin biopsies

Material	manufacturer
Ethanol absolute	Merck
Paraformaldehyde (PFA)	Merck
Paraffin	Thermo Scientific
Hematoxylin	Labor+Technik, Salzburg, Austria
Eosin Y, alcoholic	Labor+Technik
Xylene	AppliChem
Entellan®	Merck
5 mM Citrate buffer (pH 6)	Dako, Hamburg, Germany
Dako Envision+Dual Link System-HRP (DAB+)	Dako

Table 5: Buffers and solutions for histology/histochemistry

specificity	concentration	manufacturer
Polyclonal rabbit anti-human IL-12R β 2 antibody	0.7 μ g ml ⁻¹	Novus Biological, Littleton, USA
Total rabbit IgG	0.7 μ g ml ⁻¹	Sigma Aldrich

Table 6: Antibodies for histochemistry of human skin biopsies

5.6 General Material and equipment

Kit	manufacturer
Zombie NIR™ Fixable Viability Kit	BioLegend
Cytofix/Cytoperm™ Plus Kit	BD
RNeasy Mini Kit	Qiagen, Valencia, USA
RNeasy Plus Micro Kit	Qiagen
RNase-Free DNase Set	Qiagen
Pure Link RNA Micro Kit	Thermo Scientific
RevertAid H Minus First strand cDNA Synthesis Kit	Fermentas, Waltham, USA
LightCycler® FastStart DNA Master ^{PLUS} SYBR Green I	Roche, Basel, Switzerland
Mouse Lipocalin-2/NGAL-DuoSet ELISA	R&D Systems, Wiesbaden, Germany

Table 7: Commercial kits

consumable	type	manufacturer
6-well dish	cell culture	Greiner bio-one, Kremsmuenster, Austria
96 well plate	Nunc™ delta surface round-bottom	Thermo Scientific
96 well plate	Nunc™ delta surface MaxiSorp	Thermo Scientific
384 multiwell plates	LightCycler®480	Roche
Sealing foil	LightCycler®480	Roche
Cell strainer	70 µm	Greiner bio-one
Serological pipette	5 ml, 10 ml, 25 ml	Sarstedt, Nuembrecht, Germany
Syringes	Omnifix®(1, 5, 10, 20 ml)	Braun, Melsungen, Germany
Canula	Sterican 18-26G	Braun
Pipette tips	10 µl, 200 µl, 300 µl, 1000 µl	Sarstedt
Slides	SuperFrost Plus	Thermo Scientific
Coverslip	24x60 mm	Thermo Scientific
Reaction tubes	1,5 ml, 2 ml	Sarstedt
Tubes	15 ml, 50 ml	Sarstedt
PCR tubes		Eppendorf, Hamburg, Germany
FACS tube	with cell strainer snap cap	Thermo Scientific
FACS tube	Microtube	Greiner bio-one
Microvette	500 Z-Gel	Sarstedt
Surgical scalpel	disposable	Braun

Table 8: Consumables

Equipment	type	manufacturer
Agarose gel chamber	PerfectBlue	Peqlab, Erlangen, Germany
Power supply	Peqpower	Peqlab
PCR cycler	Nexus Gradient	Eppendorf
UV light image system		Intas, Goettingem, Germany
Homogenizer	TissueLyser LT	Qiagen
Microvolume spectral photometer	NanoDrop™ 1000	Peqlab
Real-Time PCR System	LightCycler® 480 System	Roche
Flow Cytometer	FACS Aria III	BD
Flow Cytometer	FACS LSR II Fortessa	BD
Flow cytometer for cell counting	Accuri™ C6	BD
Microplate washer	Hydrospeed	Tecan, Maennedorf, Switzerland
Photometer	ELISA Reader	BioTek, Winooski, USA
Pipettes	pePETTE	Peqlab
Pipettor	accu-jet pro	Brand GMBH + CO KG, Wertheim, Germany
Embedding machine	EG 1150C	Leica, Wetzlar, Germany
Microm	HM340 E	Thermo Scientific
Light microscope	Olympus BX41	Olympus, Hamburg, Germany
Camera	Olympus Color View III	Olympus
CO ₂ incubator	Galaxy 170 S	Eppendorf
Shaking incubator	Innova® 42	New Brunswick, Edison, USA
Centrifuge	5427R	Eppendorf
Centrifuge	5810R	Eppendorf
Fridge (4 °C)	MediLine	Liebherr, Bulle, Switzerland
Freezer (-20 °C)	Premium Nofrost	Liebherr
Freezer (-80 °C)	V570 HEF	New Brunswick
microwave	M935	Samsung, Seoul, Südkorea
Vortex	Vortex genie	Scientific industries, Bohemia, USA
Scale	PB303-S Delta range	Mettler ToLeDo, Columbus, USA
Scale	Scaltec SBC 31	Mettler Toledo
Water purification system	MilliQ1, EASYpure UV	Merck

Table 9: Laboratory equipment

software	software publisher
BD FACS Diva	BD
FlowJo V10	Tree Star, Ashland, USA
Olympus Cell B image acquisition software	Olympus
Gen5 2.00	BioTek
GraphPad Prism 7	GraphPad software Inc., La Jolla, USA
Nanodrop® 100 V 3.7.0	Peqlab
EndNote X8.2	Clarivate Analytics, Philadelphia, USA

Table 10: Software

5.7 Material and primers for genotyping of mice

Chemical/substance	manufacturer
EconoTaq® Plus Green	Lucigen, Middleton, USA
Proteinase K	Thermo Scientific
Agarose, wide range	SERVA Heidelberg, Germany
DNA Stain Clear G	SERVA
DNA ladder gene ruler mix	Thermo Scientific

Table 11: Material for genotyping of mice

Primer		Sequence 5`-3`
Vd1 ^{-/-} – P1	Vd1-del	CTA CTG TGG GTC AGA TA TCC AC
Vd1 ^{-/-} – P2	Vd1-1520	AGA CAA CAT CTC TGC TCA GTC
Vd1 ^{-/-} – P3	Vd1-10	AAG AGC TAG CTG GCA CTC AC
IL12rb2 ^{-/-} wt – P1	oIMR0799	GTG TG CAA GCT TGG CAC TGT GAC CGT CCA G
IL12rb2 ^{-/-} wt – P2	oIMR0800	GTT TAG CTT GCA GAC AAA CAA GGT CAT ACC
IL12rb2 ^{-/-} mut – P3	oIMR0204	CAC GGG TAG CCA ACG CTA TGT C
IL12rb2 ^{-/-} mut – P4	oIMR0221	GCC CTG AAT GAA CTG CAG GAC G
12b ^{-/-} wt – P1	oIMR0457	AGT GAA CCT CAC CTG TGA CAC G
12b ^{-/-} wt – P2	oIMR0458	TCT TTG CAC CAG CCA TGA GC
12b ^{-/-} mut – P3	oIMR6916	CTT GGG TGG AGA GGC TAT TC
12b ^{-/-} mut – P4	oIMR6917	AGG TGA GAT GAC AGG AGA TC
IL23p19 ^{-/-} – P1	BBO 0230	GGA CTA CAG AGT TAG ACT CAG
IL23p19 ^{-/-} – P2	BBO 0231	GTC ACA ACC ATC TTC ACA CTG
IL23p19 ^{-/-} – P3	BBO 0232	GAA ACG CCG AGT TAA CGC CAT
TCRd mut – P1	oIMR6916	CTT GGG TGG AGA GGC TAT TC
TCRd mut – P2	oIMR6917	AGG TGA GAT GAC AGG AGA TC
TCRd wt – P3	oIMR8744	CAA ATG TTG CTT GTC TGG TG
TCRd wt – P4	oIMR8745	GTC AGT CGA GTG CAC AGT TT

Table 12: Primers for genotyping of transgenic mice

5.8 Primers for qPCR

Primer	Sequence 5`-3`	manufacturer
Il12rb2	Forward: TGT GGG GTG GAG ATC TCA GT Reverse: TCT CCT TCC TGG ACA CAT GA	Metabion
Vg6	Forward: GAT CCA AGA GGA AAG GAA AGA CGG C Reverse: AAG GAG ACA AAG GTA GGT CCC AGC	Metabion
Cxcl9	Forward: ATT TCA TCA CGC CCT TGA GCC T Reverse: AGC CAG ACA GCT GTT GTG CAT T	Metabion
Ccl20	Forward: AAC TGGGTG AAA AGG GCT GT Reverse: GTC CAA TTC CAT CCC AAA AA	Metabion
Tnfa	Forward: CTG TAG CCC ACG TCG TAG C Reverse: TTG AGA TCC ATG CCG TTG	Metabion
Il17a	Forward: ATC AGG ACG CGC AAA CAT GA Reverse: TTG GAC ACG CTG AGC TTT GA	Metabion
Il17f	Forward: TGC TAC TGT TGA TGT TGG GAC Reverse: AAT GCC CTG GTT TTG GTT GAA	Metabion
cfs3	Forward: CAG GCT CTA TCG GGT ATT T Reverse: GGA AGG CAG AAG TGA AGG	Metabion
Il22	Forward: ATG AGT TTT TCC CTT ATG GGG AC Reverse: GCT GGA AGT TGG ACA CCT CAA	Metabion
Il1b	Forward: GAA ATG CCA CCT TTT GAC AGT G Reverse: TGG ATG CTC TCA TCA GGA CAG	Metabion
Ifng	Forward: GCA TTC ATG AGT ATT GCC AAG Reverse: GGT GGA CCA CTC GGA TGA	Metabion
Defb1	Forward: AGG TGT TGG CAT TCT CAC AAG Reverse: GCT TAT CTG GTT TAC AGG TTC CC	Metabion
Defb2	Forward: TAT GCT GCC TCC TTT TCT CA Reverse: GAC TTC CAT GTG CTT CCT TC	Metabion
Defb3	Forward: GTC TCC ACC TGC AGC TTT TAG Reverse: AGG AAA GGA ACT CCA CAA CTG C	Metabion
Defb4	Forward: ACA ATT GCC AAT CTG TCG AA Reverse: GCA GCC TTT ACC CAA ATT ATC	Metabion
S100a8	Forward: TCA AGA CAT CGT TTG AAA GGA AAT C Reverse: GGT AGA CAT CAA TGA GGT TGC TC	Metabion
S100a9	Forward: AAA GGC TGT GGG AAG TAA TTA AGA G Reverse: GCC ATT GAG TAA GCC ATT CCC	Metabion
Reg3b	Forward: CTC TCC TGC CTG ATG CTC TT Reverse: GTA GGA GCC ATA AGC CTG GG	Metabion
IL23a	Forward: AGG CTC CCC TTT GAA GAT GT Reverse: TTG TGA CCC ACA AGG ACT CA	Metabion
IL-23r	Forward: GCT CGG ATT TGG TAT AAA GG Reverse: ACT TGG TAT CTA TGT AGG TAG G	Metabion
Sgk1	Forward: GGC TAT CTG CAC TCC CTA AAC A Reverse: CCA AAG TCA GTG AGG ACG ATG T	Metabion
Foxo1	Forward: ACA TTT CGT CCT CGA ACC AGC TCA Reverse: ATT TCA GAC AGA CTG GGC AGC GTA	Metabion

Nfat5	Forward: TCA GAC TAC CTC AAC CGT TC Reverse: TTC AGG ACC AGG ATC TCT TG	Metabion
Slc5a3	Forward: ATG GTT GTC ATC AGC ATA GCA TGG Reverse: GGT GGT GTG AGA AGA CTA ACA ATC	Metabion
Akr1b1	Forward: TGA GCT GTG CCA AAC ACA AG Reverse: GGA AGA AAC ACC TTG GCT AC	Metabion
Hspa1b	Forward: CTT CTA CAC ATC CAT CAC GC Reverse: TTG AAG AAG TCC TGC AGC AG	Metabion
Ptgs2	Forward: TCT CCA ACC TCT CCT ACT AC Reverse: ACT CTC TCC GTA GAA GAA CC	Metabion
Bgt1	Forward: CTG GGA GAG ACG GGT TTT GGG TAT TAC ATC Reverse: GGA CCC CAG GTC GTG GAT	Metabion
Smit	Forward: GGA GAG ATG GCT CAT TGG TT Reverse: TTA TCA ACT GCC ATG TGG GT	Metabion
Prss8	Forward: TGC TCC TTC TCG GAT TGC TC Reverse: AAA CAT GGT TGC CAT CGT AGG	Metabion
Scnn1a	Forward: GCT CAA CCT TGA CCT AGA CCT Reverse: GGT GGA ACT CGA TCA GTG CC	Metabion
Scn7a	Forward: AAG GGC CTT GTC CCA TTT ACA Reverse: GGG AGG GTT CCA TAG GGA ATT G	Metabion
Arg1	Forward: CTC CAA GCC AAA GTC CTT AGA G Reverse: AGG AGC TGT CAT TAG GGA CAT C	Metabion
Nos2	Forward: TCA TGA CAT CGA CCA GAA GC Reverse: GGA CAT CAA AGG TCT CAC AG	Metabion
Vegf-c	Forward: GCA ATG CAT GAA CAC CAG CA Reverse: AGT TTA GAC ATG CAC CGG CA	Metabion
Gapdh	Forward: CGT CCC GTA GAC AAA ATG GT Reverse: TTG ATG GCA ACA ATC TCC AC	Metabion
Polr2a	Forward: CTG GTC CTT CGA ATC CGC ATC Reverse: GCT CGA TAC CCT GCA GGG TCA	Metabion
Lcn2	Primer Set VMPS-3457	Biomol

Table 13: Primers for qPCR

6. Methods

6.1 Animal procedures

6.1.1 Laboratory animals

The following mouse strains were used for *in vivo* experiments and/or cell isolations. C57BL/6 mice were purchased from Charles River laboratories (Sulzfeld, Germany). The knock-out mice *I112rb2^{-/-}*, *I112a^{-/-}*, *Ifng^{-/-}* and *I123a^{-/-}* were purchased from Jackson Laboratory (Bar Harbor, ME, USA) and Regeneron (Tarrytown, NY, USA), respectively. *I112b^{-/-}* mice were either purchased from Jackson Laboratory or provided by E. von Stebut and K. Schwonberg (Mainz, Germany). *Vd1^{-/-}* animals were provided by K. Kishihara (Nagasaki, Japan). *Vd1^{-/-} I112rb2^{-/-}* were generated by crossing *I112rb2^{-/-}* and *Vd1^{-/-}* mice. For all experiments female mice were used. After purchasing the animals they were bred in-house at the animal facility of the University of Zurich or at the institute of comparative medicine of the Helmholtz Centre Munich, under specific pathogen-free (SPF) conditions in individual ventilated cages (VentiRack; Biozone, Margate/UK). Mice were kept in a controlled environment under 12/12 hour light/dark cycles and provided with food and water ad libitum.

For the high salt diet experiments mice were kept under alternative housing conditions affecting food and drinking water. Salt diet conditioned mice received a sodium-rich diet containing 4% NaCl (SSNIFF, Soest, Germany) and tap water containing 0.75% NaCl ad libitum (high-salt group, HSD). In some experiments mice received a minimal salt diet containing 0.03% NaCl (SSNIFF, Soest, Germany) with tap water ad libitum (low-salt group, LSD). The control group received normal chow and tap water ad libitum. The salt diet feeding occurred for 4 weeks post weaning. All animal experiments were conducted under federal guidelines for the use and care of laboratory animals and were approved by the responsible veterinary agencies in Switzerland (33/2010 and 68/2013) and Germany (G-13-1-096).

6.1.2 Genotyping of genetically modified mice

Mice were ear-punched at 3 weeks of age for identification and biopsies were taken for genotyping. To extract genomic DNA, biopsies were digested overnight (55 °C) in a mixture of tail lysis buffer and Proteinase K (20 µg/µl). Samples were then inactivated for 15 min at 96 °C and centrifuged (10 min, 13200 rpm). For each PCR-reaction 1 µl of DNA-template (supernatant) was used. The composition of the PCR reactions for genotyping of each knock-out mouse is described in Table 14. The used primers are purchased from Metabion (Martinsried, Germany) and are listed in Table 12. PCR reactions were run in a thermocycler under the specific cycling conditions (Table 15). The PCR products were stained with DNA Stain Clear G and separated by gelelectrophoresis on an agarose gel (2 % (m/v) in TRIS-Acetate-EDTA (TAE) buffer) by electrophoresis at 120 V for 60-90 min. Bands of interest were visualised under UV light image system (Intas, Göttingen, Germany) and evaluated using a DNA ladder gene ruler mix.

PCR reaction components	Gene			
	<i>Vd1</i>	<i>Il12rb2</i>	<i>Il12b</i>	<i>Il23a</i>
H ₂ O, bidistilled	7 µl	7 µl	4,26 µl	5 µl
Go Taq® DNA polymerase	10 µl	10 µl	13,34 µl	17 µl
Primer 1 (P1)	1 µl	1 µl	1,2 µl	1 µl
Primer 2 (P2)	1 µl	1 µl	1,2 µl	1 µl
Primer 3 (P3)	1 µl		1 µl	1 µl
Primer 4 (P4)			1 µl	
DNA	1 µl	1 µl	1 µl	1 µl

Table 14: Composition of PCR reactions for genotyping of transgenic mice

Gene	Step 1 (°C/sec)	Step 2 (°C/sec)	Step 3 (°C/sec)	Step 4 (°C/sec)	Step 5 (°C/sec)	Step 6 (°C/sec)	Product size (bp)
<i>Vd1</i>	95/300	94/30	55/40	72/30	72/300	6/∞	wt 490 ko 430
<i>Il12rb2</i>	95/600	94/30	60/40	72/30	72/600	6/∞	wt 265 ko 500
<i>Il12b</i>	94/90	94/30	67/45	72/60	72/120	6/∞	wt 681 ko 280
<i>Il23a</i>	95/240	95/30	56/45	72/60	72/600	6/∞	wt 500 ko 500

Table 15: Conditions of PCR reactions and product lengths. Abbreviations: wt: wildtype; ko: knockout; ∞: infinite. Note: Step 1: pre-denaturation; Step 2: denaturation; Step 3: annealing; Step 4: elongation; Step 5: final elongation; Step 6: Hold. Steps 2-4 are repeated for 30-35 cycles

6.1.3 Induction of psoriatic plaque formation in mice

To mimic the aspects of human psoriatic plaque formation in an experimental mouse model, Aldara cream containing 5 % Imiquimod (IMQ) (3M Pharmaceuticals, Maplewood, MN, USA) was topically applied to the shaved/depilated back skin and/or the upper side of the ear.

For all experiments 7- to 11-week-old female mice of similar body weight and synchronized hair cycle were used. The back skin of mice was shaved and depilated two days before disease induction according to manufacturer's instructions (Veet; Reckitt Benckiser). Psoriatic plaque formation was induced by a daily dose of 55 mg of Aldara cream on the mouse back for 2 or 5–6 constitutive days translating in a daily dose of 2.75 mg of the active compound. In experiments in which ear skin was used, mice were treated with 7 mg of Aldara cream on each ear for 6–7 constitutive days (daily dose of 0.35 mg) if not otherwise indicated. The used dosis were empirically determined to cause most optimal and reproducible skin inflammation in C57Bl/6 mice. During the treatment period (d-2 - d5) short term anaesthesia with isoflurane was used. To avoid cage effects mice of different experimental groups were housed in the same cage. The order in which individual mice was processed for daily IMQ treatment as well as any other measurements varied each day.

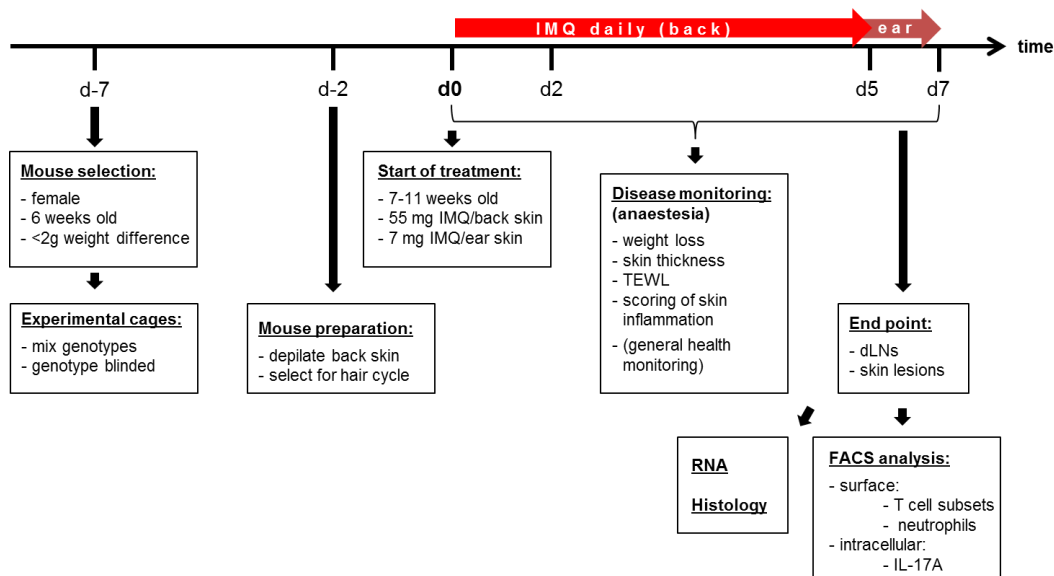


Figure 5: Protocol for the induction of psoriatic plaque formation in mice

6.1.3.1 Scoring severity of skin inflammation

To evaluate the severity of psoriatic plaque formation, mice were scored for clinical parameters of psoriatic disease on the basis of the clinical Psoriasis Area and Severity Index (PASI). Independent scoring on the degree of erythema, scaling, and thickening was performed daily starting on day 0 (baseline; prior to the first IMQ application) on a scale from 0 to 4 (Table 16). The resulting cumulative score (erythema plus scaling plus thickening) served as one measure of disease severity. Additionally, thickness of back or ear skin was measured daily with a digital caliper. Hence, the percent change in skin thickness compared to untreated skin on day 0 was calculated as an indicator for skin inflammation.

Score	Scale of severity
0	healthy, no clinical signs
1	slight
2	moderate
3	marked
4	extreme

Table 16: Psoriasis Area and Severity Index in mice

6.1.3.2 TEWL measurement

Additionally, the mouse skin was examined for transepidermal water loss (TEWL), an important non-invasive, physical parameter in dermatology to assess epithelial integrity and barrier function. Under pathological conditions, the rate of water loss from the skin's surface increases directly in proportion to the level of disease pathology. During the course of IMQ-induced plaque formation the TEWL ($\text{g}/\text{m}^2\cdot\text{h}$) of dorsal or ear skin was monitored by use of an evaporimeter equipped with a closed chamber probe (Aquaflux AF200, Biox System Ltd, London, UK).

6.1.3.3 Histology

For histological analysis, a previously defined part of the murine skin was removed and fixed in 4% paraformaldehyde in PBS for a minimum of 48 hours at room temperature. After 48 hours of fixation, the tissue was moved into 70% ethanol for long term storage. Next, tissue samples were dehydrated through a series of graded ethanol baths to displace the water, and permeated with paraffin. The samples were embedded into paraffin blocks and cut into 4 μm sections using a sliding microtome. Slides were deparaffinized and rehydrated. Subsequently, paraffin slides were put in an oven for at least 1 h at 56 °C and gradually deparaffinized by subsequent immersion in xylene followed by immersion in aqueous alcoholic solutions.

To determine the infiltration of inflammatory cells, mouse skin sections were stained with hematoxylin and eosin according to standard protocols and fixed with Entellan® (Merck, Darmstadt, Germany). To evaluate the grade of inflammation, total counts of abscesses per skin section of 2–3 independent experiments as well as the number of epidermal layers in these sections were independently quantified by two researchers.

6.1.4 Antibody treatment and application of IL-12Fc

For gain-of-function experiments local s.c.-injection of 200 ng of IL-12Fc/PBS (Vom Berg J. et al. 2013) or PBS was performed per each ear in *Il12a*^{-/-} and *Il12rb2*^{-/-} mice. Subcutaneous administration was carried out into the loose skin over the neck between the shoulders every second day starting on day -1. C57Bl/6 mice were i.p. injected with 200 μg of anti-IL12p75 (R2-9A5) or isotype control (LTF-2) antibodies every second day starting on day -1 to mimic the situation in *Il12rb2*^{-/-} mice in loss-of-function experiments. Intraperitoneal injection was performed in the lower right quadrant of the abdomen with a maximum volume of 200 μl per treatment.

The effect of IL-17A neutralization on the development of psoriatic plaque formation in *Il12rb2*^{-/-} mice was determined by i.p.-injection of 200 μg of anti-IL-17A (17F3) or isotype control (MOPC-21) antibodies every second day starting on day -1.

6.1.5 Measurement of dehydration status in mice

To evaluate possible differences in the dehydration status of mice receiving either chow or a high salt diet (**HSD**), hematocrit was measured using the scil Vet abc hematology analyzer (scil animal care company GmbH, Viernheim, Germany). Subsequently, blood from mice was collected at the end of the experiment via puncture of the orbital sinus or plexus from isoflurane anesthetized mice into Microvette® serum tubes (Sarstedt) containing EDTA. 12ul of the collected EDTA blood sample were used for calculating the hematocrit. As reference value, the hematocrit of a 7 week old female C57Bl/6 was taken which is 46.2 % \pm 1.79 (*Mouse phenome database at the Jackson laboratory*).

6.2 Cell biology methods

6.2.1 Leukocyte isolation from mice

To isolate leukocytes from various organs, mice were euthanized with CO₂. According to the organ and the cell population of interest, different isolation procedures were used.

6.2.1.1 Isolation of leukocytes from lymph nodes

The inguinal lymph nodes were removed from mice and mashed with a syringe piston through a 70 μ m nylon cell strainer. Thereafter, cell strainer was washed with PBS to receive a single cell suspension that could readily be used for further analysis.

6.2.1.2 Isolation of leukocytes from murine skin

Back and ear skin were removed from mice and placed in a six-well plate containing RPMI until further preparation was done.

Ears were splitted into halves along the cartilage and the subcutaneous fat was removed from back skin carefully by scraping it off with a scalpel. Skin was transferred into a new six-well plate with a few drops of digestion medium consisting of RPMI 1640 medium supplemented with 1 mg/ml collagenase type IV, 25 mM HEPES and 0.1 mg/ml DNase. The used collagenase was stored at 4 °C as powder and was dissolved freshly each time. The skin was cut into approximately 1 mm x 1 mm sized pieces and 5 mL digestion medium was added. Back and ear skin were

incubated for 50 min (back skin) or 20 min (ear skin) at 37°C slightly shaking. Skin samples were homogenized by pipetting up and down using a syringe with a 20G-needle and were filtered through a 70 µm cell strainer into a 50 ml tube to obtain a single-cell suspension. Cells were centrifuged at 400 g for 5 min at 4 °C. Supernatant was discarded and the pellet was resuspended in FACS buffer for further analysis.

6.3 Molecular biology methods

6.3.1 Flow cytometry

For flow cytometry analyses, single cell suspensions of lymph nodes and skin were collected in FACS buffer. Staining procedures were performed in 96-well round bottom plates. Centrifugation steps were performed at 300 x g for 5 min at 4 °C. For each washing step 200 µl FACS buffer was used. Prior to analysis, the samples were diluted in an appropriate volume of FACS buffer. All flow cytometry data was acquired on a FACS LSRII Fortessa (BD, Franklin Lakes, New Jersey, USA) using the BD FACS Diva Software and were processed with the FlowJo Software. The antibodies used for surface and intracellular staining are listed in Materials [Table 4](#).

6.3.1.1 Cell surface staining for Flow Cytometry

To block non-specific binding of immunoglobulins to Fc receptors, cells were incubated for 10 min at 4°C with 1 µg of rat anti-mouse CD16/CD32 blocking-antibody (eBioscience). After one washing step, 50 µl of mastermix containing fluorochrome-labeled antibodies was added and incubated in the dark for 25 min at 4 °C. Viability of the cells was checked by staining with NIR viability dye.

6.3.1.2 Staining procedure for Vy5/Vδ1⁺ and Vy6/Vδ1⁺ cells

To stain Vy5/Vδ1⁺ and Vy6/Vδ1⁺ cells supernatant of cultured 17D1 hybridoma cell line (anti-mouse Vy5/Vδ1, Vy6/Vδ1 and Vy1/Vδ1; rat IgM) was used, kindly provided by Robert R Tigelaar. 17D1 hybridoma cells were cultured in RPMI 1640 medium supplemented with 10% fetal bovine serum, 10 mM HEPES, penicillin, streptomycin, glutamine, sodium pyruvate and non-essential amino acids. After 3 and 6 days of culture the supernatant was collected, centrifuged, filtered and used for staining.

During the surface staining, cells were pre-stained with rat anti-mouse δTCR antibody, which is a requirement to subsequent staining of Vδ1. After a washing step cells were incubated with 100 µl of 17D1 hybridoma supernatant for 20 min. Next, cells were washed again and stained with a fluorochrome-conjugated secondary antibody against anti-rat IgM for 20 min.

6.3.1.3 Intracellular Staining for Flow Cytometry

For the detection of cytokines an intracellular staining was performed. Briefly, freshly isolated single cell suspensions were stimulated for 2h at 37°C in complete RPMI medium supplemented with 500 ng/ml ionomycin, 50 ng/ml PMA and GolgiPlug (1 µg/ml, BD). After stimulation the cells were harvested and a surface staining was performed as described above. Cells were fixed and permeabilized for 20 min by using the BD Cytfix/Cytoperm™ Plus Kit. After fixation the cells were washed twice with BD Perm/Wash™ buffer (10X concentrate diluted 1:10 in bidistilled water) and intracellular staining was performed for 1h at RT in the dark by adding 50 µl of antibody mix in permeabilization buffer. Cells were washed once with BD Perm/Wash™ buffer and once with FACS buffer.

6.3.2 Cell sorting

Single cell suspensions from back skin of Aldara-treated WT or *Il12rb2*^{-/-} mice were prepared on day 6 post treatment as described in 6.2.1.2. The whole-cell suspension was stained with a mix of fluorescence-labeled antibodies depicted in Materials [Table 4](#). Skin-associated Vy4⁺, Vy6⁺ and Vy5⁺ cells were sorted to at least 96% purity with a BD FACS Aria III (BD, Franklin Lakes, New Jersey, USA) using a 70 µm nozzle.

6.3.3 Enzyme-linked immunosorbent assay (ELISA)

For the measurement of Lipocalin 2 (Lcn2) in mouse serum a solid phase sandwich ELISA was used (mouse Lipocalin-2/NGAL-DuoSet ELISA, R&D Systems). Blood was collected from mice and centrifuged for 7 min at 5000 rpm. The assay was carried out in NUNC-Maxisorp 96-well plates, according to the manufactures instructions. Washing steps were performed three times after every incubation step with washing buffer in an automatic microplate washing system. All standards, samples as well as a positive and a negative control were assayed in duplicate. During incubation, plates were sealed to avoid evaporation.

Plates were coated with 50 µl/well of capture antibody diluted in coating-buffer as recommended by the manufacturer and incubated at 4°C over night. 300 µl blocking buffer was added for 2h at RT. 50 µl of standards, an appropriate dilution of serum samples and controls were added and incubated for 2 hours at RT. Subsequently, 50 µl of appropriate biotinylated detection antibody was added for 2 hours at RT, followed by incubation with 50 µl streptavidin-conjugated horse radish peroxidase for 30 min at RT in the dark. For detection, 50 µl TMB containing substrate buffer was added and incubated in the dark at RT until color development was visible. This process was stopped by adding 25 µl 2 M sulfuric acid.

The quantity of the resulting coloured product was measured by its optical density using a microplate ELISA reader (BioTek, Winooski, Vermont, USA) set to the appropriate wavelength (450 nm) using Gen5 2.00 Software. For the analysis the average of the duplicate readings for each standard, control, and sample were subtracted with the average zero standard optical density (O.D.). A standard curve was created by plotting the mean absorbance for each standard against the concentration drawing a curve (polynomial) through the points on the graph. The best fit line could be determined by regression analysis.

6.3.4 Gene expression analysis

6.3.4.1 RNA extraction

Isolation of total RNA from the back skin of animals was performed with the RNeasy Mini Kit (Quiagen, Valencia, CA, USA), while total RNA from mouse skin-sorted leukocytes was isolated with the Pure Link RNA Micro Kit (Invitrogen, Carlsbad, CA, USA), both according to manufactures instructions. To directly quantify total RNA concentration, 1 μ l of isolated RNA was measured using a NanoDropTM 1000 spectrophotometer (Peqlab, Erlangen, Germany). The samples were stored at -80°C prior to analyses.

6.3.4.2 cDNA-synthesis

In accordance to manufactures instructions, first strand complementary DNA (cDNA) was prepared by reverse transcription using the RevertAid H Minus First Strand cDNA synthesis Kit (Fermentas). A negative control containing every reagent for the reaction except the enzyme was used to assess for genomic DNA contamination of the RNA sample. A no template negative control was performed to assess for reagent contamination.

6.3.4.3 Quantitative real-time PCR (qRT-PCR)

Expression of murine genes was measured by quantitative real-time PCR analysis using the LightCycler[®] 480 System (Roche) and the LightCycler[®] FastStart DNA Master^{PLUS} SYBR Green I kit (Roche) according to manufacturer's instructions. Each reaction was performed in duplicate or triplicate in 284-well plates. Sequences for PCR primers are depicted in [Table 13](#). The expression levels were normalized to the Polr2a or GAPDH house-keeping gene and represented as either $2^{-\Delta C_T}$, ($\Delta C_T = C_T$ gene of interest – C_T house-keeping gene) in the case of *I12rb2* expression or $2^{-\Delta\Delta C_T}$ ($\Delta\Delta C_T = \Delta C_T - \Delta C_{Control}$), for all other transcripts.

6.4 Histochemistry of human skin biopsies

In accordance with the Code of Ethics of the World Medical Association (Declaration of Helsinki) for experiments involving humans (ethical approval number EK647) all donors signed written informed consent forms before punch biopsies from skin were taken. All samples were obtained from the University Hospital Zurich.

Human skin was immersed in 4% formaldehyde, embedded in paraffin, and sliced at a thickness of 5 μm . Deparaffinized human skin sections underwent heat-induced antigen retrieval with 5 mM citrate buffer pH 6. Sections were heated in a microwave (800 watt) 5 times for 3 min each, refilling the cuvettes between each cycle alternatively with bidistilled water or citrate buffer. After blocking and staining with polyclonal rabbit anti-human IL-12Rb2 antibody (0.7 $\mu\text{g/ml}$) or total rabbit IgG (0.7 $\mu\text{g/ml}$) staining was performed following the manufacturer's procedure (Dako Envision+Dual Link System-HRP (DAB+)). Digital images of tissue sections were recorded using an Olympus BX41 light microscope with an Olympus ColorView III camera and Olympus Cell B image acquisition software.

6.5 Data Analysis and Statistics

Analysis of data was performed using GraphPad Prism 7 or Microsoft Excel. Data are presented as mean \pm SEM, if not otherwise indicated. Significance of results were analyzed as outlined in the respective figures by unpaired two-tailed t test, one- or two-way ANOVA with Bonferroni post-test. Statistically significant differences are depicted as * $p < 0.05$, ** $p < 0.01$, *** $p < 0.001$; ns (not significant). Data presented as boxplots visualizes the distribution by minimum and maximum (whiskers), the 25th-75th percentile (box) and median (band).

7. Results

The results are divided into two parts. The first part focuses on the dissection of the distinct contribution of IL-12 and IL-23 to psoriatic plaque formation in mice. The second part deals with the impact of high dietary salt intake on the skin resident immune system and its potential as a lifestyle risk factor for the development of psoriatic plaque formation.

7.1 Divergent roles of IL-12 and IL-23 in psoriatic inflammation

The consequences of targeting IL-12 by anti-p40 therapy in psoriasis were analyzed in mice with genetic deficiency in IL-12 signaling after induction of psoriatic plaque formation by application of IMQ.

7.1.1 Reduced skin inflammation in IL-12/23p40-deficient mice

To confirm the finding of reduced skin inflammation after application of neutralizing anti-IL-12/23p40 monoclonal antibody (**mAb**) in IMQ-treated WT mice [68], psoriatic plaque formation was induced in *Il12b*^{-/-} mice with genetic deficiency in the p40 subunit shared by IL-12 and IL-23. *Il12b*^{-/-} mice showed a strongly reduced development of psoriatic lesions compared to WT mice. Correspondingly, FACS analysis of the skin revealed a significant reduction of critical markers of psoriasiform inflammation, including neutrophil invasion ([Figure 6A](#)) and accumulation of IL-17A-secreting Vγ4⁺ γδT cells in lesional skin ([Figure 6B](#)).

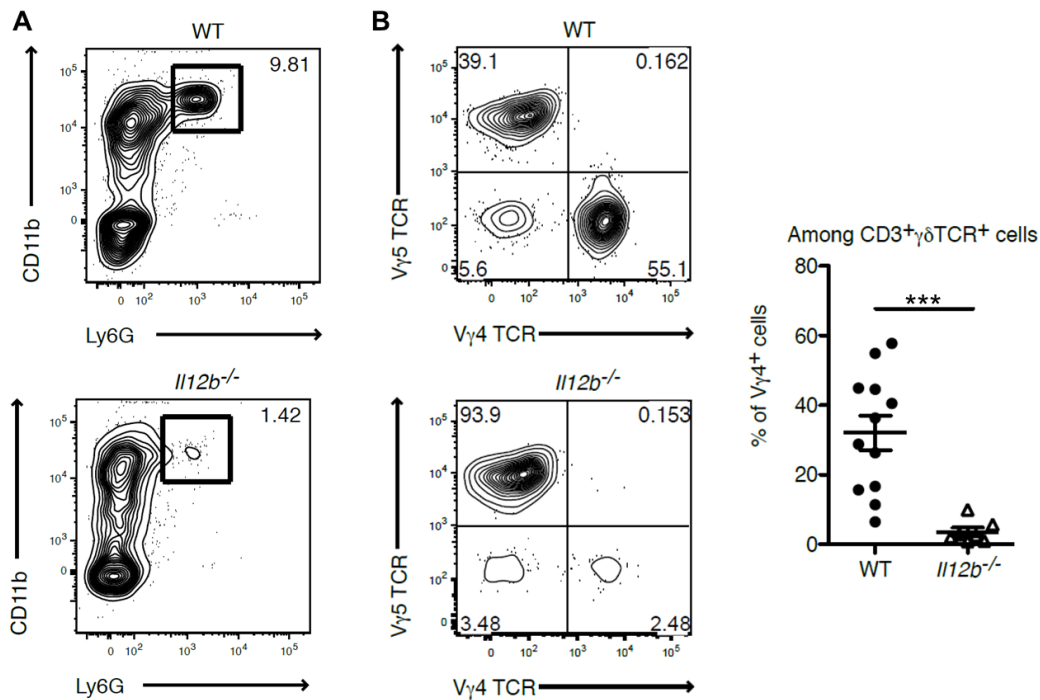


Figure 6: Analysis of inflamed skin of WT and IL-12/23p40 deficient mice. Flow cytometry analysis of inflamed skin; cells were gated on CD45⁺ leukocytes and analyzed for the presence of **(A)** neutrophils and **(B)** skin infiltrating Vγ4⁺ γδT cells. Data are given as mean ± SEM (n=12 WT, n=7 *Il12b*^{-/-}); analysis was done by unpaired two tailed t-test.

7.1.2 Exacerbated clinical phenotype on IL-12-signaling deficiency

Based on the fact that *Ifny* expression levels in psoriatic lesions correlate with disease severity, the clinical course of mice deficient in the IL-12 driven type 1 effector cytokine IFN-γ was evaluated. Confirmative to the notion that type 1 inflammation contributes to lesion formation, deficiency in IFN-γ resulted in a milder disease phenotype, reaching statistical significance to WT mice on day 4 (Figure 7).

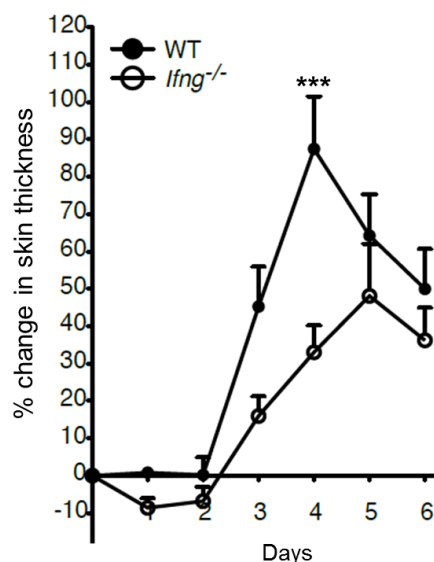


Figure 7: Disease development in WT and *Ifng*^{-/-} mice. Back skin inflammation during the whole disease course represented as a percent change in skin thickness compared to untreated skin on day 0. Data are given as mean \pm SEM (n=5-6 mice per group); analysis was done by two-way ANOVA with Bonferroni post-test.

To clarify the impact of IL-12 signaling on plaque formation signaling on plaque formation the clinical disease course was monitored in mice deficient in IL-12p35 (*Il12a*^{-/-}), in the beta subunit of the IL-12 receptor (*Il12rb2*^{-/-}), as well as in mice deficient in IL-23 (p19, *Il23a*^{-/-}) and compared to WT mice. The percental change of skin thickness during IMQ treatment served as a parameter of skin inflammation.

In WT mice, IMQ treatment of the skin led to an increase in skin thickness typically around day 2 of treatment (disease onset). The inflammation continually increased in severity with peak disease reached at day 4 and 5 of treatment (Figure 8A). *Il12a*^{-/-} mice with unaltered IL-23 signaling developed significantly more severe inflammation of the skin compared to WT mice as illustrated by a more pronounced skin thickening during peak disease on day 4 (Figure 8B, top). Likewise, mice lacking the IL-12-specific receptor subunit (*Il12rb2*^{-/-}) showed the same disease phenotype with an increased change in skin thickness from day 2 onwards and a significantly more pronounced skin thickening during peak disease on day 4 compared to WT mice (Figure 8A and B, bottom). Further evaluation of disease severity was performed on the basis of the clinical Psoriasis Area and Severity Index (PASI), including daily independent scoring of the degree of erythema, scaling and thickening of back skin. *Il12rb2*^{-/-} mice showed significantly higher disease scores ranging from 8 to 9 during disease development compared to WT mice with 6 as a maximum score (Figure 8C). Of note, when skin thickness of mice only deficient in

IL-23 signaling ($Il23a^{-/-}$) was compared to $Il12b^{-/-}$ mice (lacking IL-12 and IL-23), a trend towards a reduced skin inflammation could be observed (Figure 8A).

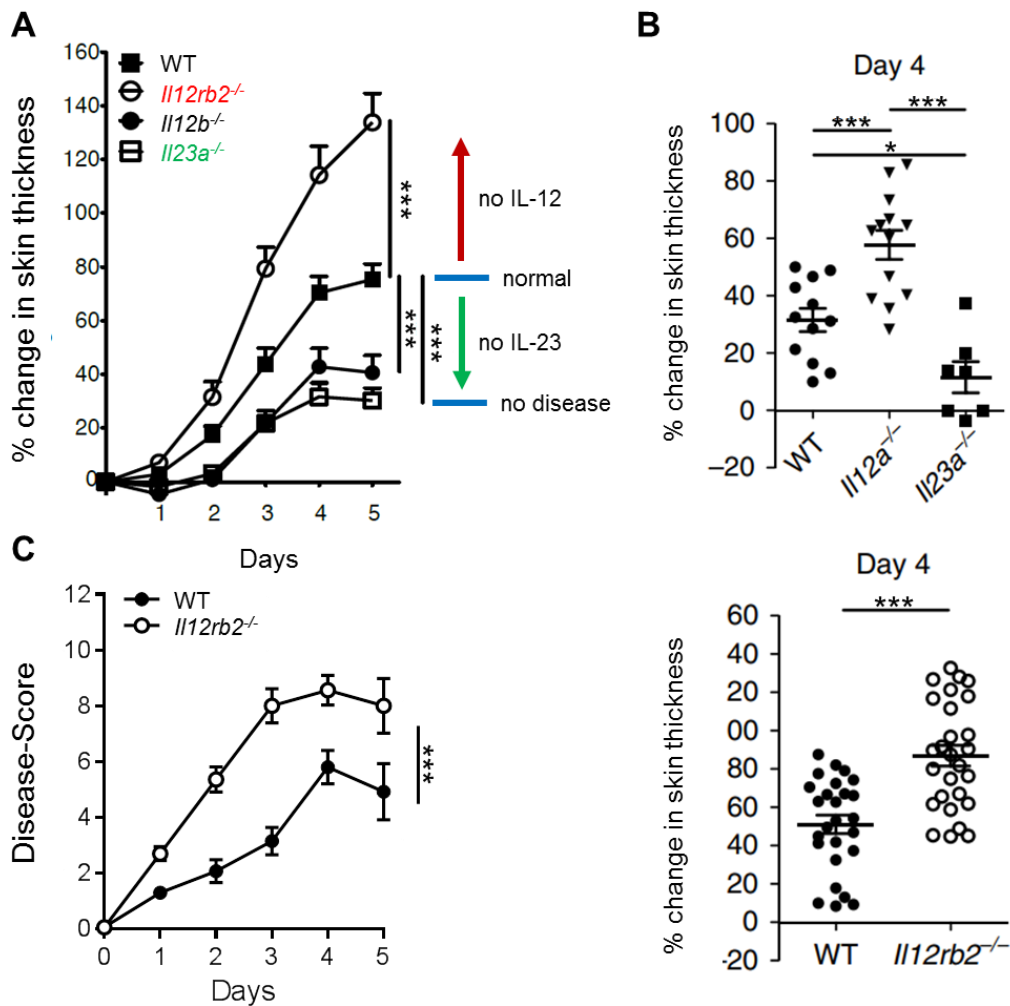


Figure 8: Skin inflammation in IMQ-treated WT, $Il12a^{-/-}$, $Il12b^{-/-}$, $Il23a^{-/-}$ and $Il12rb2^{-/-}$ mice. Back skin inflammation represented as a percent change in skin thickness compared to untreated skin on day 0 (A) during the whole disease course (n=21 WT, n=15 $Il12rb2^{-/-}$, n=16 $Il12b^{-/-}$, n=9 $Il23a^{-/-}$) and (B) during peak disease on day 4 (top: n=7-13; bottom: n=26-27 mice per group). (C) Disease score of WT and $Il12rb2^{-/-}$ mice starting on day 0 (n=15 mice per group). Data are given as means \pm SEM. Analyses were done by (A, C) two-way, (B) one-way ANOVA with Bonferroni post-test.

The phenotype of aggravated skin inflammation in IL-12 signaling-deficient mice already became visible on day 3 of IMQ treatment as signs of erythema and scaling were more pronounced compared to WT mice (Figure 9A). Quantification of the barrier integrity by measuring transepithelial water loss (TEWL) indicated that in absence of IL-12 signaling treatment with IMQ resulted in a more pronounced breach of the epithelial barrier as the water loss through the epidermis significantly increased from day 2 onwards compared to WT mice (Figure 9B).

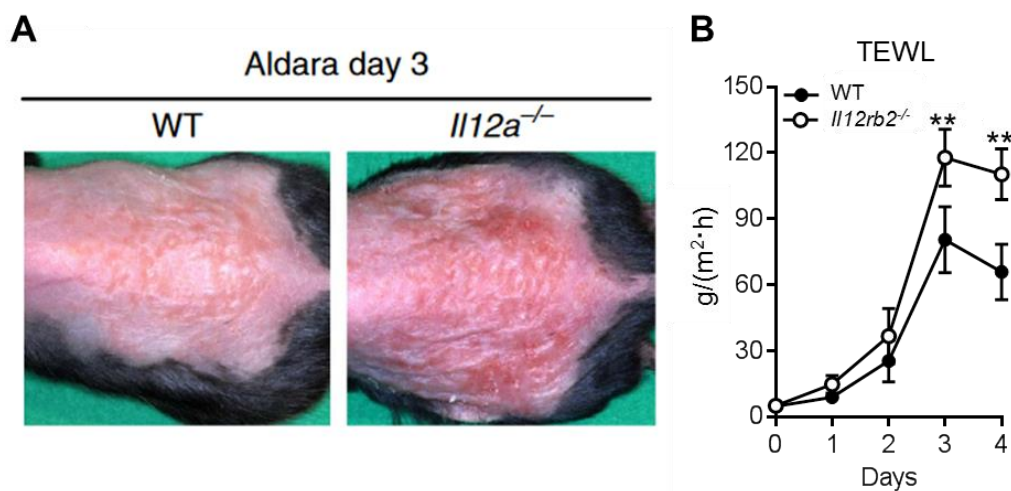


Figure 9: Appearance of skin lesions and TEWL in WT and IL-12-signaling deficient mice. (A) Representative photos taken on day 3 post IMQ treatment. **(B)** TEWL in IMQ-treated back skin. Data are given as mean + SEM (n=9 WT, n=10 *Il12rb2^{-/-}*); analysis was done by two-way ANOVA with Bonferroni post-test.

Going more into detail, histopathologic features of psoriatic plaque formation were also more pronounced when IL-12 was absent. They were represented by a significant increase of the epidermal layers (acanthosis) (Figure 10A and B, top), caused by hyperproliferation of keratinocytes and an altered differentiation of keratinocytes (parakeratosis), indicated by the retention of nuclei in the *stratum corneum* (Figure 10A). To complete the picture of disease aggravation in IL-12-deficient mice, significantly increased frequencies of neutrophilic micro-abscesses per mm in the *stratum corneum* were measured compared to WT mice (Figure 10B, bottom).

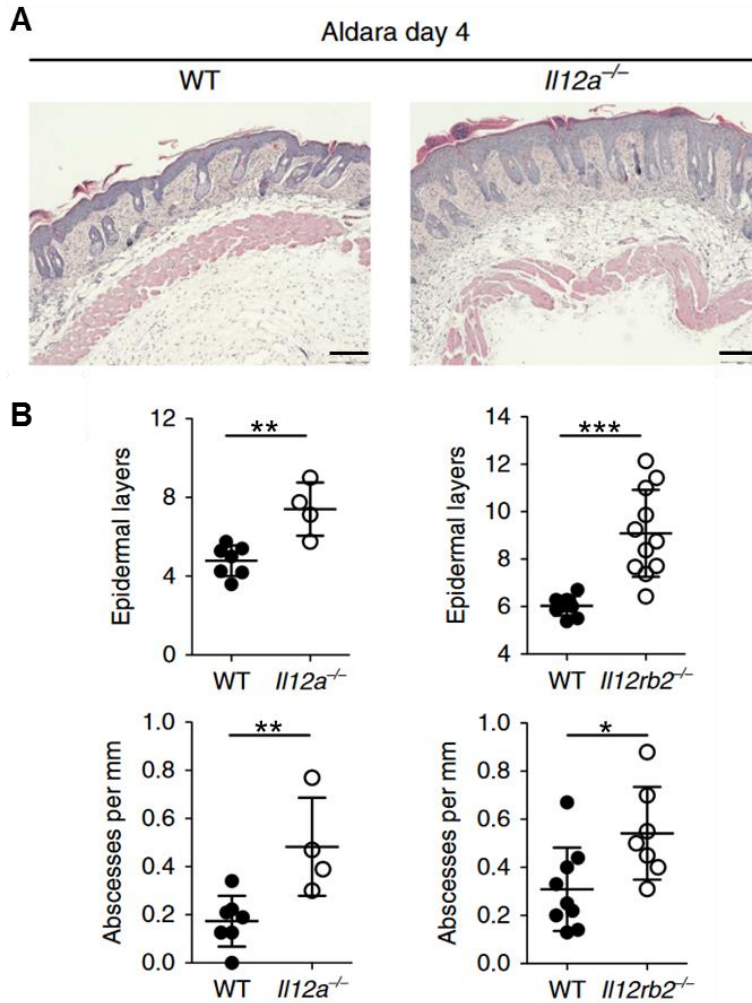


Figure 10: Histopathology of skin lesions of WT and IL-12-signaling deficient mice. (A) Back skin sections on day 4 post treatment were stained with H&E; scale bar 200 μm . (B) quantification of total counts of epidermal layers and skin abscesses ($n=7-9$ WT, $n=4$ *Il12a^{-/-}*, $n=7-11$ *Il12rb2^{-/-}*). Data are given as means \pm SEM; results were analyzed by unpaired two tailed t-test.

In order to find the mechanism behind the aggravated psoriatic response in IL-12 signaling-deficient mice, transcript analyses of lesional skin were performed focussing on hallmark pathogenic pathways in psoriasis.

Looking into the effector cytokine profile in the skin lesions of *Il12rb2^{-/-}* mice, it was striking that particularly IL-17A and IL-17F as well as other effector molecules of the type 17 immune response were drastically increased, pointing towards an increased type 17 bias in the absence of IL-12 (Figure 11A). At the same time, the inflamed skin of *Il12rb2^{-/-}* mice showed a marked decrease of typical type 1 inflammation markers including IFN- γ - and IFN- γ -dependent CXCL9 due to the lack of upstream induction by IL-12 (Figure 11A and C). The increased type 17 response in IL-12-deficient mice strengthened as analyzed effector pathways downstream of IL-17

identified a range of antimicrobial peptides, including β -defensins, S100 proteins and Reg3b to be significantly upregulated (Figure 11B). Noteworthy, lipocalin 2 (*Lcn2*) was significantly enhanced, which corresponded to local neutrophil and epithelial activation in *Il12rb2*^{-/-} lesions and was therefore also an indicator of a type 17 bias (Figure 11B). Furthermore, the ligand of CCR6, CCL20, was found to be significantly increased in lesions of *Il12rb2*^{-/-} mice indicating the involvement of dermato-tropic type 17 effector T cells, like $\gamma\delta$ T17 and T_H17 cells in the exaggerated disease phenotype of IL-12 signaling deficient mice (Figure 11C).

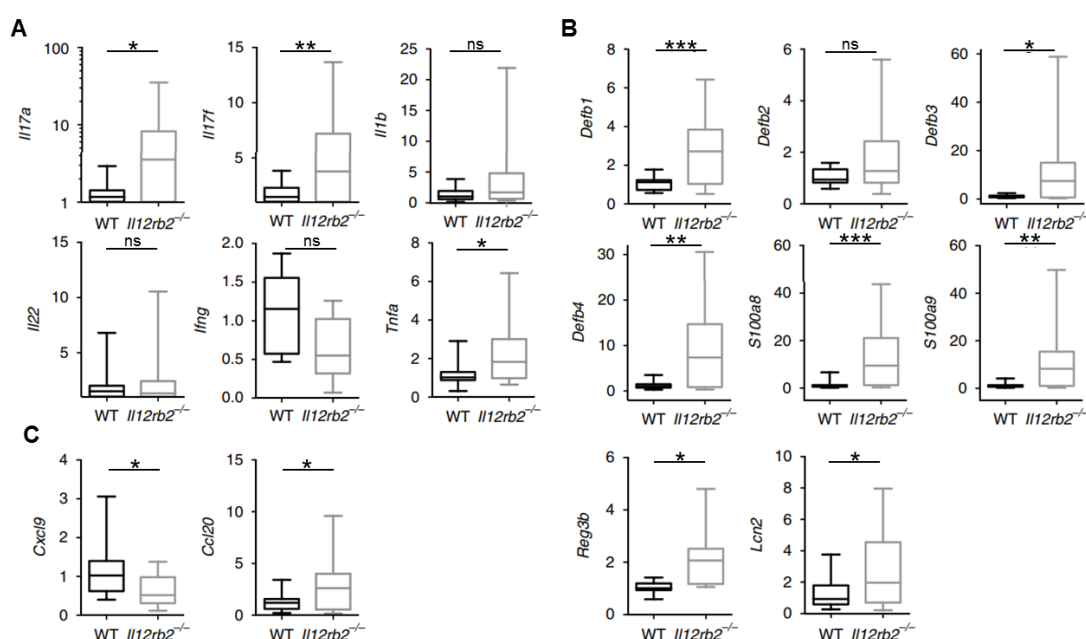


Figure 11: Transcript analysis of lesional skin of WT and *Il12rb2*^{-/-} mice. RT-qPCR analyses of the whole skin on day 5 post treatment represented as fold changes relative to the average WT expression levels (n=10–18 WT and n=10–15 *Il12rb2*^{-/-}). Results were analyzed by unpaired two-tailed t-test.

It has to be noted that IL-12 (p35/p40) shares its p35 subunit with another member of the IL-12 superfamily, IL-35 (p35/EBI3). Although IL-35 has been demonstrated to have predominantly regulatory functions [172], it is possible that this cytokine could play a role in the phenotype observed. Therefore, our collaborators induced psoriatic plaque formation in *Ebi3*^{-/-} mice to clarify the impact of IL-35 in disease development. Deficiency in IL-35 did not phenocopy the exacerbated pathology of IL-12 deficient mice, as they showed unaltered disease development (published in [173]).

7.2 IL-12 controls accumulation and effector functions of $\gamma\delta$ T17 cells in the skin

7.2.1 Characterization of accumulating V γ 6V δ 1⁺ $\gamma\delta$ T17 cells in psoriatic skin

Building up on the characterization of the disease phenotype observed in IL-12 signaling-deficient mice, the next step was to identify the cellular immune mechanism behind this phenotype. In a recent study, Pantelyushin and colleagues showed that IL-17A-producing V γ 4⁺ $\gamma\delta$ T cells are the essential drivers of psoriasiform inflammatory processes in the skin and are therefore a marker for disease severity in the IMQ-model [68]. Since *Il12rb2*^{-/-} mice showed an enhanced disease severity, it was hypothesized that IL-17A-producing V γ 4⁺ $\gamma\delta$ T cells are increased in the lesions of these mice.

Although flow cytometric analysis (gating strategy, [Figure 12A](#)) revealed an increase in total $\gamma\delta$ T cell infiltration in the lesional skin of *Il12rb2*^{-/-} mice, the frequency of the V γ 4⁺ $\gamma\delta$ T cell subset was decreased ([Figure 12B and C](#)). Hence, the observed increase in total $\gamma\delta$ T cell numbers could only be explained by the appearance of another $\gamma\delta$ T cell subpopulation typically unaccounted for the disease context. The emergence of a third distinct $\gamma\delta$ T cell subset even became apparent by looking at the CD3 vs. δ TCR FACS plot. Here, three populations of $\gamma\delta$ T cells could clearly be distinguished in *Il12rb2*^{-/-} mice with one being very low in frequency in WT but drastically elevated in *Il12rb2*^{-/-} mice ([Figure 12B](#)). At the time of observation, no third $\gamma\delta$ T cell subset had been reported to populate the skin. The specific staining for the γ -chains revealed that this $\gamma\delta$ T cell subpopulation neither expressed the V γ 4 chain, which is characteristic for the highly mobile IL-17A-secreting, skin-invading $\gamma\delta$ T cell subset, nor the V γ 5 chain, invariantly expressed by dendritic epidermal $\gamma\delta$ T cells ([Figure 12C](#)).

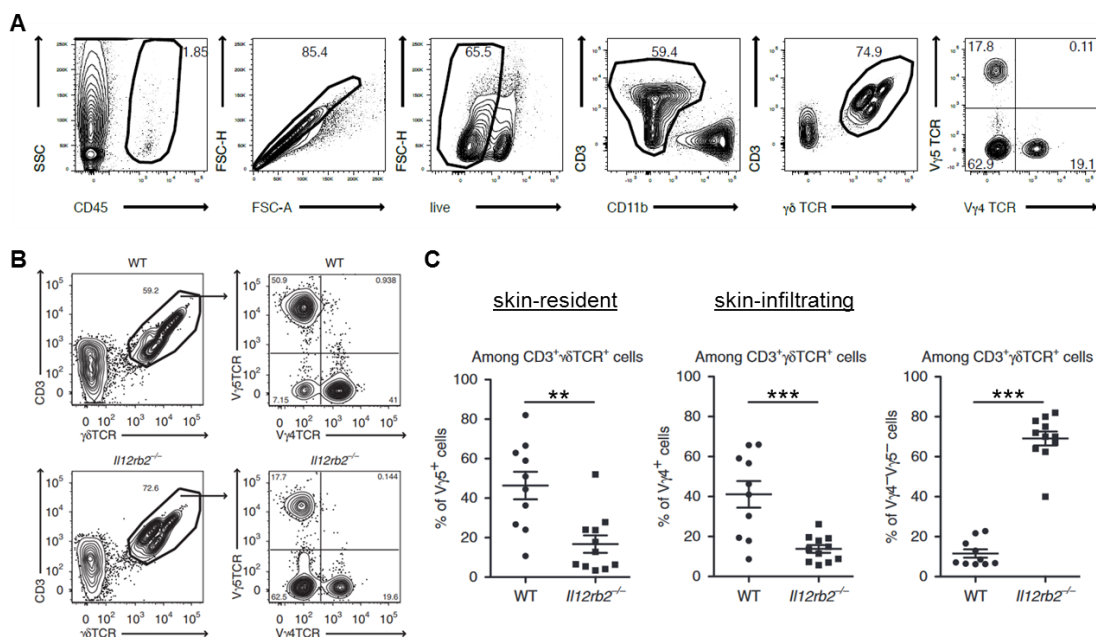


Figure 12: Analysis of $\gamma\delta$ T cell distribution in lesional skin of WT and *Il12rb2*^{-/-} mice. (A) Representative flow cytometry gating strategy for mouse skin. Cells were gated on CD45⁺/singlets⁺/live⁺/CD11b⁻ leukocytes and analyzed for $\gamma\delta$ T cell subsets. (B) Representative plots and (C) flow cytometry analysis of inflamed skin for presence of skin-resident and skin-infiltrating $\gamma\delta$ T cells. Data are given as means \pm SEM (n=10-11 mice per group); results were analyzed by unpaired two-tailed t-test.

To identify the novel $\gamma\delta$ T cell subset, real-time quantitative PCR was performed on V γ 4⁺, V γ 5⁺ and V γ 4⁻V γ 5⁻ $\gamma\delta$ T cells isolated from lesional skin of *Il12rb2*^{-/-} mice (data not shown). The result provided evidence that the V γ 4⁻V γ 5⁻ $\gamma\delta$ T cell population could be invariant V γ 6⁺ $\gamma\delta$ T cells. This was verified on the single cell level by FACS analysis taking advantage of the 17D1 antibody, which stains the typical invariant TCR composition found on V γ 6⁺ $\gamma\delta$ T cells, V γ 6/V δ 1. Additionally, the antibody stains V γ 5/V δ 1⁺, which can be differentiated by co-staining with a V γ 5-specific antibody and subsequent gating for V γ 5⁺17D1⁺ $\gamma\delta$ T cells. The FACS analysis clearly identified the V γ 4⁻V γ 5⁻ $\gamma\delta$ T cell subset as the invariant $\gamma\delta$ T cell subpopulation expressing V γ 6⁺V δ 1⁺ TCR chains. Figure 13 depicts the three subpopulations of $\gamma\delta$ T cells, which were identified in the skin of C57/BL6 mice.

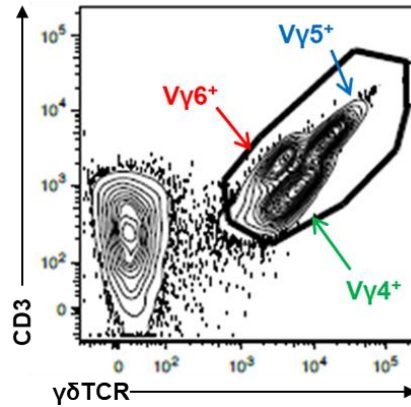


Figure 13: Identification of three subpopulations of $\gamma\delta$ T cells in the murine skin. Representative FACS plot showing the distribution of $\gamma\delta$ T cell subsets in the murine skin after treatment with IMQ.

Next, the question was addressed whether the accumulation of $V\gamma 6^+$ $\gamma\delta$ T cells in the skin is directly linked to deficiency of IL-12 or a consequence of elevated IL-23 levels during increased inflammation in the mutant mice (*Il12rb2^{-/-}* and *Il12a^{-/-}*). To this end, IMQ-treated *Il12b^{-/-}* and *Il23a^{-/-}* mice, which both lack IL-23 and only differ in their deficiency (*Il12b^{-/-}*) or sufficiency (*Il23a^{-/-}*) of IL-12, were analyzed for the appearance of $V\gamma 6^+$ $\gamma\delta$ T cells in the skin and the ratio of $V\gamma 6^+/V\gamma 4^+$ $\gamma\delta$ T cells was calculated.

As expected, mice deficient only in IL-12 signaling showed a high ratio of $V\gamma 6^+/V\gamma 4^+$ $\gamma\delta$ T cells due to the massive accumulation of $V\gamma 6^+$ $\gamma\delta$ T cells in these mice. Interestingly, depending on the absence or presence of IL-12 in mice lacking IL-23 (*Il23a^{-/-}* vs *Il12b^{-/-}*) and thus full-blown inflammation, significant differences in $V\gamma 6^+$ $\gamma\delta$ T cell accumulation were still visible (Figure 14).

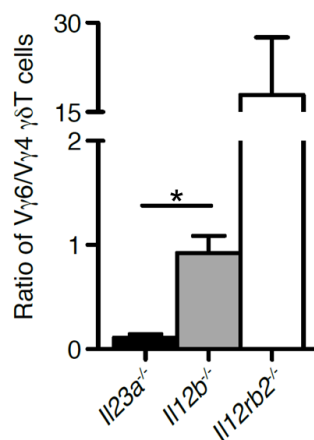


Figure 14: Ratio of skin effector $\gamma\delta$ T cells in IMQ-treated *Il23a^{-/-}*, *Il12b^{-/-}* and *Il12rb2^{-/-}* mice. Mice were treated with IMQ for 6 days followed by flow cytometry analysis of treated skin. Calculated ratio of $V\gamma 6^+/V\gamma 4^+$ $\gamma\delta$ T cells ($n=4$ *Il12rb2^{-/-}*, $n=9$ *Il12b^{-/-}*, $n=3$ *Il23a^{-/-}*). Data are given as mean + SEM; analysis was done by unpaired two tailed t-test.

The increased type 17 response in IL-12-deficient mice was further analyzed by intracellular FACS staining revealing that the overall levels of IL-17A in *Il12rb2*^{-/-} mice were increased compared to WT mice. As reported before, typically V γ 4⁺ $\gamma\delta$ T cells are the main IL-17A-secreting cells in the lesional skin during psoriatic plaque formation. However, in the case of IL-12 deficiency, the main producers of IL-17A were found to be V γ 6⁺ $\gamma\delta$ T cells aberrantly accumulating in the skin (Figure 15).

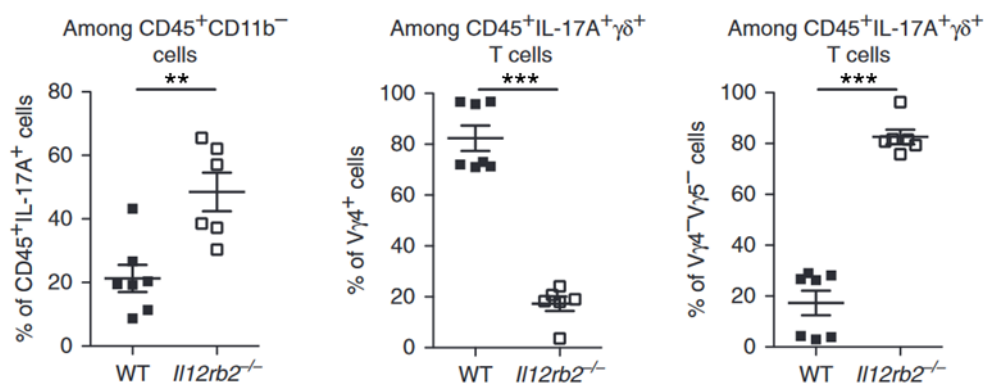


Figure 15: IL-17A production in IMQ-treated WT and *Il12rb2*^{-/-} mice. Flow cytometry analysis of inflamed skin; cells were gated on CD45⁺CD11b⁻ leukocytes and analyzed for the expression of IL-17A in CD45⁺ T cells, V γ 4⁺ and V γ 4⁻V γ 5⁻ $\gamma\delta$ T cells. Data are given as means \pm SEM (n=6-7 mice per group); results were analyzed by unpaired two-tailed t-test.

7.2.2 Effect of IL-17A neutralization in IMQ-treated *Il12rb2*^{-/-} mice

The current data showed that V γ 6⁺ $\gamma\delta$ T cells accumulate in the absence of IL-12 and that these cells are able to produce high amounts of the effector cytokine IL-17A. To determine whether the elevated IL-17A levels are responsible for the increased inflammatory response in *Il12rb2*^{-/-} mice, IL-17A was blocked during disease induction by application of an IL-17A neutralizing antibody (Figure 16).

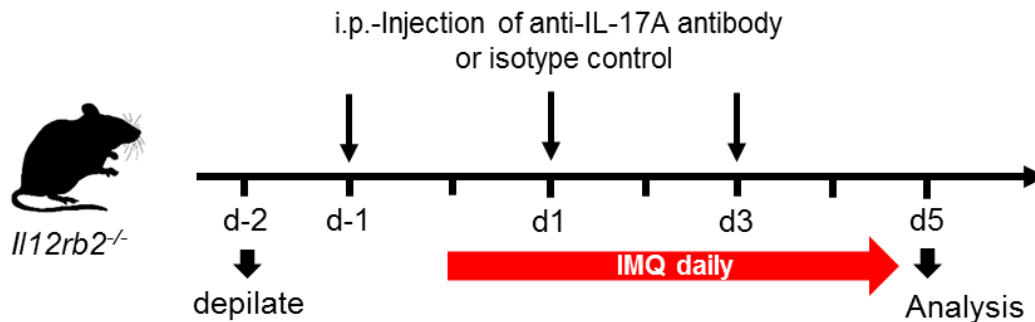


Figure 16: Treatment protocol of IL-17A neutralization in IMQ-treated *Il12rb2*^{-/-} mice. Mice were treated with IMQ for 5 days. Intraperitoneal injection of 200 μ g of anti-IL-17A antibody or isotype control was performed every second day starting on day -1.

Neutralization of IL-17A led to a significant reduction in skin thickness and an improved epidermal integrity determined by TEWL measurement (Figure 17A and B). Furthermore, a significant reduction of neutrophil invasion into the lesions was observed after treatment with anti-IL-17A antibody (Figure 17C). The dissection of overall cell numbers of effector V γ 4⁺ and V γ 6⁺ $\gamma\delta$ T cells showed that they were not altered by anti-IL-17A antibody application (Figure 17D). Although not statistically significant, there was the trend that anti-IL-17A mAb treated *Il12rb2*^{-/-} mice had an even lower disease outcome than WT mice (Figure 17A and B).

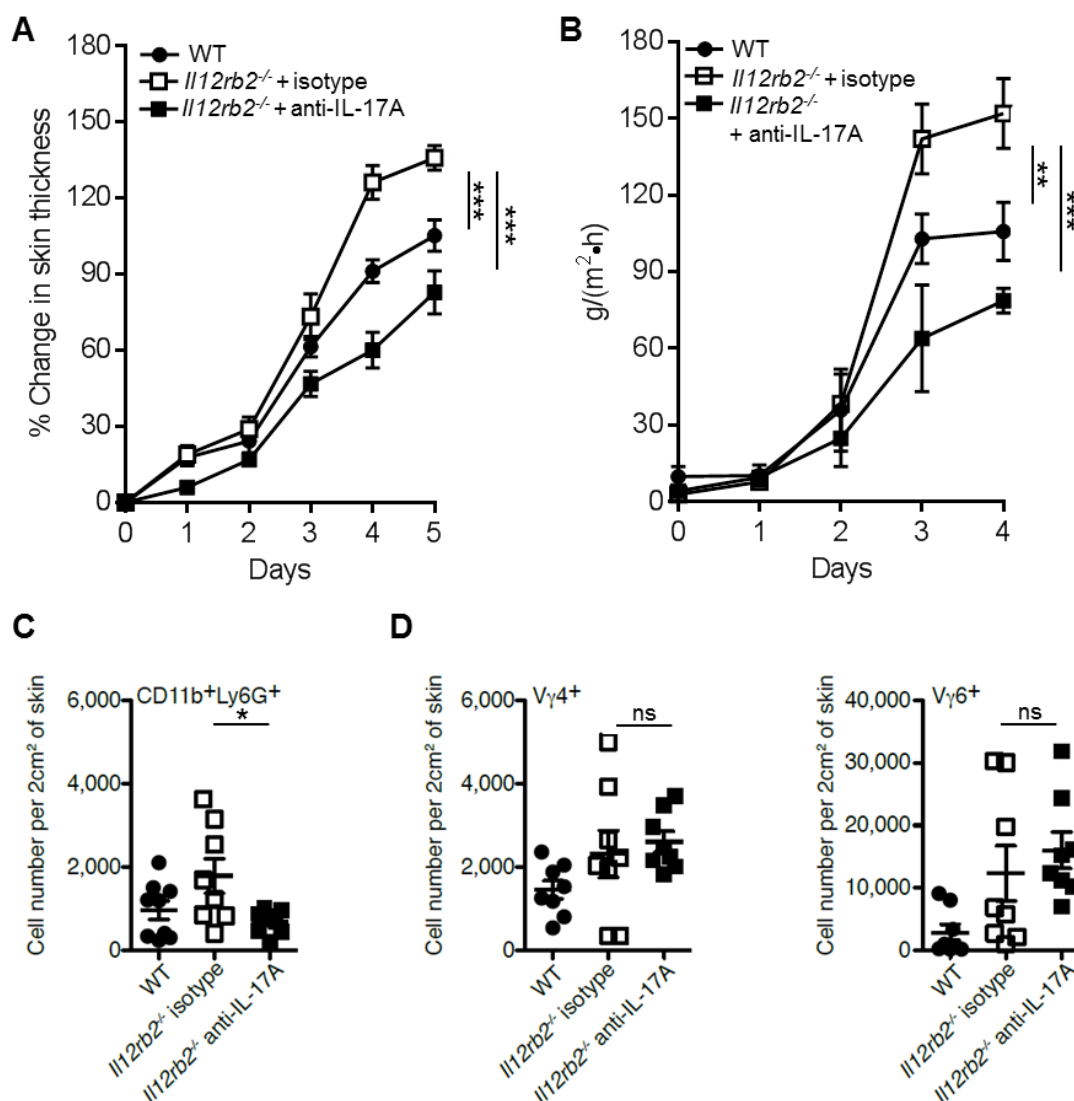


Figure 17: Analysis of inflamed skin in WT and anti-IL-17A-treated *Il12rb2*^{-/-} mice. (A) Back skin inflammation during the whole disease course represented as a percent change in skin thickness compared to untreated skin on day 0 (B) TEWL in IMQ-treated back skin (C, D) Flow cytometry analysis of inflamed skin; cells were gated on CD45⁺ leukocytes and analyzed for (C) neutrophils and (D) skin infiltrating V γ 4⁺ (left) and V γ 6⁺ (right) $\gamma\delta$ T cells (n=8 mice per group). Data are given as means \pm SEM. Analyses were done by (A, B) two-way ANOVA with Bonferroni post-test, (C, D) unpaired two tailed t-test.

7.2.3 Reduced skin inflammation in mice functionally lacking V γ 6⁺ $\gamma\delta$ T cells

To test if the specific accumulation of V γ 6⁺ $\gamma\delta$ T17 cells is causative in the aggravation of disease symptoms when IL-12 is missing, *Vd1*^{-/-} mice, which selectively lack functional V γ 6⁺V δ 1⁺ $\gamma\delta$ T cells [174], were bred on to the *Il12rb2*^{-/-} background and psoriatic plaque formation was induced.

Mice lacking functional $V\gamma 6^+V\delta 1^+$ $\gamma\delta T$ cells developed a significantly reduced skin inflammation compared to the exaggerated disease phenotype seen in IL-12R mutants. Moreover, the observed inflammation was reduced to the levels of WT mice (Figure 18).

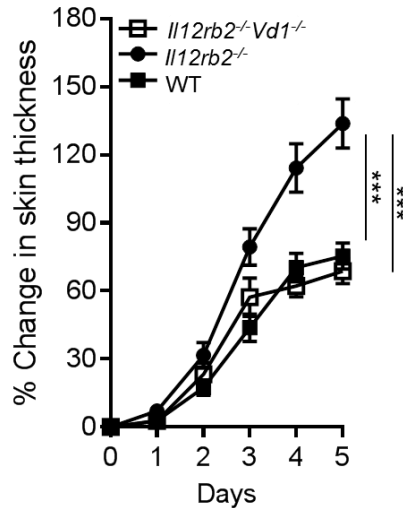


Figure 18: Analysis of skin inflammation in mice functionally lacking $V\gamma 6^+V\delta 1^+$ T cells. Back skin inflammation represented as percent change in skin thickness compared with untreated skin on day 0. Data are given as mean + SEM ($n=17$ WT, $n=15$ *Il12rb2^{-/-}*, $n=12$ *Il12rb2^{-/-}Vd1^{-/-}*); analysis was done by two-way ANOVA with Bonferroni post-test.

To analyze whether $V\gamma 6^+$ effector $\gamma\delta T17$ cells are in general involved in the modulation of disease severity also in non-mutant mice, the varying frequencies of $V\gamma 6^+$ $\gamma\delta T$ cells in the dermis of WT mice were correlated with their individual disease severities during peak disease (skin thickness). The data revealed a positive correlation between the frequencies of $V\gamma 6^+$ effectors and skin thickness in WT mice (Figure 19).

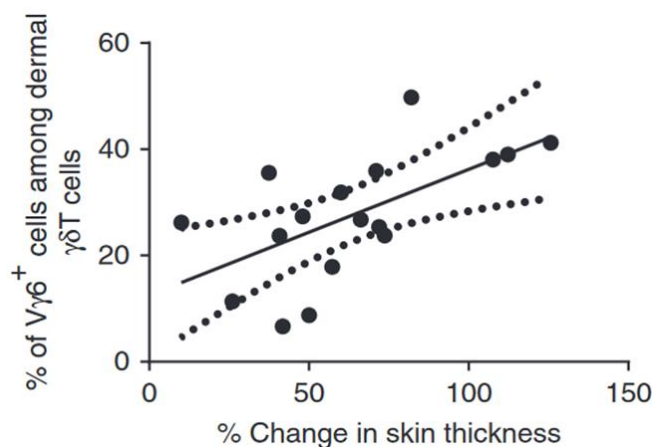
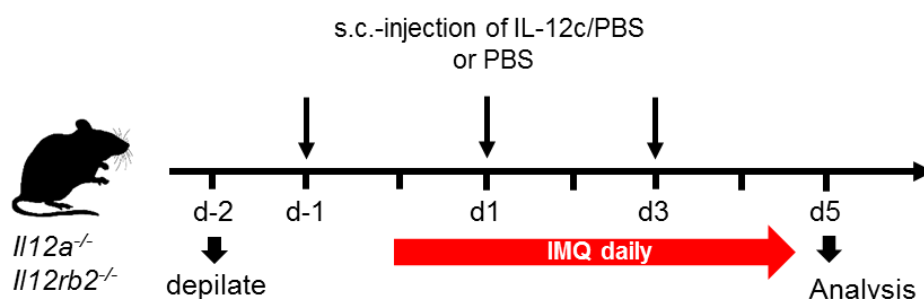


Figure 19: Correlation analysis of $V\gamma 6^+V\delta 1^+$ $\gamma\delta T$ cells with skin thickness in WT mice. Pearson's correlation analysis of $V\gamma 6^+$ $\gamma\delta T$ cells in inflamed back skin calculated as percent of all dermal $\gamma\delta T$ cells and percent change in epidermal thickening in WT mice ($n=17$). Each data point represents an individual mouse (Pearson's $r=0.615$, $p=0.0086$).

7.2.4 IL-12 limits psoriasiform skin inflammation

To further highlight the decisive role of IL-12 in psoriatic plaque formation, gain- and loss-of-function experiments were performed either by means of local administration of IL-12Fc into the skin of *Il12a*^{-/-} and *Il12rb2*^{-/-} mice or by injection of an anti-IL-12p70 antibody into WT mice (Figure 20).

gain-of function:



loss-of function:

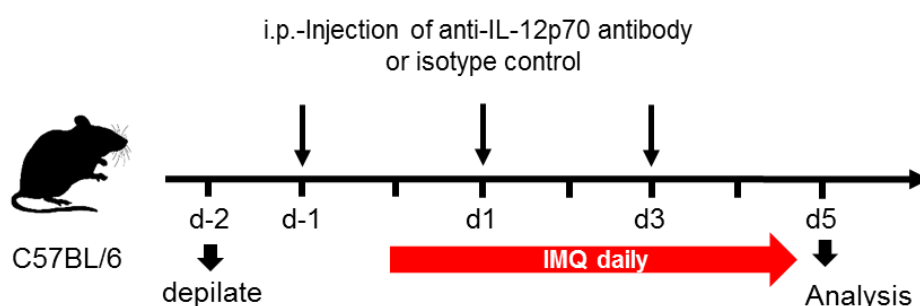


Figure 20: Treatment protocol of loss- and gain-of-function experiments. Mice were treated with IMQ for 5 days. For gain-of-function experiments ears of mice deficient in IL-12 signaling were s.c.-injected with IL-12Fc/PBS or PBS. For loss-of-function experiments WT mice were i.p.-injected with anti-IL-12p70 antibody or isotype control. Injection was performed every second day starting on day -1.

Administration of IL-12 directly into the ears of *Il12a*^{-/-} mice led to significantly reduced skin inflammation (Figure 21A) whereas this did not occur if the receptor of IL-12 was deleted (Figure 21B). Correspondingly, the presence of IL-12 with unhindered IL-12 signaling significantly diminished the overall production of IL-17A and prevented the accumulation of Vγ6⁺ γδT17 cells independent of Vγ4⁺ γδT17 cell numbers, which were not altered (Figure 21C).

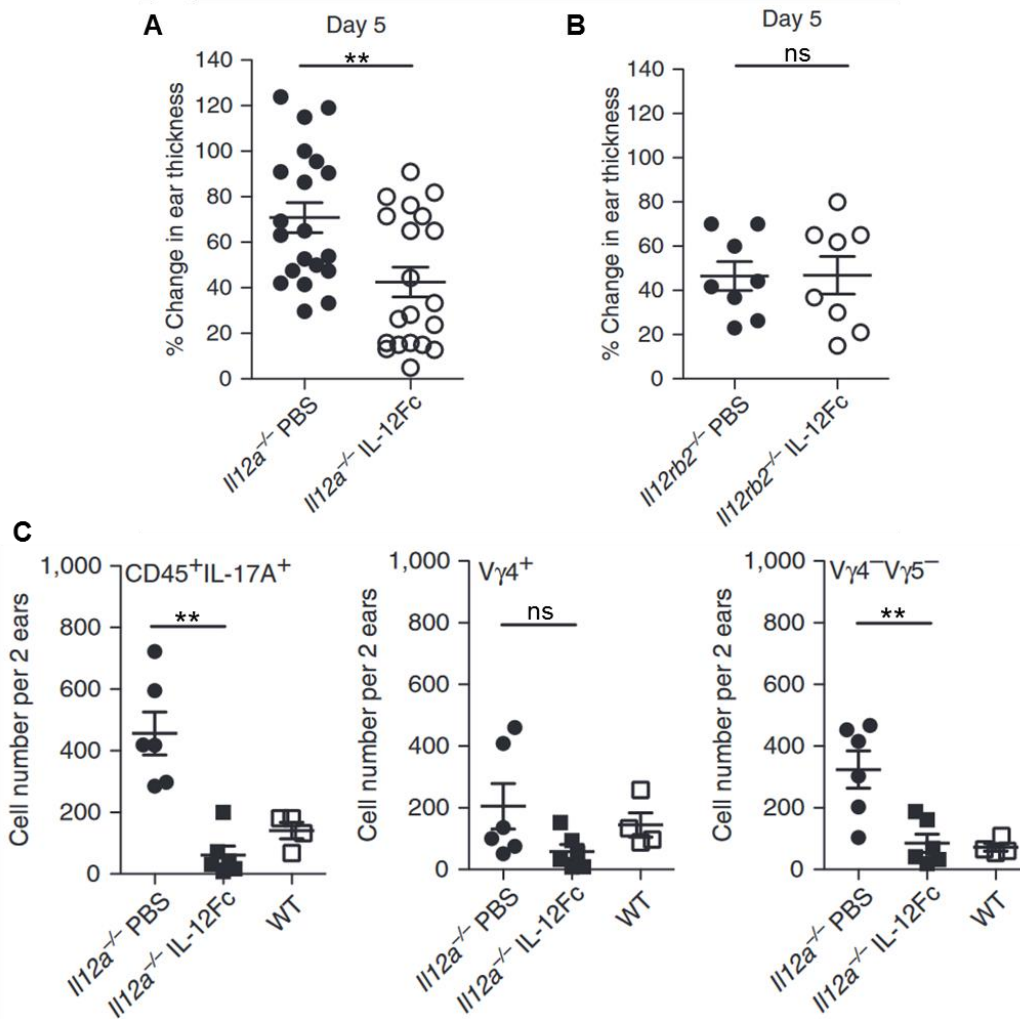


Figure 21: Skin inflammation in IL-12Fc-treated mice deficient in IL-12-signaling. (A, B) Ear skin inflammation represented as percent change in ear thickness on day 5 compared with untreated skin on day -1 ($n=20$ *Il12a^{-/-}* and $n=8$ *Il12rb2^{-/-}*) (C) Flow cytometry analysis of inflamed back skin; absolute numbers of skin-infiltrating CD45⁺IL-17A⁺ leukocytes, V γ 4⁺ and V γ 4⁻V γ 5⁻ $\gamma\delta$ T cells ($n=4$ WT, $n=6$ *Il12a^{-/-}*). Data are given as means \pm SEM; results were analyzed by unpaired two-tailed t-test.

Injection of anti-IL-12p70 heterodimer-specific neutralizing antibody into WT mice was performed to control potential aberrancies in the genetically targeted mouse lines. The phenotype observed in *Il12rb2^{-/-}* mice could be recapitulated as blocking of IL-12 signaling in WT mice led to a more pronounced skin thickness and reduced skin integrity comparable with that found in *Il12rb2^{-/-}* mice (Figure 22A and B). Furthermore, FACS analysis revealed an increase of the absolute numbers of inflammatory infiltrates compared to isotype-treated WT mice, which are mostly represented by neutrophils, effector $\gamma\delta$ T cell subsets and other IL-17A-producing cells (Figure 22C).

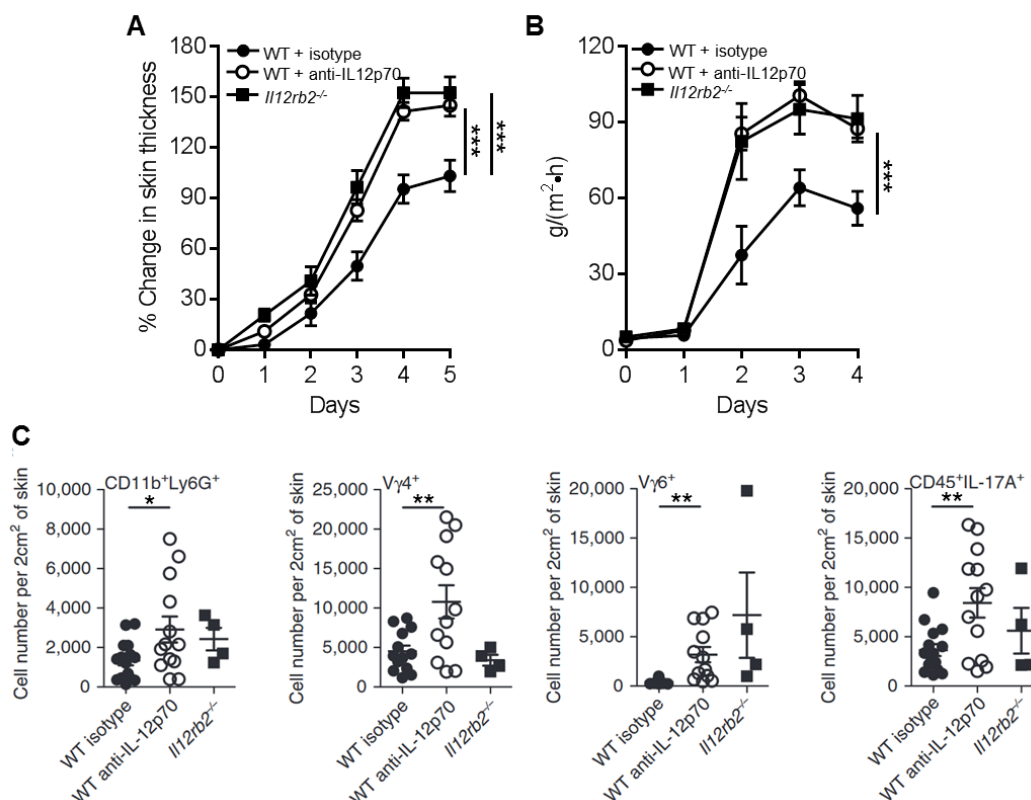


Figure 22: Skin inflammation in WT mice after neutralization of IL-12. (A) Back skin inflammation represented as percent change in skin thickness compared with untreated skin on day 0 and **(B)** TEWL in IMQ-treated back skin ($n=8$ WT isotype, $n=13$ WT anti-IL12p70, $n=10$ *Il12rb2*^{-/-}). **(C)** Flow cytometry analysis of inflamed back skin; absolute numbers of skin infiltrating neutrophils, V γ 4⁺ $\gamma\delta$ T cells, V γ 6⁺ $\gamma\delta$ T cells and CD45⁺IL-17A⁺ leukocytes ($n=13$ WT isotype, $n=12$ WT anti-IL12p70, $n=4$ *Il12rb2*^{-/-}). Data are given as means \pm SEM. Analyses were done by (A, B) two-way ANOVA with Bonferroni post-test (C) unpaired two-tailed t-test.

7.3 Screening for IL-12 responders in the skin

The IL-12R complex is expressed on certain subsets of natural killer cells, NKT cells, $\gamma\delta$ T cells and activated $\alpha\beta$ T cells [175]. As $\gamma\delta$ T17 cells accumulate in psoriatic skin in absence of IL-12 signaling, a direct response of $\gamma\delta$ T17 cells to IL-12 was hypothesized. Therefore, our collaborators determined the expression of *Il12rb2* by RT-qPCR analysis directly on skin-associated $\gamma\delta$ T cells (V γ 4⁺, V γ 6⁺ and V γ 5⁺ subset) sorted from psoriatic WT and *Il12rb2*^{-/-} skin.

As expected, high levels of *Il12rb2* RNA were detected in V γ 5⁺ DETCs (positive control), as they are known respond to IL-12 by inducing a type 1 response dominated by IFN γ [176]. Importantly, no *Il12rb2* transcripts were measured in the V γ 4⁺ and V γ 6⁺ $\gamma\delta$ T cell subsets (Figure 23).

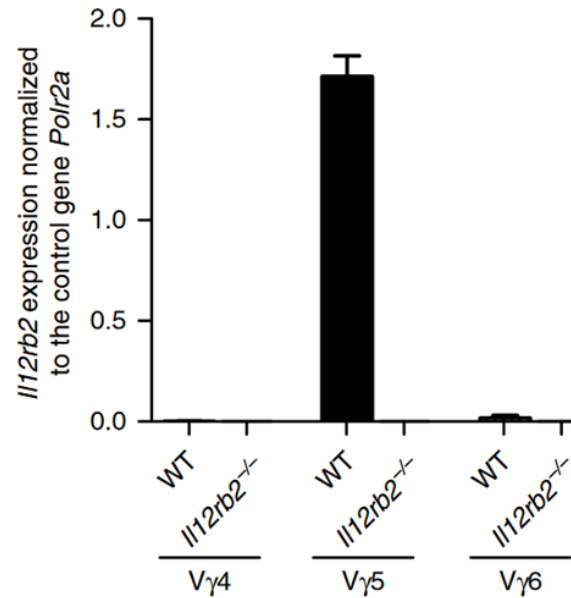


Figure 23: Expression of *Il12rb2* on murine $\gamma\delta$ T cell subsets. V γ 4⁺, V γ 5⁺ and V γ 6⁺ $\gamma\delta$ T cells were sorted by flow cytometry from WT and *Il12rb2*^{-/-} mice treated with IMQ for 6 days. The sort of pooled material of two mice was analyzed by RT-qPCR for *Il12rb2* expression with *Polr2a* as a house-keeping gene. Data are given as mean + SEM.

Since no direct link between IL-12 and $\gamma\delta$ T cells was found, our collaborators further screened for alternative IL-12 responders and pin-pointed mouse keratinocytes as potential responders with very high *Il12rb2* transcript expression (published in [173]). To this effect they generated bone marrow chimeras showing an increased inflammation when IL-12R was missing from the radio-resistant compartment, pointing to non-immune cells like keratinocytes as critical IL-12 responders in this disease model (published in [173]).

To translate the murine findings to the human situation, clinical biopsies of psoriatic lesions and healthy controls were examined by immunohistochemistry for IL-12 receptor expression. Using a specific antibody against human IL-12R β 2, high expression of IL-12R β 2 protein in healthy human epidermis (Figure 24A) as well as in the epidermis of psoriatic lesions was detected (Figure 24B).

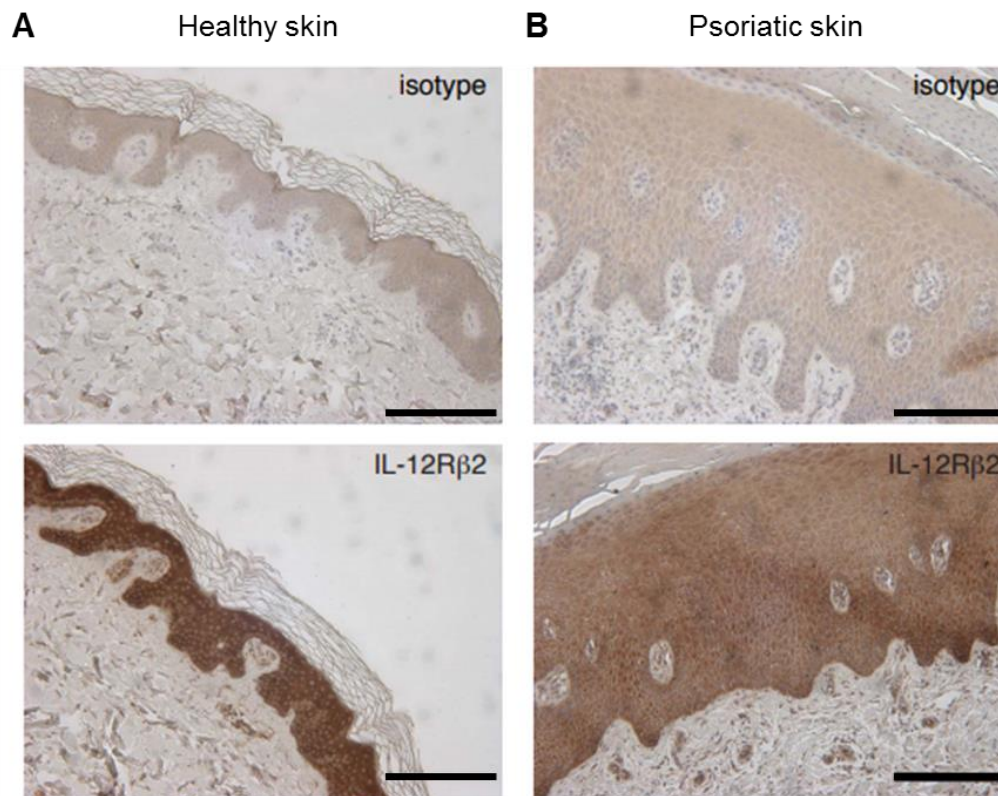


Figure 24: IL-12Rβ2 expression in healthy and psoriatic human skin. Skin sections from (A) a healthy human donor and (B) a psoriatic patient were stained with antibodies against human IL-12Rβ2 or isotype control for immunohistochemistry; scale bar: 200 μm.

For deeper and unbiased insights into the molecular processes induced by IL-12 signaling in keratinocytes, our collaborators sorted keratinocytes from IMQ-treated WT and *Il12rb2*^{-/-} mice and performed transcriptomic analysis by next-generation sequencing (published in [173]). Comparing genes on high variance between IMQ-treated *Il12rb2*^{-/-} versus IMQ-treated WT mice, they highlighted IL-12 to specifically modify transcriptional programmes, which affect tissue structure remodelling, keratinocyte differentiation and basement membrane integrity. Importantly, they also observed a high increase of inflammatory elements related to type 17 immune responses as well as factors enhancing neutrophil engagement in *Il12rb2*^{-/-} lesions (published in [173]). These findings fit to the increased disease severity observed in *Il12a*^{-/-} and *Il12rb2*^{-/-} mice (Figures 8-11).

7.4 Effect of nutritional salt on psoriatic plaque formation in mice

It was previously described that long-term intake of excess dietary salt with increased storage of osmotically inactive Na⁺ in extra-renal organs is a potential lifestyle risk factor for the development of autoimmune diseases by affecting immune cell function [163, 164]. Therefore, the consequence of an excessive intake of salt on the tissue-resident immune system in the skin was investigated in WT mice receiving either chow (0.5% NaCl) or high salt diet (HSD; 4% NaCl; 0.75% in H₂O) for four weeks directly after weaning. Subsequently, to study the impact of increased sodium concentrations in the skin tissue on the development of inflammatory skin diseases psoriatic plaque formation was induced by application of IMQ (Figure 25). By use of the IMQ model of psoriasiform inflammation the focus was set on tissue-resident innate lymphocytes represented mostly by $\gamma\delta$ T cells as potential responders to changes in local sodium concentrations.

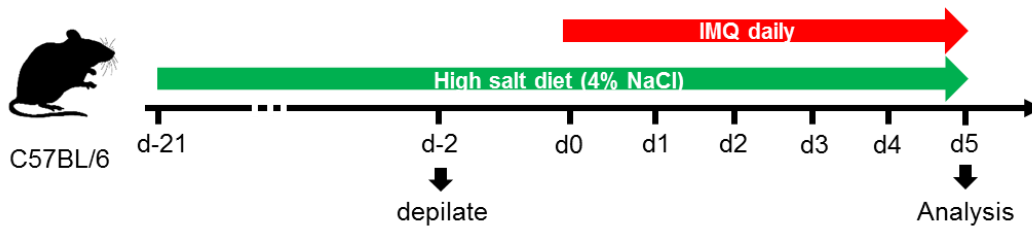


Figure 25: Treatment protocol for HSD-experiments in WT mice. Mice received HSD containing 4% NaCl and tap water added with 0.75% NaCl, while the control group was fed with chow. After 3 weeks, psoriatic plaque formation was induced by treatment with IMQ for 5 days.

7.4.1 High salt diet exacerbates psoriatic plaque formation in mice

First, to evaluate possible differences in the dehydration status of mice receiving either chow or HSD and to rule out that HSD resulted in a status of pathological dehydration, the hematocrit was measured. As depicted in [Figure 26](#), there were no relevant differences in the hydration status between the two diets irrespective of disease induction.

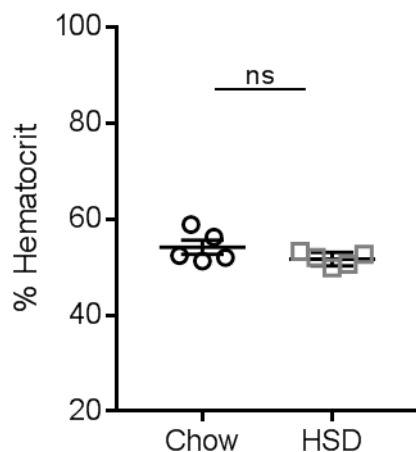


Figure 26: Measurement of the hematocrit in WT mice fed with chow or HSD. Data are given as mean \pm SEM (n=5 mice per group); analysis was done by unpaired two tailed t-test.

Next, the clinical disease course in mice was monitored. Independent of diet, both treatment groups showed the same reduction in body weight ([Figure 27A](#)). Interestingly, mice that received HSD showed an exacerbated disease course compared to chow-fed mice. This was illustrated by an increased change in skin thickness during disease development and a significantly more pronounced skin thickening during peak disease on day 4 ([Figure 27B](#)). Correspondingly, these mice suffered from an exaggerated physical barrier disruption, indicated by a significant increase in TEWL from day 3 onwards ([Figure 27C](#)). Feeding of HSD in untreated WT mice *per se* had no measurable effect on skin thickness or TEWL.

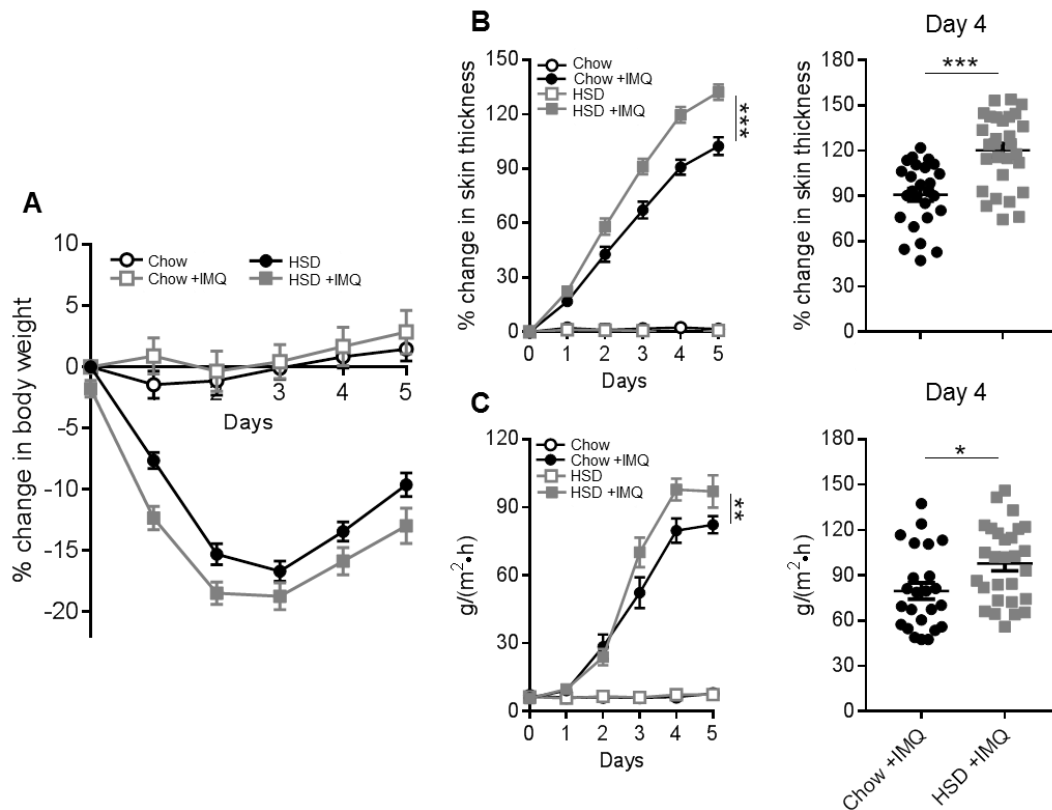


Figure 27: Analysis of skin inflammation in IMQ-treated WT mice fed with chow or HSD. (A) Percent change in body weight and **(B)** back skin inflammation during the whole disease course (left) or peak disease on day 4 (right) represented as a percent change in skin thickness compared to untreated skin on day 0. **(C)** TEWL in back skin during disease course (left) and peak disease on day 4 (right). Data are given as means \pm SEM (n=19 Chow, n=24 Chow +IMQ, n=23 HSD, n=29 HSD +IMQ). Analyses were done by (B, C) two-way ANOVA with Bonferroni post-test, (day 4) unpaired two tailed t-test.

The more severe clinical outcome in IMQ-treated mice on HSD was also visible by means of histopathologic scoring. Correcting the initial finding that HSD alone had no effect on skin thickness when measured with caliper, histology revealed that in fact a slight increase in epidermal layers could be observed in untreated WT mice on HSD compared to control mice on chow. The increased acanthosis became even more prominent after disease induction and was further accompanied with clear elongated rete ridges and an extensive infiltration of leukocytes into the dermis (Figure 28A). Quantification of epidermal layers confirmed a significant increase in the treated HSD group compared to IMQ-treated mice fed with chow (Figure 28 B). During inflammation, the levels of the acute phase protein lipocalin 2 (Lcn2) in the serum became significantly upregulated after induction of psoriatic plaques in both diet groups. Although no differences in the levels of Lcn2 were observable between mice without disease induction, a slight trend to higher Lcn2 levels in treated HSD-fed mice compared to their control group was detectable (Figure 28C).

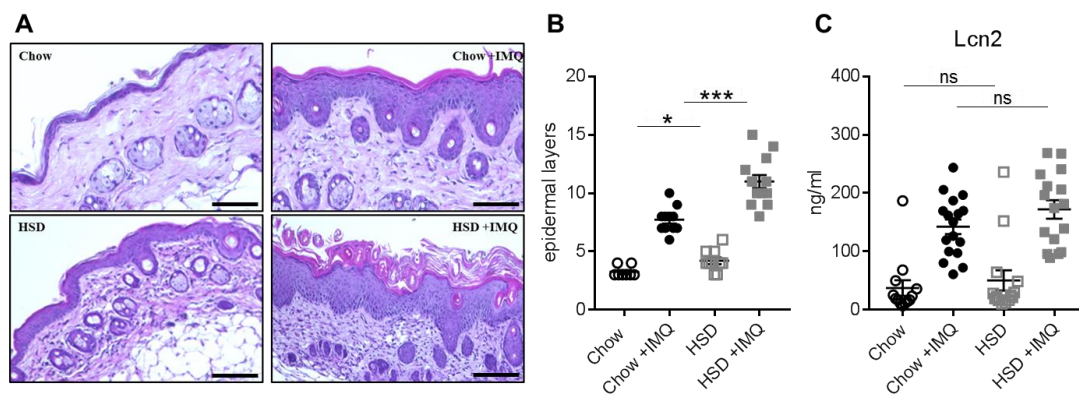


Figure 28: Histopathology and Lcn2-levels of IMQ-treated WT mice fed with chow or HSD. Representative sections of back skin on day 5 post treatment were **(A)** stained with H&E; scale bar, 50 μ m and **(B)** total counts of epidermal layers were quantified (n=8-13 mice per group). **(C)** ELISA of Lcn2 in the serum (n=13-17 mice per group). Data are given as means \pm SEM; results were analyzed by unpaired two-tailed t-test.

To further investigate the contribution of HSD on the inflammatory response, hallmark pathways of psoriasis were analyzed by transcript analyses in the skin of treated and untreated mice in the presence or absence of HSD (Figure 29). Skin lesions of mice under high-salt condition displayed a stronger type 17 phenotype compared to treated mice on chow, as most key signature cytokines of T_H17 cells including *Il17A*, *Il17F*, as well as expression of *IL23a* were significantly upregulated. The increase also included levels of *Gcsf* transcript, a stromal factor directly downstream of IL-17A and an important marker for neutrophil activity, as it stimulates survival, proliferation, differentiation, and function of neutrophils (Figure 29A). This further strengthened an enhanced involvement of an IL-17 response in this model. High salt conditions further amplified the up-regulation of the pro-inflammatory cytokines *Tnfa* and *Il1 β* during psoriatic plaque formation. No differences were observed in the cytokines *Il22* and *Ifny* (Figure 29A), as well as in the chemokine *Cxcl9*, which is dominantly controlled by IFN- γ (Figure 29B). In contrast, a slight increase of *Ccl20* was detectable in the lesions of HSD-fed mice (Figure 29B). Looking at downstream transcripts induced by type 17 cytokines and *Lcn2* levels revealed a range of antimicrobial peptides, including β -defensins (*defb1-4*) and S100 proteins (*S100a8* and *9*), whose induction during disease is mostly upregulated by HSD (Figure 29C). Strikingly, some of the pro-psoriatic markers increased only in response to HSD alone without any further disease induction. Such an increase was most prominent in the case of *Il17A* and parts of its downstream signature (*defb4*, *s100a8*, *s100a9*, *lcn2*; Figure 29C).

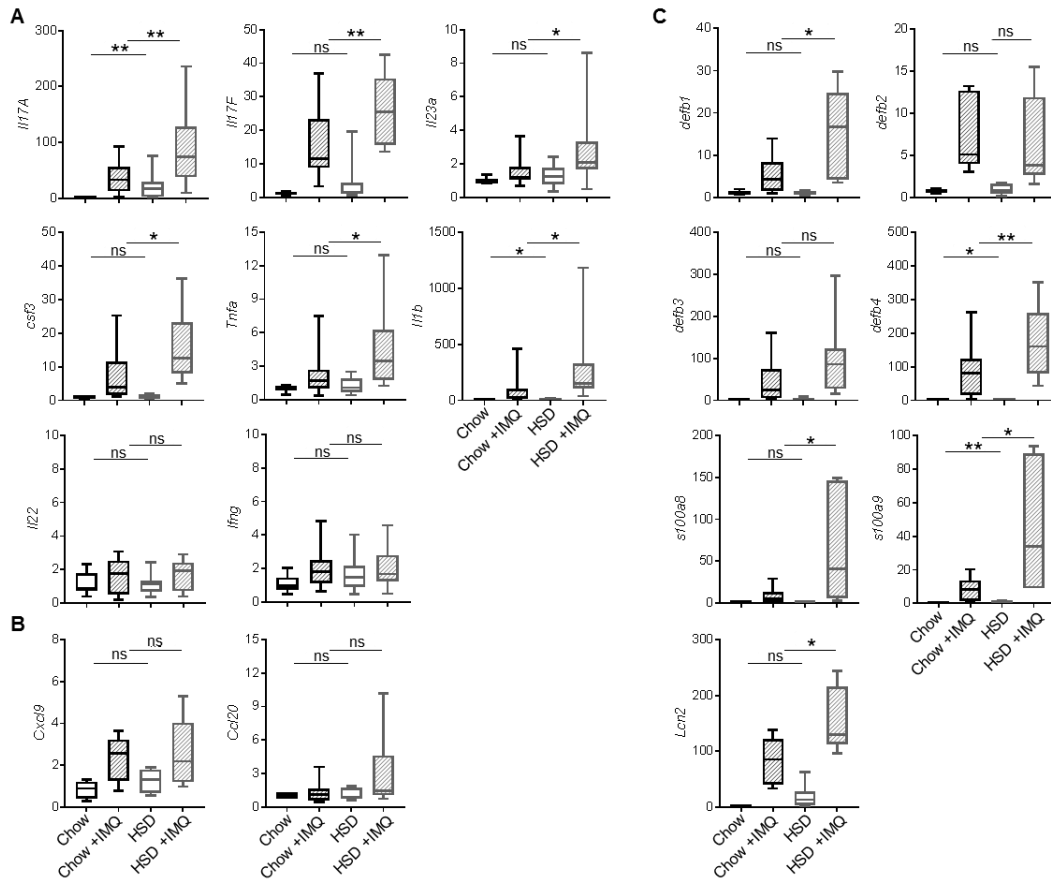


Figure 29: Transcript analysis of lesional skin of WT mice fed with chow or HSD. RT-qPCR analyses of the whole skin on day 5 post treatment represented as fold change relative to the average WT expression levels of **(A)** inflammatory cytokines **(B)** chemokines **(C)** antimicrobial peptides (n=4–14 Chow, n=5–21 Chow +IMQ, n=5–19 HSD, n=6–24 HSD +IMQ); results were analyzed by unpaired two-tailed t-test.

7.5 $\gamma\delta$ T17 cells drive disease aggravation after high salt diet feeding

7.5.1 Effect of HSD on effector $\gamma\delta$ T17 cells in skin and skin-dLNs

To follow-up on the lead that there is an exaggerated IL-17A footprint in the psoriatic tissue of mice fed with HSD, the skin was analyzed for Ror γ t-dependent $\gamma\delta$ T17 cells as they are the main drivers of psoriasiform inflammation in mice by production of IL-17A, IL-17F, and IL-22. As already mentioned, there are two independent $\gamma\delta$ T cell effector subsets located in the dermis that are able to induce an IL-17 response, V γ 4⁺ and V γ 6⁺ $\gamma\delta$ T cells. Both are resident in the dermis at steady state but take up different functional roles during inflammation. To analyse if both subsets respond to the high sodium environment, their distribution in the skin (Figure 30) as well as their surface expression of CD27 and CD44 (Figure 31), an indicative marker for IL-17 producing effector T cells, in skin-dLNs were analysed via flow cytometry.

The generated FACS plots indicated that HSD changes the cellular composition of the dermal immune network as V γ 6⁺ $\gamma\delta$ T cells strongly accumulated in the high sodium environment whereas V γ 4⁺ $\gamma\delta$ T cells seemed to be unaffected or even reduced (Figure 30).

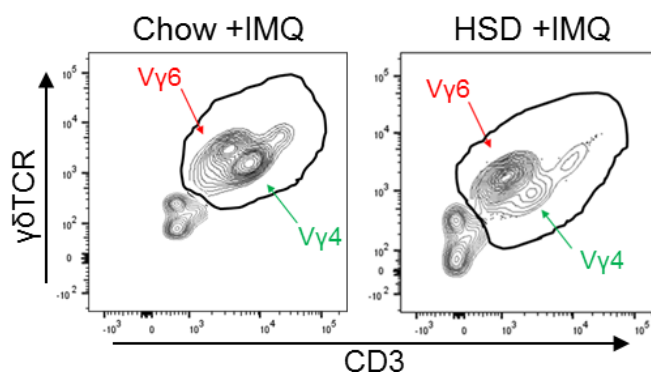


Figure 30: $\gamma\delta$ T17 cell contribution in skin of IMQ-treated WT mice fed with chow or HSD. Representative FACS plots of CD3⁺γδTCR⁺ cells showing the distribution of $\gamma\delta$ T cell subsets in the skin of IMQ-treated mice 5 days post treatment. Cells were pre-gated on CD45⁺CD11b⁻ leukocytes.

Going more into detail, the surface expression of CD44 and CD27 on $\gamma\delta$ T cells was analysed in the skin-draining lymph nodes (skin-dLN; Figure 31). The expression of CD44 on total $\gamma\delta$ T cells already revealed that under high salt condition mice expand $\gamma\delta$ T cells of a type 17 polarity (CD44^{hi}CD27⁻). This effect already occurs on HSD

alone (49%) reaching comparable expression levels to IMQ-treated mice on chow (46%). In the context of disease this effect indeed became even more pronounced under high salt condition (79%; [Figure 31A](#)).

A closer look into the two $\gamma\delta$ T17 subsets confirmed the dominance of $CD44^{hi}V\gamma 4^{+}$ $\gamma\delta$ T cells in chow +IMQ mice (~66%; [Figure 31B](#)), while $CD44^{hi}V\gamma 6^{+}$ $\gamma\delta$ T cells only represent a small population in these mice (~27%; [Figure 31C](#)). Interestingly, type 17 polarized $V\gamma 4^{+}$ $\gamma\delta$ T cell numbers seem to be not affected by the diet alone (~35% chow vs. ~41% HSD), but disease induction in a high salt environment increased their numbers compared to normal salt condition (~66% chow vs ~80% HSD; [Figure 31B](#)). Surprisingly, a different response pattern was observed for $V\gamma 6^{+}$ $\gamma\delta$ T cells, which in contrast to $V\gamma 4^{+}$ $\gamma\delta$ T cells, were measurably affected due to higher salt concentrations. Here, feeding untreated mice with HSD resulted in nearly twice of the expression levels of CD44 (~44%) compared to IMQ-treated WT mice fed with chow (~27%). Induction of disease under high salt diet further potentiated this effect as a clear and dominant type 17 polarity of $V\gamma 6^{+}$ $\gamma\delta$ T cells occurred (~81%; [Figure 31C](#)).

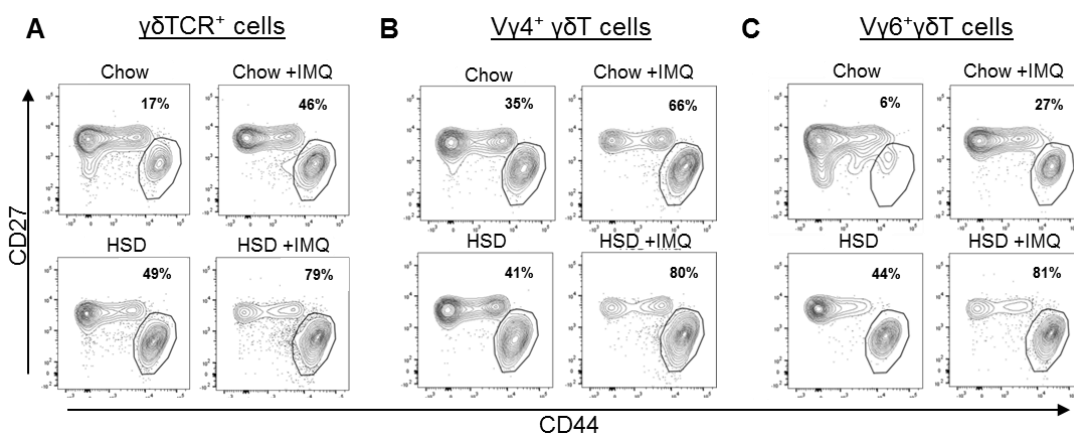


Figure 31: Expression levels of CD44 in $\gamma\delta$ T cells in skin-dLN in mice on chow or HSD. Representative FACS plots of $CD44^{hi}CD27^{-}$ $\gamma\delta$ T cells from skin-dLNs 5 days post IMQ treatment. **(A)** total $\gamma\delta$ T cells, **(B)** $V\gamma 4^{+}$ and **(C)** $V\gamma 6^{+}$. Cells were gated on $CD45^{+}CD11b^{-}CD3^{+}\gamma\delta$ TCR⁺ leukocytes.

7.5.2 V γ 6⁺ $\gamma\delta$ T cells highly respond to high salt conditions

These results so far indicated that V γ 6⁺ $\gamma\delta$ T cells are most affected by local sodium changes in the skin as well as in the skin-dLN. To further strengthen these observations, skin inflammation was monitored in chow *versus* HSD fed V δ 1^{-/-} mice, functionally lacking V γ 6⁺ $\gamma\delta$ T cells [174], to analyze if they contribute to the exacerbated disease phenotype observed in mice after HSD feeding (Figure 32).

Under high salt conditions IMQ treatment in V δ 1^{-/-} mice did not recapitulate the salt induced increase in skin thickness and breach of skin barrier but remained unaltered to the level of chow fed littermates (Figure 32B and C). Whereas skin inflammation in V δ 1^{-/-} chow +IMQ mice was not significantly reduced compared to WT chow +IMQ mice, a significant reduction was visible in V δ 1^{-/-} HSD +IMQ mice compared to WT HSD +IMQ mice.

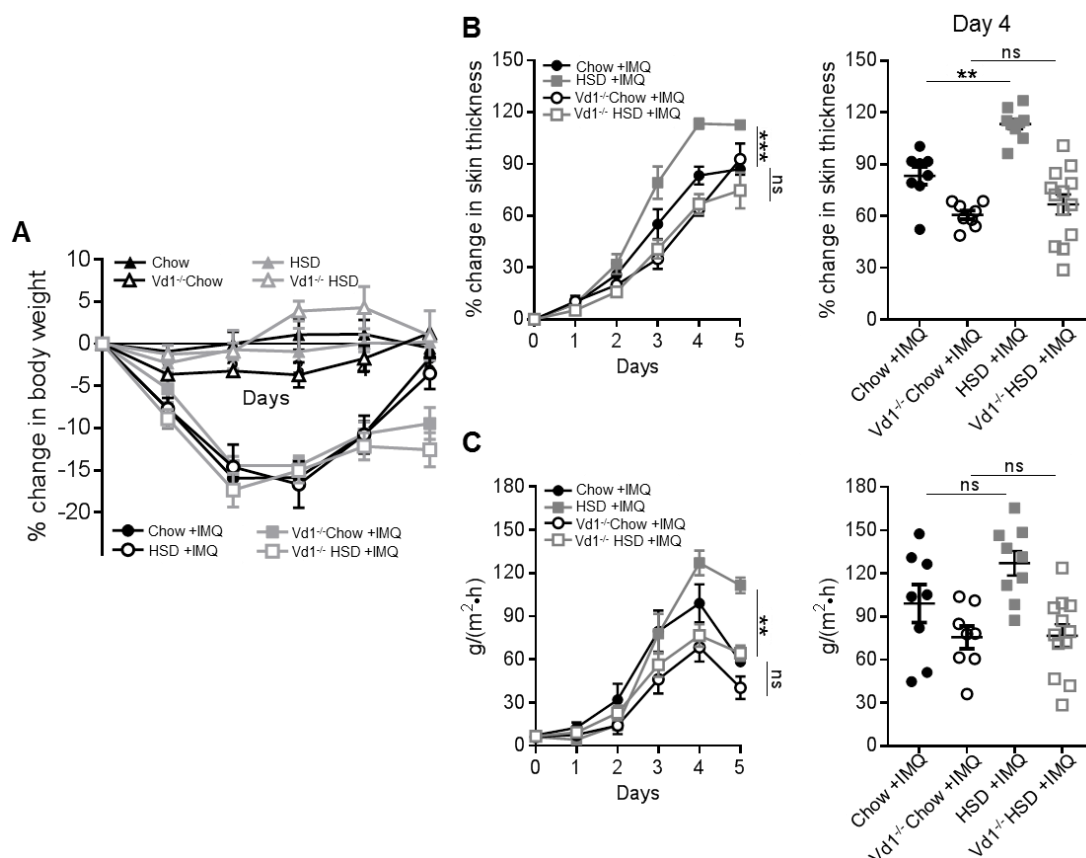


Figure 32: Skin inflammation in HSD-fed mice functionally lacking V γ 6⁺V δ 1⁺ T cells. WT and Vd1^{-/-} mice receiving either chow or HSD were treated with IMQ for 5 days. **(A)** Percent change of body weight. **(B)** Back skin inflammation during the whole disease course (left) or peak disease on day 4 (right) represented as a percent change in skin thickness compared to untreated skin on day 0. **(C)** TEWL of back skin during disease course (left) and peak disease on day 4 (right). Data are given as means \pm SEM (n=8-13 mice per group). Analyses were done by (B, C) two-way ANOVA with Bonferroni post-test, (day 4) unpaired two tailed t-test.

7.6 Effect of a minimal salt diet on psoriatic plaque formation

So far, it could be shown that HSD leads to a more pronounced disease development. In all previous experiments chow was used as a control for HSD. Since the composition of chow and HSD do not only differ in their content of salt (NaCl) but also slightly in other basic food components (e.g. fibre content), the experiments were repeated using the best technical control available. This control diet, the minimal salt diet (LSD; 0.03%), comprised the identical composition to HSD but contained the lowest salt concentration available, even below that of chow (0.43%). To test if LSD would have a comparable effect to chow and result in a lesser disease severity compared to HSD, WT mice were fed either HSD or LSD before and during IMQ treatment.

Independent of the diet, all IMQ-treated mice showed a comparable loss of weight ([Figure 33A](#)). The aggravated phenotype under high salt conditions disappeared when mice were fed a minimal salt diet. This was illustrated, as mice receiving LSD showed a significant reduction in change of skin thickness during the whole disease course as well as on peak disease on day 4 compared to HSD-fed mice ([Figure 33B](#)). The same tendency was apparent concerning skin barrier integrity, as mice on LSD showed slightly reduced levels of TEWL ([Figure 33C](#)). Importantly, the clinical disease parameters in LSD fed mice were comparable to the disease progression in mice receiving chow ([Figure 27](#)).

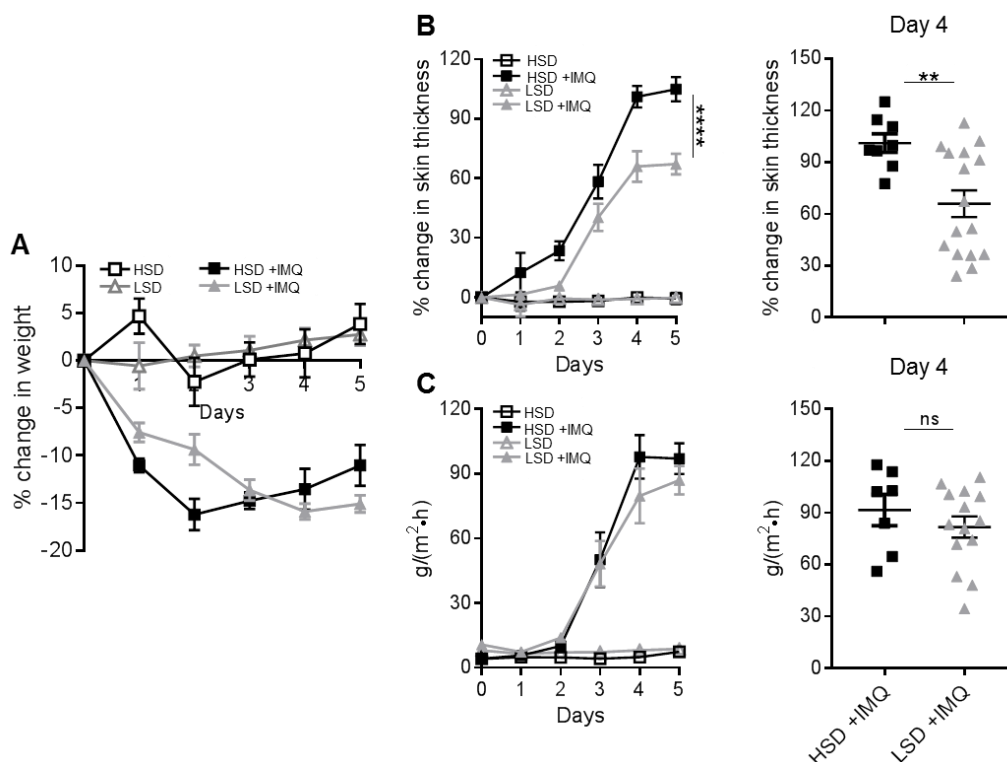


Figure 33: Analysis of skin inflammation in IMQ-treated WT mice fed with HSD or LSD. (A) Percent change of body weight. (B) Back skin inflammation during the whole disease course (left) or peak disease on day 4 (right) represented as a percent change in skin thickness compared to untreated skin on day 0. (C) TEWL in back skin during disease course (left) and peak disease on day 4 (right). Data are given as means \pm SEM (n=8 HSD +IMQ, n=16 LSD +IMQ). Analyses were done by (B, C) two-way ANOVA with Bonferroni post-test, (day 4) unpaired two tailed t-test.

7.7 Molecular pathways induced by HSD

To determine the molecular mechanisms by which salt mediates the induction of effector $\gamma\delta$ T17 cells and, therefore consequently has an impact on the inflammatory phenotype, analyses of the transcriptional response in back skin was performed, focusing particularly on regulatory pathways induced by hypertonicity.

Accumulation of sodium in the tissue was accompanied with the induction of the osmosensitive transcription factor *Nfat5* as its expression was significantly increased under high salt conditions only and was further potentiated by the combination of HSD and psoriatic plaque formation (Figure 34A). NFAT5 elicits a genetic program of osmoadaptive responses to restore cellular homeostasis. One important target of NFAT5 is the serum- and glucocorticoid-inducible kinase 1 (SGK1), which enhances *Il23r* expression due to deactivation of its direct repressor, the Forkhead box protein O1 (FOXO1) [164]. No differences were observed in response to HSD concerning

either *Skgl1* or *Foxo1* expression (Figure 34A). However, a significant increase in *I/23r* expression could be detected in treated HSD-fed mice in comparison to treated WT mice fed with chow.

Further, it was investigated whether a signature of increased NFAT5 activity was detectable. Therefore, downstream targets of NFAT5 were analyzed, which are involved in restoring biochemical homeostasis under hypertonic stress, collectively known as osmoprotective genes. Except for prostaglandin *Ptgs2* and *Smit*, which were significantly increased in treated mice under high salt conditions, the transporters *Slc5a3* and *Bgt1* as well as the enzymes *Akr1b1* and *Hspa1b* showed unaltered gene expression (Figure 34B).

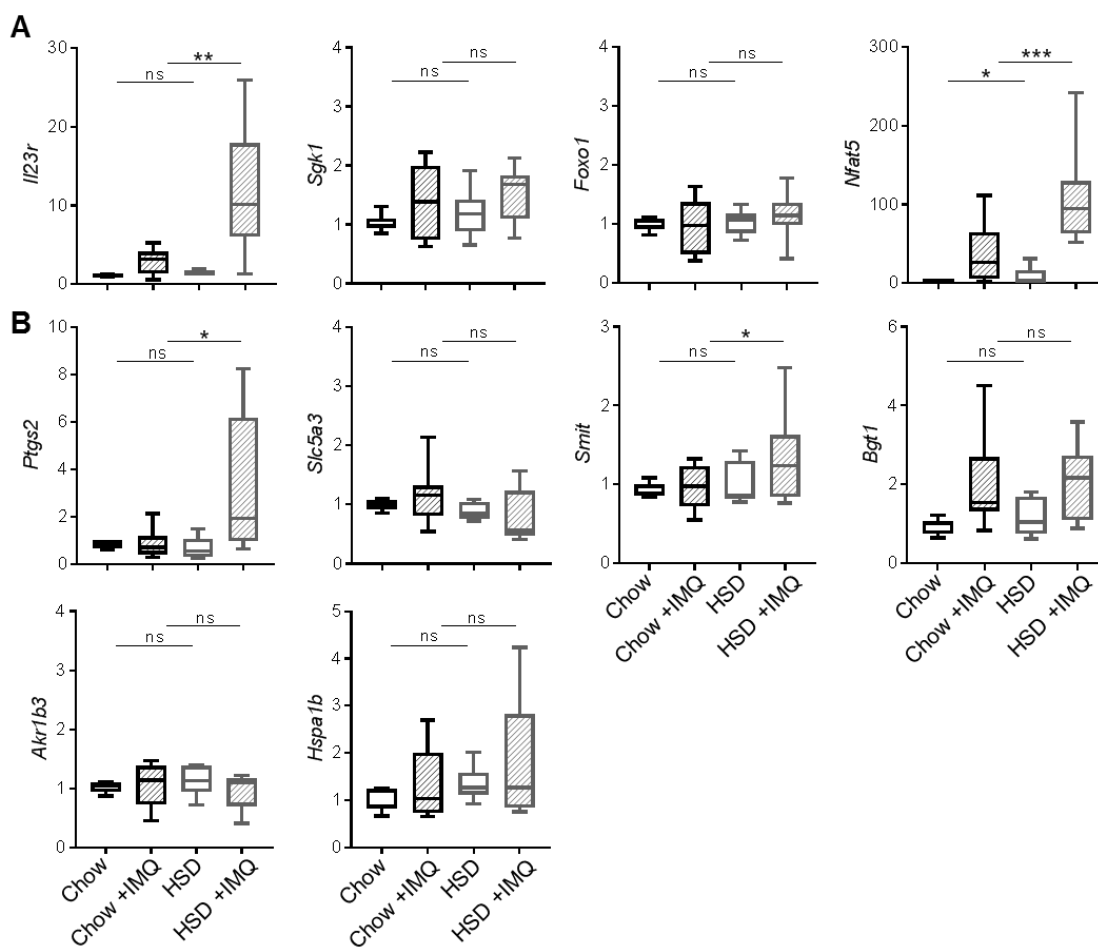


Figure 34: Transcript analysis of the NFAT5-induced osmoadaptive response. RT-qPCR analyses of the whole skin on day 5 post treatment represented as fold changes relative to the average WT expression levels (n=4–12 chow, n=8–20 chow +IMQ, n=4–14 HSD, n=11–18 HSD +IMQ); results were analyzed by unpaired two-tailed t-test.

Beneath the NFAT5-induced osmoadaptive pathway, hypertonicity in the skin can be sensed by the sodium channel Na_x (*Scn7a*). This entails an upregulation of prostasin (*Prss8*), which results in an activation of the sodium channel ENaC (*Scnn1a*), leading to an increased sodium flux. This is further accompanied by downstream mRNA synthesis of inflammatory mediators [157]. The sodium channel Na_x (*SCN7a*) was found to be affected by the high sodium concentrations in the diet only in combination with disease induction, where its expression was significantly increased (Figure 35). No effect was observable in the expression levels of *Prss8* and *Scnn1a* on the transcript level.

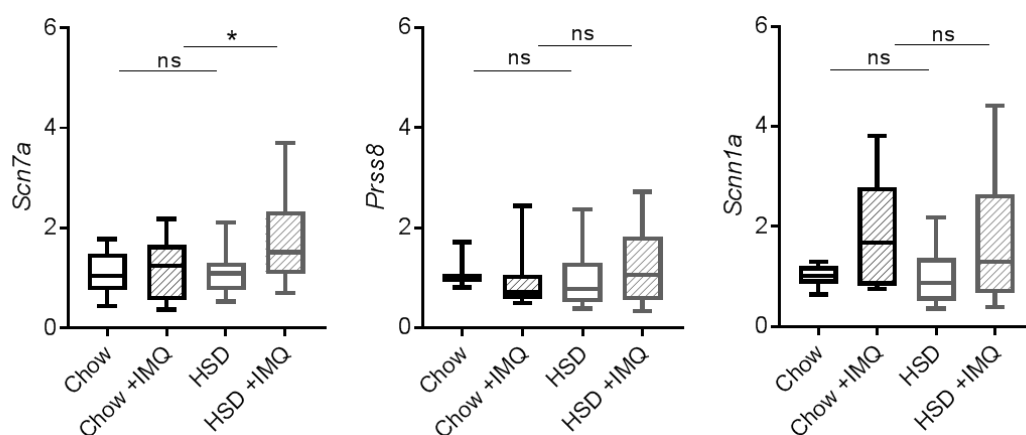


Figure 35: Transcript analysis of sodium channels in the skin. RT-qPCR analyses of the whole skin on day 5 post treatment represented as fold changes relative to the average WT expression levels (n=10–13 chow, n=17–19 chow +IMQ, n=14–15 HSD, n=20–24 HSD +IMQ); results were analyzed by unpaired two-tailed t-test.

A high salt environment in the skin was shown to have direct stimulatory effects on the migration and activation status of $\text{M}\Phi$ [148]. HSD in IMQ-treated mice resulted in a significantly increased expression of the enzyme arginase-1 (*Arg1*), while no differences could be observed concerning *nos2* expression. $\text{M}\Phi$ can further release a variety of growth factors, including vascular endothelial growth factor-C (**VEGF-C**) and are therefore involved in salt-induced hypertension triggered by lymphoangiogenesis, which allows sodium clearance through cutaneous lymph vessels. While *Vegfc* expression increased due to IMQ treatment, no further upregulation was detected under high salt conditions (Figure 36).

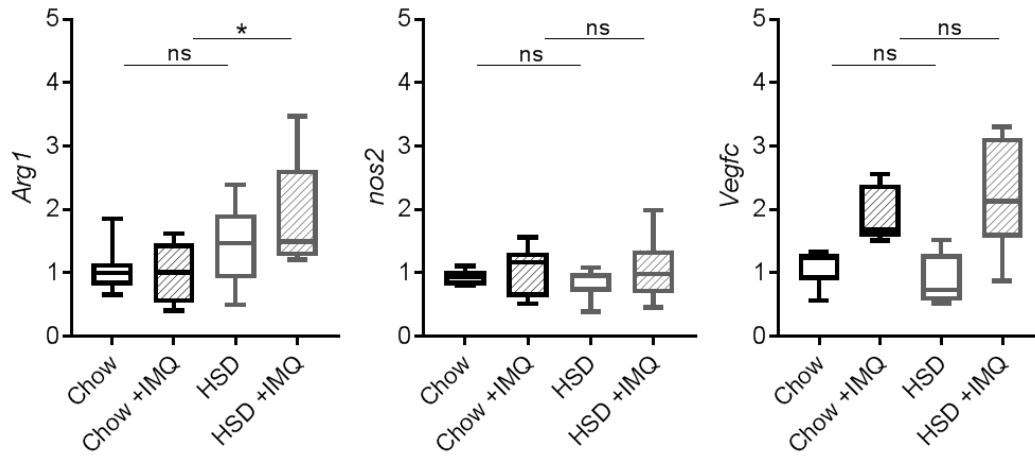


Figure 36: Transcript analysis of selected expression markers of macrophages in the skin. RT-qPCR analyses of the whole skin on day 5 post treatment represented as fold changes relative to the average WT expression levels (n=6–7 chow, n=7–11 chow +IMQ, n=5–6 HSD, n=5–9 HSD +IMQ); results were analyzed by unpaired two-tailed t-test.

8. Discussion

This study investigates the efficacy of current treatment options in psoriasis, focusing on the parallel targeting of IL-12 by anti-p40 therapy and also analyzes the impact of high dietary salt intake on the development of psoriasiform inflammation.

8.1 Targeting IL-12 by anti-p40 therapy is counterproductive in psoriasis treatment

Psoriasis is a chronic, immune-mediated disease with dramatic effects on life quality without a curative treatment available. Currently, ustekinumab is applied for moderate to severe psoriasis vulgaris providing good clinical efficacy in psoriasis patients [127]. But the parallel targeting of IL-12 and IL-23 questioned if the therapeutic activity of the p40-specific antibody Ustekinumab is possibly due to the inhibition of the IL-23 and not IL-12 signaling pathway. Furthermore, mechanistic data on the putative role of either IL-12 or IFN- γ in psoriatic lesions is still lacking. This study aimed to dissect the individual contribution of IL-12 and IL-23 to the formation of psoriatic lesions and to estimate the extent of their therapeutic co-targeting by anti-p40 antibodies.

In the first step treatment with IMQ in $p40^{-/-}$ mice resulted in a greatly decreased psoriatic plaque formation, which is in concordance to the injection of murine IL-12/23p40 antibody into IMQ-treated WT mice [68]. Thus, both findings in mice confirm the reported clinical efficacy of Ustekinumab in psoriasis patients [127], thus presuming that parallel inhibition of IL-12 to IL-23 might amplify the drug's anti-inflammatory effect.

At the time point of the development of IL-12p40 neutralizing antibodies, psoriasis vulgaris was considered a T_H1 effector cell-driven disease with the IL-12/IFN- γ axis as the key mediator of pathogenesis [124]. Focusing on its potential role in plaque development, this study showed that IFN- γ exerts a pro-psoriatic function in the skin, as IMQ-treatment in $IFN\gamma^{-/-}$ mice resulted in a robust amelioration of the disease. This fits to the presence of increased levels of IFN- γ in peripheral blood as well as in skin lesions of patients [73, 74, 76]. These levels further showed a positive correlation with all indices of disease severity, thus serving as a severity and prognostic marker [177]. Moreover, two small pilot studies using a neutralizing humanized anti-IFN- γ antibody (Fontolizumab), demonstrated an improvement of

inflammatory parameters and disease-related gene expression. Although the therapy was well tolerated and safe in psoriasis patients, the clinical efficacy was only minimal, suggesting that it might not be the dominant pathway [123].

With the discovery of IL-23 [78], more and more data obtained from clinical studies as well as mouse models demonstrated the predominant role of IL-23 and its downstream effector cytokines IL-17A, IL-17F and IL-22 in psoriasis development [39]. This is also supported by increased IL-23p19 and IL-23p40 transcripts in psoriatic lesions but not of IL-12p35 [81].

As IL-12 drives the differentiation of naive T cells into IFN- γ -producing T_H1 cells [25], the next step was to investigate its causal relationship in the formation of psoriatic plaques. Therefore, mice with sole IL-12 deficiency were analysed for their response to IMQ treatment. The first key observation in this study was the development of significantly more severe skin inflammation in these mice compared to IMQ-treated WT mice, which was further accompanied with an increased type 17 immune response. This finding strongly contrasts the notion of a dominant pro-psoriatic role of IL-12 in the skin. In addition, these observations reveal that the protective function of IL-12 in skin inflammation is independent of IFN- γ , which itself was found to be pro-inflammatory and to promote plaque formation in this study.

The finding of a protective function of IL-12 in the skin has been described before in the context of UVB-induced inflammation and photocarcinogenesis [178, 179]. Here IL-12 exerts its protective function by inducing DNA damage repair, while its deficiency is associated with a higher risk of UV radiation-induced skin tumors [180, 181]. Furthermore, IL-12 reduces UV-specific DNA lesions in keratinocytes and suppresses their UV-mediated apoptosis [179, 180]. There are also reports showing that IL-12 is able to restrain parts of the inflammatory response in organs other than the skin as mice deficient in IL-12 signaling were more susceptible to the induction of autoimmune inflammation of the central nervous system. In the latter case, however, IFN- γ also exerts a partially protective function [182].

8.1.1 Long-term consequences of IL-12 neutralization in psoriasis treatment

So far, the observations in this study indicate that IL-12, unlike IL-23, has a positive effect in the skin affected by psoriasis. This contrasts to the hypothesis of an enhanced anti-inflammatory effectiveness by additionally blocking IL-12 and points towards a possible counterproductive element in the anti-p40-therapy in psoriasis treatment. Concerning the long-term treatment perspective of psoriasis patients

receiving anti-p40 therapy it is of pivotal importance to clearly specify all aspects of the drug's biological effect.

An important aspect is the antitumor and antimetastatic role of IL-12. Early studies in mice already demonstrated the anti-tumor activity of IL-12 in different murine tumor models [183], which are in part mediated by the induction of T_H1 and cytotoxic T cell responses [184, 185]. The presence of IL-12 at the tumor site further highlights its critical role in tumor regression [186]. Although the therapeutic anti-p40 antibodies Briakinumab and Ustekinumab are very effective and positively evaluated, different clinical trials reported a conspicuously increased rate of cancer after their application [187, 188]. This suggests a potential risk of anti-p40 therapy in psoriasis and highlights once more the importance and necessity of a more specific targeting approach in therapeutic intervention.

At present, clinical trials highlight the therapeutic efficacy of Ustekinumab in Crohn's disease (CD) as both the IL-12/T_H1 and the IL-23/T_H17 axis seem to be relevant in its pathogenesis [189, 190]. In these studies, Ustekinumab showed similar therapeutic efficacy to TNF- α inhibitors [191], the current first line biologic for CD and could induce remission in patients who are resistant to TNF- α inhibitors or have lost responsiveness over time [192]. Due to its rapid onset of action with high response rates, long duration effect and mode of administration, Ustekinumab was approved for the treatment of moderate-to-severe CD by the FDA in 2016 and has the potential to become the first-line treatment option for CD.

These data and own data highlight that depending on the organ and the inflammatory context, cytokines can mediate different effector functions. Therefore, each treatment should aim to target specifically the involved organ and the local cytokines involved in the pathogenesis of a disease.

8.1.2 Future perspectives in psoriasis treatment

As this study strongly points towards a positive role of IL-12 in the skin and discusses the possible consequences of its longterm targeting, the use of IL-12p40 antibodies in psoriasis treatment has to be revised. The use of IL-17A blocking antibodies in this study demonstrates one effective approach to more selectively targeting the relevant pathogenic immune responses, as treatment with anti-IL-17A significantly reduced skin inflammation in mice. Moreover, mice deficient only in IL-23p19 signaling (IL23a^{-/-}) developed no visible signs of inflammation, thus targeting solely IL-23 might be another targeting approach, which minimizes the risk of interference with potential beneficial ones.

Currently, data from past and ongoing comparative clinical studies support a superior clinical efficacy of mAbs targeting solely the IL-23/IL-17 axis, including Secukinumab [132], Ixekizumab [134] and Brodalumab [133] and the IL23p19 inhibitors, Risankizumab [140] and Guselkumab [141], compared to the former approach of targeting the shared subunit of IL-23 and IL-12 with Ustekinumab. At that time, no explanation was available for these observations. This thesis provides for the first time a novel protective role of IL-12 in the skin that may be of relevance for the therapeutic efficacy of selective inhibition of the IL-23/IL-17 axis. This new generation of drugs that target specifically the IL-23/IL-17 axis have the advantage of leaving the T_H1 pathway untouched and thus, consequently sustain the pivotal role of IL-12/IFN- γ signaling in anti-cancer immune-surveillance as previously discussed. In agreement with the findings presented here, anti-IL-23p19 and anti-IL17 therapies will replace Ustekinumab in future psoriasis treatment.

Still open is the questions whether specific inhibition of IL-23p19 may offer comparable or even higher efficacy to IL-17 inhibitors in the treatment of psoriasis. Different outcomes of both inhibitor classes have already been demonstrated in the context of colonic inflammation. Here, deficiency of IL-17A aggravates disease pathology in murine colitis models [193, 194]. Furthermore, inhibition of IL-17 by Secukinumab or Brodalumab in human IBD is not only ineffective, but results in an exacerbated disease activity [195, 196], whereas anti-IL-23p19 mAb are highly efficient [197]. Plausible explanations for the contraindication of IL-17 inhibitors in IBD involve the homeostatic as well as non-immune functions of IL-17A at steady-state, which are independent of IL-23 signaling. To this effect, IL-17A is deeply involved in regular physiological body processes in various tissues e.g. by maintaining epithelial cell barrier integrity in the gut [198]. Moreover, its local expression in adipose tissue was shown to inhibit adipogenesis and to critically regulate glucose metabolism as well as thermogenesis [199, 200]. In contrast, IL-23 seems to be an essential cytokine, which drives maturation and maintenance of pathogenic T_H17 cells, thus, contributing to certain autoimmune and chronic inflammatory diseases [38].

Although targeting IL-17A is efficacious in psoriasis, its contraindication in treatment of IBD demonstrates the dramatic consequences of the pleiotropic effects of cytokines used as therapeutics and emphasizes the context-dependent immunologic roles of IL-17A and IL-23. First results of the ongoing ECLIPSE Phase 3 head-to-head study, which directly compares the anti-IL-23p19 mAb Guselkumab with the IL-17A inhibitor Secukinumab, indicates that Guselkumab can be superior to

Secukinumab in treating moderate to severe plaque psoriasis in adults (clinicaltrials.gov; Identifier: NCT03090100).

Thus, in psoriasis treatment targeting solely IL-23, leaving the homeostatic functions of IL-17 intact, might be a more effective therapeutic approach. Another therapeutic alternative would be the targeted delivery of these cytokine blocking drugs directly to psoriatic skin, thus, bypassing global cytokine inhibition by means of a tissue specific anchor or topical application of smaller therapeutic binders than mAbs.

8.2 IL-12 limits skin inflammation in mice by regulating pathogenic V γ 6⁺ γ δ T17 cells

In mice it is well described that the main drivers of IMQ-induced psoriasiform inflammation are γ δ T17 cells discriminated by their V γ 4⁺ TCR. These skin-invading dermal V γ 4⁺ cells were shown to be necessary and sufficient to drive psoriatic plaque formation by collective delivery of type 17 signature cytokines into the skin, thus, becoming an established marker for disease severity [68]. Although this study confirmed V γ 4⁺ γ δ T17 cells as main drivers of skin inflammation in IMQ-treated WT mice, in mice with IL-12 deficiency another IL-17-producing γ δ T cell sub-population, identified as dermal V γ 6⁺ γ δ T17 cells, aberrantly accumulated in the skin and contributed to the aggravated disease phenotype. Their potential to take up a pathogenic phenotype corresponds well with a report, in which V γ 6⁺ γ δ T cells were characterized as an IL-17-producing effector subset with the capability to induce psoriatic skin inflammation [103]. This work further demonstrated the biological relevance of their pathogenic potential in IMQ-treated WT mice as their frequencies positively correlate with disease severity (skin thickness). By the use of loss- and gain-of-function experiments, this study generated a conclusive picture in which IL-12, produced locally in the inflammatory lesion, exclusively protects the skin from psoriatic inflammation by restricting the numbers of pathogenic V γ 6⁺ γ δ T17 cells, independently of IL-23 and V γ 4⁺ γ δ T17 cells (illustrated in [Figure 37](#)).

The reason why both γ δ T17 subsets perform similar effector functions within the same tissue, but are differently affected by IL-12 signaling, remains an open question. Although a differential regulation program of V γ 4⁺ and V γ 6⁺ γ δ T cells can be assumed, a molecular mechanism accounting for these differences is currently not known. To answer this question, it would be necessary to perform comparative transcriptomic analyses (e.g. next generation sequencing) to gain deeper insights into the molecular pathways driving both subsets.

8.2.1 Significance of the murine findings for humans

Although the IMQ model has proven itself to be a valuable experimental system to understand cellular TLR-specific interactions, it still remains to be established to what extent these findings in mice can be translated into psoriasis of man. While in the murine IMQ model IL-12 restrains the invasion of pathogenic $V\gamma 6^+$ $\gamma\delta T17$ cells, this response is taken over by a different subset or cell population in man. In contrast to murine $\gamma\delta T$ cells, less is known about the precise nature and subsequent steps of functional differentiation of human $\gamma\delta T$ cells and what exact roles they play in host defense, homeostasis and inflammatory skin diseases, like psoriasis.

So far, less is known about tissue resident subsets, preferentially residing at epithelial sites such as the skin [109]. The best characterized subset is represented by the one expressing a peculiar semi-invariant $V\gamma 9^+V\delta 2^+$ TCR. This subset is generated during gestation with pre-programmed effector functions and a restricted TCR specificity [201], thus exhibiting some common features to murine $\gamma\delta T$ cell subsets. As their numbers rapidly increase with age by proliferation of already existing cells, they form the major blood borne $\gamma\delta T$ cell effector subset in healthy adult peripheral blood [202]. Clinical data from psoriasis patients implicated a pathogenic role of $V\gamma 9^+V\delta 2^+$ cells as they can exit the blood and highly accumulate in the inflamed skin producing high amounts of pro-inflammatory mediators such as IL-17A [70, 116]. However, the question if this $\gamma\delta T$ cell subset represents the equivalent to mouse $\gamma\delta T17$ cells remains presently unsolved and needs further investigation, again by performing comparative studies using next generation sequencing technology.

Previously, another unconventional subset of human $V\delta 2^+$ T cells has been identified, which does not co-express $V\gamma 9$. This subset exhibits a naïve phenotype in peripheral blood and can be polarized into different functional effector subsets depending on the cytokine milieu and inflammatory signals [203].

There is also the possibility that the equivalent population to murine $\gamma\delta T$ cells is not represented by human $\gamma\delta T$ cells, but by a cell population, which carries similar functional properties, express the same specific molecules/markers or localizes in the same tissue [204]. Thus, a possible alternative innate cell population in man, which might take over the role of $\gamma\delta T17$ cells in mice, is represented by ILC3s. Even in mice, ILC3s and $\gamma\delta T17$ cells share substantial characteristics, as both specifically localize in certain tissues and are innate-like responders with pre-programmed effector functions [18].

Furthermore, the human skin and in particular the epidermis, is mainly populated by CD8⁺ T_{RM} cells, which are rare in SPF-housed mice due to the lack of immune challenges of the skin immune system under this condition. Following infection or inflammation, memory CD8⁺ T cells populate the skin and become long-lived tissue-resident memory T cells providing a first line of defense against reinfection [205]. These cells stay in close contact with the basement membrane displaying a dendritic morphology similar to that of DETCs [206]. Moreover, CD8⁺ T_{RM} cells were shown to perform innate immune functions including cytokine secretion upon innate signals without any need of TCR engagement comparable to TLRs on innate immune cells [207]. Importantly, in mice their formation is accompanied with a reduction of DETCs suggesting a competition of both populations for local survival signals (e.g. IL-2 and -15) and space within an epidermal niche [208]. Thus, the emerging differences in cell populations might not originate between mouse and man, but develop between an experienced-mature and an unexperienced-immature immune system. Therefore, skin-resident memory T cells might replace innate T cells as they compete more effectively for an epidermal niche and take over some of their functions.

8.3 IL-12 initiates a tissue-protective response in keratinocytes

The accumulation of pathogenic V γ 6⁺ $\gamma\delta$ T17 cells in the skin of mice was shown to be limited by IL-12. Unexpectedly, $\gamma\delta$ T17 cells did not directly respond to IL-12 in this study, as *I12rb2* was only expressed by DETCs and keratinocytes (published in [173]). DETCs respond to IL-12 inducing a type 1 response dominated by IFN- γ [176], which did not mediate the observed, protective effect in psoriatic plaque formation. Generation of bone marrow/thymocyte chimeras suggested the stromal compartment of the skin to be the essential IL-12 signal recipient, as treatment with IMQ led to a more severe skin inflammation when IL-12R was absent on the skin stroma (published in [173]). Although stromal cells mainly provide an important structural component for tissues under physiological conditions, they are also involved in the regulation of immune responses by directing immune cell migration, activation and survival, as well as their organization within the tissue. Moreover, in situations of pathogen threat or during inflammation they can acquire novel features [209, 210]. In fibroblasts, signals derived from infiltrating cells such as IL-4, IFN- γ and TNF- α can influence the persistence of inflammatory processes by modification of their transcriptional profile [211]. Similarly, TNF- α has been shown to interact with

both haematopoietic and stromal cells, thus exacerbating epithelial inflammation [212]. The observed expression of high levels of *Il12rb2* by murine and human keratinocytes in this study demonstrates that they are able to respond to IL-12, and thus to regulate subsiding immune responses in the psoriatic skin. Moreover, after pre-activation with TNF- α , the application of IL-12 to primary human keratinocytes resulted in an enhancement of biological processes (e.g. multicellular organismal and system development, cytoskeleton rearrangement, published in [173]), which are known to be downregulated in psoriatic compared to healthy skin [213]. Additionally, similar processes were observed in the comparison of IMQ-treated *Il12rb2*^{-/-} versus WT mice, with the majority of transcriptional changes found in gene families involved in tissue structure, keratinocyte differentiation and basement membrane integrity (published in [173]). This data fits to the findings by Molenda and colleagues, in which they could show that pre-treatment of keratinocytes with IL-12 has a modulatory effect on the transcriptional profile, which was initiated by UV (e.g. cytoskeletal, junctional, extracellular matrix and signaling proteins, RNA processing enzymes), thereby enhancing protective and at the same time dampening deleterious processes [214]. Thus, in contrast to its function on lymphocytes, under inflammatory conditions the transcriptional profile of murine and human keratinocytes is visibly modulated by IL-12, including changes in trafficking, tissue structure and remodeling [published in [173]]. Identification of common regulatory elements in the IL-12-dependent subset of inflammation-regulated genes may shed light on the underlying molecular mechanisms of how IL-12 counter-regulates the transcriptional changes in keratinocytes caused by psoriasiform inflammation.

8.4 Nutritional salt shapes the psoriatic skin microenvironment through induction of pathogenic $\gamma\delta$ T17 cells

Psoriasis results from an interplay of genetic and environmental risk factors as well as involvement of a complex network of inflammatory cells and cytokines. As the incidence of psoriasis has increased during recent decades, especially in developed countries [215] where no fundamental changes in the genetic basis can be expected, lifestyle factors are in the focus to play a substantial part in it [144]. Currently, consumption of excess dietary salt (>5g/day) is under discussion to favor the development of autoimmunity by increasing the differentiation of naive $\alpha\beta$ T cells into pro-inflammatory T_H17 cells [163, 164]. Thus, the second aim of this study was

to investigate the effect of high dietary salt intake on psoriasis development. Therefore, psoriatic plaque formation was induced in wildtype mice fed with high salt diet using the IMQ-model. Special focus was put on $\gamma\delta$ T cells as critical triggers in psoriasis development and important producers of IL-17.

This study shows that excessive intake of dietary salt exacerbates skin inflammation by priming the skin-resident immune system towards a pro-inflammatory environment with a type 17 signature, thereby promoting immune-pathogenic processes. This is in concordance with the findings in other murine models of autoimmune diseases, where HSD also accelerated the onset and aggravated disease severity of e.g. EAE and IBD due to higher frequencies of IL-17-producing $CD4^+$ T cells [163, 168]. Furthermore, supportive human data comes from studies on MS patients, showing that increased sodium concentrations found within inflammatory lesions are associated with greater disability and worse clinical progression [216, 217].

Studies in rats on HSD [153] as well as long-term observations in humans [149, 150] identified the skin as one major kidney-independent Na^+ reservoir. As this storage is dynamic and can be actively induced, the skin is able to regulate its own electrolyte microenvironment by creating a local osmotic Na^+ -gradient from epidermis to dermis, which has functional implications [152, 153]. Thus, focusing on skin tissue-resident $\gamma\delta$ T cells as local drivers of psoriasiform skin inflammation revealed that high salt intake had some remarkable effects on $V\gamma 6^+$ $\gamma\delta$ T cells. These cells increased in number in the skin, even in absence of any inflammatory stimuli, whereas $V\gamma 4^+$ $\gamma\delta$ T cell numbers did not change dramatically. The fact, that the inflammatory effects of HSD are not limited to $\alpha\beta$ T cells, was recently shown as induction of colitis in HSD-fed *RAG*^{-/-} mice, which lack mature B and T cells, induced detectable signs of inflammation, suggesting an involvement of innate, tissue resident IL-17-producing cells, like ILC3s and $\gamma\delta$ T cells [218].

More importantly, the accumulation of $V\gamma 6^+$ $\gamma\delta$ T cells under high salt conditions was causative for disease aggravation as HSD-fed *V δ 1*^{-/-} mice did not show the high salt-induced disease phenotype. These observations favor the notion that in a high salt environment, rather than $V\gamma 4^+$ $\gamma\delta$ T cells, $V\gamma 6^+$ $\gamma\delta$ T cells are the dominant and critical source of IL-17A, thus, contributing to the exacerbated formation of acute psoriasiform lesions (Figure 37).

At present, it is unclear if skin-invading $V\gamma 6^+$ $\gamma\delta$ T17 cells can directly sense and respond to elevated salt concentrations as opposed to $V\gamma 4^+$, which might not be able to. Preliminary *in vitro* data indicate that $\gamma\delta$ T cells are indeed directly affected by an increase of sodium concentration and respond with increased IL-17A production

(data not shown). The future steps for this work will be to confirm *in vitro* the high salt-induced expression of higher IL-17A levels by the V γ 6⁺ $\gamma\delta$ T cell subset. Besides performing these additional *in vitro* studies, it should be taken into account that also other cells could be involved as direct responders to high salt conditions. Potential responders in the skin could be ILCs [68] and stromal cells [157]. Thus, high salt intake in the skin may affect the cellular activity of stromal cells by e.g. inducing transcriptional modifications, which in turn could alter the local immune cell composition. Due to the cross-talk between lymphocytes and stromal cells, salt might therefore indirectly regulate V γ 6⁺ $\gamma\delta$ T cells by creating an environment that supports their accumulation and survival in the skin, making them competitive to other cell populations.

8.4.1 Molecular mechanism of the high salt induced effect on $\gamma\delta$ T17 cells

So far, the postulated underlying molecular mechanism how naive CD4⁺ T cells are polarized into T_H17 cells under high salt conditions includes the involvement of p38/mitogen-activated protein kinase (**p38/MAPK**), nuclear factor of activated T cells-5 (**NFAT5**) as well as serum- and glucocorticoid-inducible kinase 1 (**SGK1**)-dependent signaling [163, 164, 219]. A high sodium concentration increases the phosphorylation of p38/MAPK, which induces the expression of *Nfat5* and thus activates SGK1. This further leads to enhanced *Il23r* expression by deactivation of its direct repressor, the Forkhead box protein O1 (**FOXO1**) and as a consequence to an enhanced T_H17 cell differentiation [164].

In this thesis a significant induction of *Nfat5* expression was detected in the skin of HSD-fed mice with further increase after disease induction, while *Sgk1* and *Foxo1* were neither up- nor downregulated in response to HSD. For *Il23r* expression a significant increase was observed in mice on HSD, but only after IMQ treatment. This would fit to an increase of cells carrying the IL-23R, like $\gamma\delta$ T17 cells and to an increased amount of IL-23R on the surface of these cells, but it may also not necessarily be associated with an induction of this receptor by SGK-1. It should be noted that the time-point of transcriptional analysis may be critical, as SGK-1 is a kinase and might therefore rapidly change its expression in the inflammatory process. This has been demonstrated by a recent study, which analyzed the expression levels of *Sgk1* in colon tissue after oral administration of a high concentrated salt solution. Here, an increase in *Sgk1* was only measurable after 90 min, whereas it decreased after 120 h or 3 weeks of HSD consumption [218]. Therefore, in the current work *Sgk1* expression might increase within hours at the

beginning of HSD consumption and then further decreases to normal levels during 4 weeks of HSD, due to compensatory mechanisms.

Although an increase of *Nfat5* expression was detected no osmoprotective response signature was observed in the skin (unaltered expression of NFAT5 downstream effector molecules e.g. *Slc5a3*, *Smit*, *Ptgs2*). This could mean that no osmotic stress is induced in the tissue by the diet or that NFAT5 exerts a more cell and context-specific functional role through alternative pathways, as NFAT5 is able to induce cell-specific gene expression in e.g. M Φ , T and B cells under hypertonic conditions [158, 220, 221]. The discovery of additional pathways of NFAT5, especially in T cells, and the conditions on which they become induced, may give a deeper insight into its functional role.

Additionally, perturbations of epithelial sodium homeostasis are sensed by the sodium channel Na_x (*SCN7a*). Its activation manipulates sodium flux through upregulation of prostasin (*PRSS8*) and activation of ENaC (*Scnn1a*) on keratinocytes and is also regulated, at least in part, by NFAT5 and SGK-1 [157, 222]. As an induction was only observed for Na_x by the combination of HSD and disease, further analyses of Na_x, prostasin and ENaC expression levels, specifically in keratinocytes, are necessary. This will evaluate if they play a decisive role during HSD and are involved in the aggravated disease phenotype by increasing synthesis of inflammatory mediators (PTGS2, IL-1 β , IL-8) [157].

A hypertonic microenvironment due to increased Na⁺ concentrations in the skin was shown to act as a chemotactic stimulus for infiltrating M Φ , which become activated and support the antimicrobial host defense in the skin in situations of bacterial skin infections in mice and humans [148]. Moreover, HSD in EAE-diseased mice led to a polarization of M Φ into M Φ 1 effector cells, which infiltrate the central nervous system and contribute to a more severe disease phenotype, while the development and functionality of alternative M Φ 2 is impaired [161, 162]. However, the results presented in this thesis do not sustain a potential involvement of M Φ , as expression of *Arg1* (M Φ 2), *nos2* (M Φ 1) as well as *Vegf-c* remained unaltered.

The lack of alteration in gene expression (sodium channels, NFAT5 and downstream molecules) could be attributed to the fact that whole tissue lysates were used for the analysis. These qPCR experiments are therefore limited in resolution and the measured effects are integrals of different independent effects in different cells of the tissue. Thus, it is of special interest to further analyze the relevance of the discussed pathways, specifically in $\gamma\delta$ T cells, and to uncover potential additional mechanisms, contributing to the inflammatory effects triggered by high salt. One difficulty concerning $\gamma\delta$ T cells, especially the individual subsets, will be their highly

limited number, which makes it often difficult to get enough material. Therefore, a small molecule screen of FACS sorted $\gamma\delta$ T cell subsets from either HSD-fed mice or from WT mice with subsequent *in vitro* expansion under high salt conditions is now investigated. A following gene expression analysis of these sorted/harvested cells is planned by either qPCR or, what might be an even better approach, with RNA sequencing. The advantage of RNA sequencing is provided by the sensitive analysis of the whole transcriptome, which includes mRNA as well as non-coding and small RNA, in a single cell assay without the limitation of prior knowledge. Moreover, to verify the involvement of NFAT5 or SGK-1, these molecules will be specifically inhibited by the use of small molecule inhibitors or silencing short hairpin RNA in *in vitro* cultured $\gamma\delta$ T cells with subsequent analysis of the cytokine profile. The use of knock-out mice lacking one of these factors in $\gamma\delta$ T cells will provide additional prove *in vivo*.

8.4.2 Impact of high salt diet on the skin microbiome

In addition to its direct immune effects, salt might also affect the composition of the skin microbiome leading to transient or persistent modifications in the resident bacteria [223]. So far, a first published study only focuses on the influence of HSD on the gut microbiome, demonstrating the suppression of several intestinal bacteria by HSD, with species of *Lactobacillus spp.* being nearly depleted in mice and reduced intestinal survival in humans. Supplementation of this species ameliorated the salt-induced aggravation in the EAE-model by reduction of T_H17 cells [224].

Preliminary collected data already identified changes in the skin microbiome when mice received HSD for one week without disease induction (data not shown). Striking in this context was the reduced alpha-diversity after HSD, which can be explained by the dominance of a fewer number of bacterial phyla, mainly *Firmicutes*, above all others. This can be due to their halophilic or halotolerant characteristics in addition to an inhibitory effect of salt on the other bacteria. A deeper look into the sub-species revealed an increase of the pathogens *Aerococcus viridans* and *Staphylococcus lentus*, which may display harmful effects under longer periods of HSD. These changes in the skin microbiome could further influence local T cell functions through their capacity in tuning the local innate immune milieu. Under inflammatory conditions these findings might have even more relevance as the skin microbiome of psoriasis patients already differs from healthy subjects by means of reduced community stability and decreased levels of immunoregulatory bacteria (e.g. *Staphylococcus epidermidis*, *Propionibacterium acnes*). A potential consequence is the colonization of lesional skin with pathogens (e.g.

Staphylococcus aureus), which might aggravate cutaneous inflammation via the type 17 axis [225]. To further analyze the possible impact of the HSD-induced bacteria on disease aggravation, they should be isolated and applied on mouse skin. This may unravel if the abundance of specific commensal bacteria that populate the skin under HSD affects $V\gamma 6^+$ $\gamma\delta T17$ cells by supporting their accumulation in specific skin niches.

8.5 Conclusion

In summary, this study indicates that targeting IL-12 by anti-p40 therapy is counterproductive in psoriasis treatment as it exerts a positive effect in the skin affected by psoriasis. Furthermore, this study identifies a direct communication of IL-12 with the stromal microenvironment and presents a new concept of how the local stroma can be modified by a single cytokine. This modification of tissue structure by IL-12 might open or close a cellular niche, which in turn might allow specific immune cell subsets to populate and accumulate in the tissue. It has to be considered that IL-12 might not exclusively mediate its anti-psoriatic effect through the keratinocyte compartment. Therefore screening of additional IL-12-responsive cell types e.g. other tissue forming cells, like fibroblasts, mesenchymal cells or nerve cells will be necessary. Depending on the type of stromal cell involved and its cellular activity, the composition of adaptive and innate immune cells may differ, which could determine the outcome of immune responses in autoimmune and inflammatory diseases. Although this study demonstrated that, in absence of IL-12R on murine keratinocytes and under high salt condition, the affected immune cell population contributing to the aggravated disease phenotype is represented by pathogenic $V\gamma 6^+$ $\gamma\delta T17$ cells (illustrated in [Figure 37](#)), in humans this function might be carried out by other cell types.

Furthermore, this thesis provides evidence that besides a single cytokine, also a single nutritional component has the ability to modulate not only adaptive, but also innate immune cells as well as their responses. Therefore, dietary salt represents one possible lifestyle factor that, in combination with others (e.g. infection, injury), can trigger psoriasis development (illustrated in [Figure 37](#)).

Future studies on the compartmentalization and dynamic regulation of salt in distinct tissues will be necessary to discover the full repertoire of the immunomodulatory effects in health and disease. Currently, only few human studies are available, which suggests an association between high salt intake and development of immune-

mediated diseases [169, 170]. Robustly powered prospective intervention studies of high salt-consuming individuals and their risk for developing autoimmune diseases with strong type 17 components (e.g. MS, psoriasis) as well as clinical trials studying the effect of salt restriction in patients already suffering from them are missing until now. Considering excessive salt intake as a potential risk factor for autoimmune diseases, including psoriasis, EAE or IBD, salt restriction and development of salt-lowering treatments may have potential clinical relevance in alleviating the disease severity of affected patients.

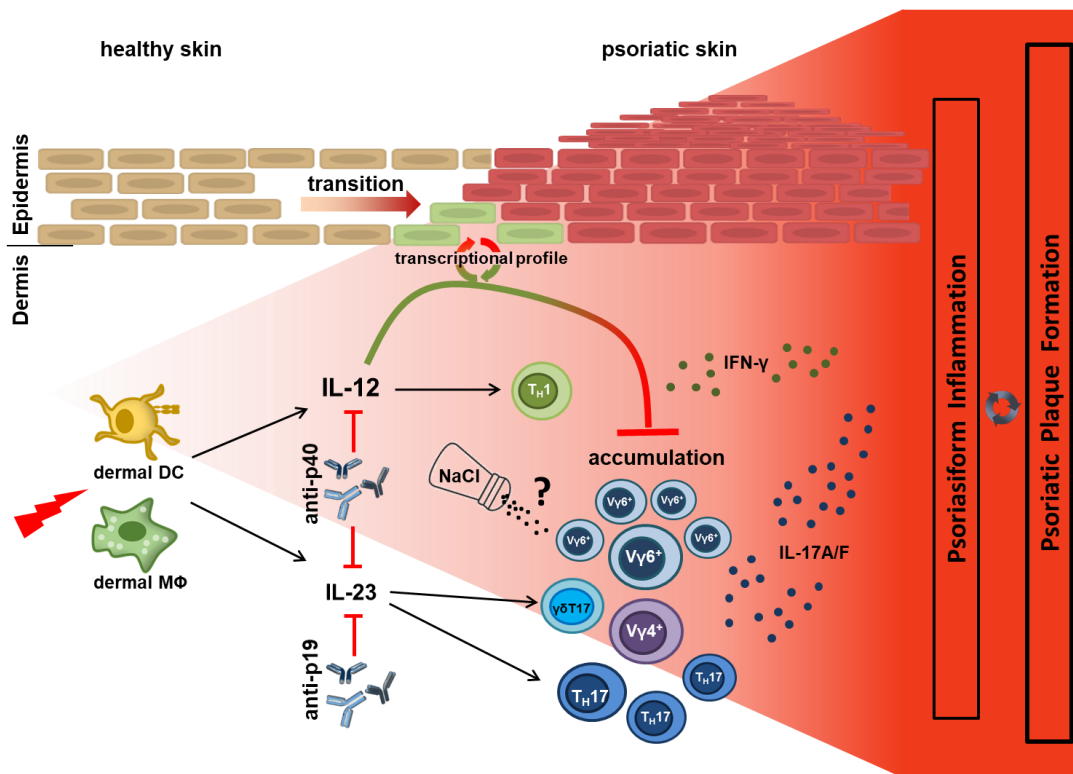


Figure 37: Protective function of IL-12 in the skin and the effect of high dietary salt intake on the development of psoriatic plaque formation. New concept of how the local stroma can be modified by IL-12, which counter-regulates changes in keratinocytes induced by inflammatory stimuli, while in absence of IL-12R on murine keratinocytes pathogenic Vγ6+ γδT17 cells accumulate in the skin contributing to psoriasis development. Dietary salt is one possible lifestyle factor with the ability to modulate innate immune cells as well as their responses, thus triggering psoriasis development.

Literature

1. Abbas, A.K., A.H. Lichtman, and S. Pillai, *Cellular and molecular immunology*. Eighth edition. ed. 2015, Philadelphia, PA: Elsevier Saunders. viii, 535 pages.
2. Murphy, K. and C. Weaver, *Janeway's immunobiology*. 9th edition. ed. 2016, New York, NY: Garland Science/Taylor & Francis Group, LLC. xx, 904 pages.
3. Streilein, J.W., *Skin-associated lymphoid tissues (SALT): origins and functions*. *J Invest Dermatol*, 1983. **80 Suppl**: p. 12s-16s.
4. Matejuk, A., *Skin Immunity*. *Arch Immunol Ther Exp (Warsz)*, 2018. **66**(1): p. 45-54.
5. Nestle, F.O., et al., *Skin immune sentinels in health and disease*. *Nat Rev Immunol*, 2009. **9**(10): p. 679-91.
6. Watt, F.M., *Terminal differentiation of epidermal keratinocytes*. *Curr Opin Cell Biol*, 1989. **1**(6): p. 1107-15.
7. Lebre, M.C., et al., *Human keratinocytes express functional Toll-like receptor 3, 4, 5, and 9*. *J Invest Dermatol*, 2007. **127**(2): p. 331-41.
8. Albanesi, C., et al., *Keratinocytes in inflammatory skin diseases*. *Curr Drug Targets Inflamm Allergy*, 2005. **4**(3): p. 329-34.
9. Kennedy-Crispin, M., et al., *Human keratinocytes' response to injury upregulates CCL20 and other genes linking innate and adaptive immunity*. *J Invest Dermatol*, 2012. **132**(1): p. 105-13.
10. Janeway, C.A., Jr. and R. Medzhitov, *Innate immune recognition*. *Annu Rev Immunol*, 2002. **20**: p. 197-216.
11. Hashimoto, D., et al., *Tissue-resident macrophages self-maintain locally throughout adult life with minimal contribution from circulating monocytes*. *Immunity*, 2013. **38**(4): p. 792-804.
12. Yanez, D.A., et al., *The role of macrophages in skin homeostasis*. *Pflugers Arch*, 2017. **469**(3-4): p. 455-463.
13. Kissenpfennig, A., et al., *Dynamics and function of Langerhans cells in vivo: dermal dendritic cells colonize lymph node areas distinct from slower migrating Langerhans cells*. *Immunity*, 2005. **22**(5): p. 643-54.
14. Kubo, A., et al., *External antigen uptake by Langerhans cells with reorganization of epidermal tight junction barriers*. *J Exp Med*, 2009. **206**(13): p. 2937-46.
15. Krystel-Whittemore, M., K.N. Dileepan, and J.G. Wood, *Mast Cell: A Multi-Functional Master Cell*. *Front Immunol*, 2015. **6**: p. 620.
16. Hamerman, J.A., K. Ogasawara, and L.L. Lanier, *NK cells in innate immunity*. *Curr Opin Immunol*, 2005. **17**(1): p. 29-35.

17. Kronenberg, M., *Toward an understanding of NKT cell biology: progress and paradoxes*. *Annu Rev Immunol*, 2005. **23**: p. 877-900.
18. Yang, J., et al., *Establishment and function of tissue-resident innate lymphoid cells in the skin*. *Protein Cell*, 2017. **8**(7): p. 489-500.
19. Uchida, Y., et al., *Role for E-cadherin as an inhibitory receptor on epidermal gammadelta T cells*. *J Immunol*, 2011. **186**(12): p. 6945-54.
20. Jameson, J., et al., *A role for skin gammadelta T cells in wound repair*. *Science*, 2002. **296**(5568): p. 747-9.
21. Macleod, A.S. and W.L. Havran, *Functions of skin-resident gammadelta T cells*. *Cell Mol Life Sci*, 2011. **68**(14): p. 2399-408.
22. Sumaria, N., et al., *Cutaneous immunosurveillance by self-renewing dermal gammadelta T cells*. *J Exp Med*, 2011. **208**(3): p. 505-18.
23. Clark, R.A., et al., *The vast majority of CLA+ T cells are resident in normal skin*. *J Immunol*, 2006. **176**(7): p. 4431-9.
24. Watanabe, R., et al., *Human skin is protected by four functionally and phenotypically discrete populations of resident and recirculating memory T cells*. *Sci Transl Med*, 2015. **7**(279): p. 279ra39.
25. Manetti, R., et al., *Natural killer cell stimulatory factor (interleukin 12 [IL-12]) induces T helper type 1 (Th1)-specific immune responses and inhibits the development of IL-4-producing Th cells*. *J Exp Med*, 1993. **177**(4): p. 1199-204.
26. Szabo, S.J., et al., *A novel transcription factor, T-bet, directs Th1 lineage commitment*. *Cell*, 2000. **100**(6): p. 655-69.
27. Zheng, W. and R.A. Flavell, *The transcription factor GATA-3 is necessary and sufficient for Th2 cytokine gene expression in CD4 T cells*. *Cell*, 1997. **89**(4): p. 587-96.
28. Mosmann, T.R., et al., *Two types of murine helper T cell clone. I. Definition according to profiles of lymphokine activities and secreted proteins*. *J Immunol*, 1986. **136**(7): p. 2348-57.
29. Park, H., et al., *A distinct lineage of CD4 T cells regulates tissue inflammation by producing interleukin 17*. *Nat Immunol*, 2005. **6**(11): p. 1133-41.
30. Harrington, L.E., et al., *Interleukin 17-producing CD4+ effector T cells develop via a lineage distinct from the T helper type 1 and 2 lineages*. *Nat Immunol*, 2005. **6**(11): p. 1123-32.
31. Ivanov, II, et al., *The orphan nuclear receptor RORgammat directs the differentiation program of proinflammatory IL-17+ T helper cells*. *Cell*, 2006. **126**(6): p. 1121-33.
32. Aggarwal, S., et al., *Interleukin-23 promotes a distinct CD4 T cell activation state characterized by the production of interleukin-17*. *J Biol Chem*, 2003. **278**(3): p. 1910-4.
33. Acosta-Rodriguez, E.V., et al., *Surface phenotype and antigenic specificity of human interleukin 17-producing T helper memory cells*. *Nat Immunol*, 2007. **8**(6): p. 639-46.

34. Veldhoen, M., et al., *TGFbeta in the context of an inflammatory cytokine milieu supports de novo differentiation of IL-17-producing T cells*. *Immunity*, 2006. **24**(2): p. 179-89.
35. McGeachy, M.J., et al., *The interleukin 23 receptor is essential for the terminal differentiation of interleukin 17-producing effector T helper cells in vivo*. *Nat Immunol*, 2009. **10**(3): p. 314-24.
36. Korn, T., et al., *IL-17 and Th17 Cells*. *Annu Rev Immunol*, 2009. **27**: p. 485-517.
37. Curtis, M.M. and S.S. Way, *Interleukin-17 in host defence against bacterial, mycobacterial and fungal pathogens*. *Immunology*, 2009. **126**(2): p. 177-85.
38. Langrish, C.L., et al., *IL-23 drives a pathogenic T cell population that induces autoimmune inflammation*. *J Exp Med*, 2005. **201**(2): p. 233-40.
39. Di Cesare, A., P. Di Meglio, and F.O. Nestle, *The IL-23/Th17 axis in the immunopathogenesis of psoriasis*. *J Invest Dermatol*, 2009. **129**(6): p. 1339-50.
40. Eyerich, S., et al., *Th22 cells represent a distinct human T cell subset involved in epidermal immunity and remodeling*. *J Clin Invest*, 2009. **119**(12): p. 3573-85.
41. Sakaguchi, S., et al., *Foxp3+ CD25+ CD4+ natural regulatory T cells in dominant self-tolerance and autoimmune disease*. *Immunol Rev*, 2006. **212**: p. 8-27.
42. Di Meglio, P., F. Villanova, and F.O. Nestle, *Psoriasis*. *Cold Spring Harb Perspect Med*, 2014. **4**(8).
43. World Health Organization (WHO). *Global Report on Psoriasis*. 2016 [cited 2019 May]; Available from: <https://apps.who.int/iris/handle/10665/204417>.
44. Trembath, R.C., et al., *Identification of a major susceptibility locus on chromosome 6p and evidence for further disease loci revealed by a two stage genome-wide search in psoriasis*. *Hum Mol Genet*, 1997. **6**(5): p. 813-20.
45. Nair, R.P., et al., *Evidence for two psoriasis susceptibility loci (HLA and 17q) and two novel candidate regions (16q and 20p) by genome-wide scan*. *Hum Mol Genet*, 1997. **6**(8): p. 1349-56.
46. Capon, F., et al., *Sequence variants in the genes for the interleukin-23 receptor (IL23R) and its ligand (IL12B) confer protection against psoriasis*. *Hum Genet*, 2007. **122**(2): p. 201-6.
47. Cargill, M., et al., *A large-scale genetic association study confirms IL12B and leads to the identification of IL23R as psoriasis-risk genes*. *Am J Hum Genet*, 2007. **80**(2): p. 273-90.
48. Nair, R.P., et al., *Genome-wide scan reveals association of psoriasis with IL-23 and NF-kappaB pathways*. *Nat Genet*, 2009. **41**(2): p. 199-204.
49. Stuart, P.E., et al., *Genome-wide association analysis identifies three psoriasis susceptibility loci*. *Nat Genet*, 2010. **42**(11): p. 1000-4.
50. Ellinghaus, E., et al., *Genome-wide association study identifies a psoriasis susceptibility locus at TRAF3IP2*. *Nat Genet*, 2010. **42**(11): p. 991-5.

51. de Cid, R., et al., *Deletion of the late cornified envelope LCE3B and LCE3C genes as a susceptibility factor for psoriasis*. Nat Genet, 2009. **41**(2): p. 211-5.
52. Huffmeier, U., et al., *Replication of LCE3C-LCE3B CNV as a risk factor for psoriasis and analysis of interaction with other genetic risk factors*. J Invest Dermatol, 2010. **130**(4): p. 979-84.
53. Gelfand, J.M., et al., *Risk of myocardial infarction in patients with psoriasis*. JAMA, 2006. **296**(14): p. 1735-41.
54. Ahlehoff, O., et al., *Psoriasis is associated with clinically significant cardiovascular risk: a Danish nationwide cohort study*. J Intern Med, 2011. **270**(2): p. 147-57.
55. Lonnberg, A.S., et al., *Association of Psoriasis With the Risk for Type 2 Diabetes Mellitus and Obesity*. JAMA Dermatol, 2016. **152**(7): p. 761-7.
56. Gisondi, P., et al., *Prevalence of metabolic syndrome in patients with psoriasis: a hospital-based case-control study*. Br J Dermatol, 2007. **157**(1): p. 68-73.
57. Cohen, A.D., J. Driehar, and S. Birkenfeld, *Psoriasis associated with ulcerative colitis and Crohn's disease*. J Eur Acad Dermatol Venereol, 2009. **23**(5): p. 561-5.
58. Gelfand, J.M., et al., *The risk of mortality in patients with psoriasis: results from a population-based study*. Arch Dermatol, 2007. **143**(12): p. 1493-9.
59. Abuabara, K., et al., *Cause-specific mortality in patients with severe psoriasis: a population-based cohort study in the U.K.* Br J Dermatol, 2010. **163**(3): p. 586-92.
60. Chuang, S.Y., et al., *Murine models of psoriasis and their usefulness for drug discovery*. Expert Opin Drug Discov, 2018. **13**(6): p. 551-562.
61. van der Fits, L., et al., *Imiquimod-induced psoriasis-like skin inflammation in mice is mediated via the IL-23/IL-17 axis*. J Immunol, 2009. **182**(9): p. 5836-45.
62. Gilliet, M., et al., *Psoriasis triggered by toll-like receptor 7 agonist imiquimod in the presence of dermal plasmacytoid dendritic cell precursors*. Arch Dermatol, 2004. **140**(12): p. 1490-5.
63. Beutner, K.R., et al., *Treatment of genital warts with an immune-response modifier (imiquimod)*. J Am Acad Dermatol, 1998. **38**(2 Pt 1): p. 230-9.
64. Geisse, J.K., et al., *Imiquimod 5% cream for the treatment of superficial basal cell carcinoma: a double-blind, randomized, vehicle-controlled study*. J Am Acad Dermatol, 2002. **47**(3): p. 390-8.
65. Szeimies, R.M., et al., *Imiquimod 5% cream for the treatment of actinic keratosis: results from a phase III, randomized, double-blind, vehicle-controlled, clinical trial with histology*. J Am Acad Dermatol, 2004. **51**(4): p. 547-55.
66. Fanti, P.A., et al., *Generalized psoriasis induced by topical treatment of actinic keratosis with imiquimod*. Int J Dermatol, 2006. **45**(12): p. 1464-5.
67. Rajan, N. and J.A. Langtry, *Generalized exacerbation of psoriasis associated with imiquimod cream treatment of superficial basal cell carcinomas*. Clin Exp Dermatol, 2006. **31**(1): p. 140-1.

68. Pantelyushin, S., et al., *Rorgammat+ innate lymphocytes and gammadelta T cells initiate psoriasiform plaque formation in mice*. J Clin Invest, 2012. **122**(6): p. 2252-6.
69. Ueyama, A., et al., *Mechanism of pathogenesis of imiquimod-induced skin inflammation in the mouse: a role for interferon-alpha in dendritic cell activation by imiquimod*. J Dermatol, 2014. **41**(2): p. 135-43.
70. Cai, Y., et al., *Pivotal role of dermal IL-17-producing gammadelta T cells in skin inflammation*. Immunity, 2011. **35**(4): p. 596-610.
71. Ellis, C.N., et al., *Cyclosporine improves psoriasis in a double-blind study*. JAMA, 1986. **256**(22): p. 3110-6.
72. Gottlieb, S.L., et al., *Response of psoriasis to a lymphocyte-selective toxin (DAB389IL-2) suggests a primary immune, but not keratinocyte, pathogenic basis*. Nat Med, 1995. **1**(5): p. 442-7.
73. Uyemura, K., et al., *The cytokine network in lesional and lesion-free psoriatic skin is characterized by a T-helper type 1 cell-mediated response*. J Invest Dermatol, 1993. **101**(5): p. 701-5.
74. Schlaak, J.F., et al., *T cells involved in psoriasis vulgaris belong to the Th1 subset*. J Invest Dermatol, 1994. **102**(2): p. 145-9.
75. Yawalkar, N., et al., *Expression of interleukin-12 is increased in psoriatic skin*. J Invest Dermatol, 1998. **111**(6): p. 1053-7.
76. Austin, L.M., et al., *The majority of epidermal T cells in Psoriasis vulgaris lesions can produce type 1 cytokines, interferon-gamma, interleukin-2, and tumor necrosis factor-alpha, defining TC1 (cytotoxic T lymphocyte) and TH1 effector populations: a type 1 differentiation bias is also measured in circulating blood T cells in psoriatic patients*. J Invest Dermatol, 1999. **113**(5): p. 752-9.
77. Johnson-Huang, L.M., et al., *A single intradermal injection of IFN-gamma induces an inflammatory state in both non-lesional psoriatic and healthy skin*. J Invest Dermatol, 2012. **132**(4): p. 1177-87.
78. Oppmann, B., et al., *Novel p19 protein engages IL-12p40 to form a cytokine, IL-23, with biological activities similar as well as distinct from IL-12*. Immunity, 2000. **13**(5): p. 715-25.
79. Parham, C., et al., *A receptor for the heterodimeric cytokine IL-23 is composed of IL-12Rbeta1 and a novel cytokine receptor subunit, IL-23R*. J Immunol, 2002. **168**(11): p. 5699-708.
80. Presky, D.H., et al., *A functional interleukin 12 receptor complex is composed of two beta-type cytokine receptor subunits*. Proc Natl Acad Sci U S A, 1996. **93**(24): p. 14002-7.
81. Lee, E., et al., *Increased expression of interleukin 23 p19 and p40 in lesional skin of patients with psoriasis vulgaris*. J Exp Med, 2004. **199**(1): p. 125-30.
82. Chiricozzi, A., et al., *Scanning the Immunopathogenesis of Psoriasis*. Int J Mol Sci, 2018. **19**(1).
83. Lande, R., et al., *Plasmacytoid dendritic cells sense self-DNA coupled with antimicrobial peptide*. Nature, 2007. **449**(7162): p. 564-9.

84. Morizane, S., et al., *Cathelicidin antimicrobial peptide LL-37 in psoriasis enables keratinocyte reactivity against TLR9 ligands*. J Invest Dermatol, 2012. **132**(1): p. 135-43.
85. Ganguly, D., et al., *Self-RNA-antimicrobial peptide complexes activate human dendritic cells through TLR7 and TLR8*. J Exp Med, 2009. **206**(9): p. 1983-94.
86. Villanova, F., et al., *Characterization of innate lymphoid cells in human skin and blood demonstrates increase of NKp44+ ILC3 in psoriasis*. J Invest Dermatol, 2014. **134**(4): p. 984-991.
87. Nograles, K.E., et al., *Th17 cytokines interleukin (IL)-17 and IL-22 modulate distinct inflammatory and keratinocyte-response pathways*. Br J Dermatol, 2008. **159**(5): p. 1092-102.
88. Chiricozzi, A., et al., *Integrative responses to IL-17 and TNF-alpha in human keratinocytes account for key inflammatory pathogenic circuits in psoriasis*. J Invest Dermatol, 2011. **131**(3): p. 677-87.
89. Boniface, K., et al., *IL-22 inhibits epidermal differentiation and induces proinflammatory gene expression and migration of human keratinocytes*. J Immunol, 2005. **174**(6): p. 3695-702.
90. Nestle, F.O., D.H. Kaplan, and J. Barker, *Psoriasis*. N Engl J Med, 2009. **361**(5): p. 496-509.
91. Brenner, M.B., et al., *Identification of a putative second T-cell receptor*. Nature, 1986. **322**(6075): p. 145-9.
92. Carding, S.R. and P.J. Egan, *Gammadelta T cells: functional plasticity and heterogeneity*. Nat Rev Immunol, 2002. **2**(5): p. 336-45.
93. Prinz, I., B. Silva-Santos, and D.J. Pennington, *Functional development of gammadelta T cells*. Eur J Immunol, 2013. **43**(8): p. 1988-94.
94. Heilig, J.S. and S. Tonegawa, *Diversity of murine gamma genes and expression in fetal and adult T lymphocytes*. Nature, 1986. **322**(6082): p. 836-40.
95. Jensen, K.D., et al., *Thymic selection determines gammadelta T cell effector fate: antigen-naive cells make interleukin-17 and antigen-experienced cells make interferon gamma*. Immunity, 2008. **29**(1): p. 90-100.
96. Martin, B., et al., *Interleukin-17-producing gammadelta T cells selectively expand in response to pathogen products and environmental signals*. Immunity, 2009. **31**(2): p. 321-30.
97. Sutton, C.E., et al., *Interleukin-1 and IL-23 induce innate IL-17 production from gammadelta T cells, amplifying Th17 responses and autoimmunity*. Immunity, 2009. **31**(2): p. 331-41.
98. Ribot, J.C., et al., *CD27 is a thymic determinant of the balance between interferon-gamma- and interleukin 17-producing gammadelta T cell subsets*. Nat Immunol, 2009. **10**(4): p. 427-36.
99. Zachariadis, O., et al., *gammadelta T cells regulate the early inflammatory response to bordetella pertussis infection in the murine respiratory tract*. Infect Immun, 2006. **74**(3): p. 1837-45.

100. Hamada, S., et al., *IL-17A produced by gammadelta T cells plays a critical role in innate immunity against listeria monocytogenes infection in the liver*. J Immunol, 2008. **181**(5): p. 3456-63.
101. Di Meglio, P., et al., *Activation of the aryl hydrocarbon receptor dampens the severity of inflammatory skin conditions*. Immunity, 2014. **40**(6): p. 989-1001.
102. Gray, E.E., K. Suzuki, and J.G. Cyster, *Cutting edge: Identification of a motile IL-17-producing gammadelta T cell population in the dermis*. J Immunol, 2011. **186**(11): p. 6091-5.
103. Cai, Y., et al., *Differential developmental requirement and peripheral regulation for dermal Vgamma4 and Vgamma6T17 cells in health and inflammation*. Nat Commun, 2014. **5**: p. 3986.
104. Gray, E.E., et al., *Deficiency in IL-17-committed Vgamma4(+) gammadelta T cells in a spontaneous Sox13-mutant CD45.1(+) congenic mouse substrain provides protection from dermatitis*. Nat Immunol, 2013. **14**(6): p. 584-92.
105. Malhotra, N., et al., *A network of high-mobility group box transcription factors programs innate interleukin-17 production*. Immunity, 2013. **38**(4): p. 681-93.
106. Hayday, A.C., *[gamma][delta] cells: a right time and a right place for a conserved third way of protection*. Annu Rev Immunol, 2000. **18**: p. 975-1026.
107. Zheng, B.J., et al., *Anti-tumor effects of human peripheral gammadelta T cells in a mouse tumor model*. Int J Cancer, 2001. **92**(3): p. 421-5.
108. Eberl, M., et al., *A rapid crosstalk of human gammadelta T cells and monocytes drives the acute inflammation in bacterial infections*. PLoS Pathog, 2009. **5**(2): p. e1000308.
109. Holtmeier, W., et al., *The TCR-delta repertoire in normal human skin is restricted and distinct from the TCR-delta repertoire in the peripheral blood*. J Invest Dermatol, 2001. **116**(2): p. 275-80.
110. Ebert, L.M., S. Meuter, and B. Moser, *Homing and function of human skin gammadelta T cells and NK cells: relevance for tumor surveillance*. J Immunol, 2006. **176**(7): p. 4331-6.
111. De Rosa, S.C., et al., *Ontogeny of gamma delta T cells in humans*. J Immunol, 2004. **172**(3): p. 1637-45.
112. Holtmeier, W. and D. Kabelitz, *gammadelta T cells link innate and adaptive immune responses*. Chem Immunol Allergy, 2005. **86**: p. 151-83.
113. Deusch, K., et al., *A major fraction of human intraepithelial lymphocytes simultaneously expresses the gamma/delta T cell receptor, the CD8 accessory molecule and preferentially uses the V delta 1 gene segment*. Eur J Immunol, 1991. **21**(4): p. 1053-9.
114. Uyemura, K., et al., *Evidence for clonal selection of gamma/delta T cells in response to a human pathogen*. J Exp Med, 1991. **174**(3): p. 683-92.
115. Toulon, A., et al., *A role for human skin-resident T cells in wound healing*. J Exp Med, 2009. **206**(4): p. 743-50.

116. Laggner, U., et al., *Identification of a novel proinflammatory human skin-homing Vgamma9Vdelta2 T cell subset with a potential role in psoriasis*. J Immunol, 2011. **187**(5): p. 2783-93.
117. Caccamo, N., et al., *Differentiation, phenotype, and function of interleukin-17-producing human Vgamma9Vdelta2 T cells*. Blood, 2011. **118**(1): p. 129-38.
118. Krueger, G.G., et al., *A randomized, double-blind, placebo-controlled phase III study evaluating efficacy and tolerability of 2 courses of alefacept in patients with chronic plaque psoriasis*. J Am Acad Dermatol, 2002. **47**(6): p. 821-33.
119. Leonardi, C.L., et al., *Etanercept as monotherapy in patients with psoriasis*. N Engl J Med, 2003. **349**(21): p. 2014-22.
120. Gordon, K.B., et al., *Clinical response to adalimumab treatment in patients with moderate to severe psoriasis: double-blind, randomized controlled trial and open-label extension study*. J Am Acad Dermatol, 2006. **55**(4): p. 598-606.
121. Chaudhari, U., et al., *Efficacy and safety of infliximab monotherapy for plaque-type psoriasis: a randomised trial*. Lancet, 2001. **357**(9271): p. 1842-7.
122. Conrad, C., et al., *TNF blockade induces a dysregulated type I interferon response without autoimmunity in paradoxical psoriasis*. Nat Commun, 2018. **9**(1): p. 25.
123. Harden, J.L., et al., *Humanized anti-IFN-gamma (HuZAF) in the treatment of psoriasis*. J Allergy Clin Immunol, 2015. **135**(2): p. 553-6.
124. Hong, K., et al., *IL-12, independently of IFN-gamma, plays a crucial role in the pathogenesis of a murine psoriasis-like skin disorder*. J Immunol, 1999. **162**(12): p. 7480-91.
125. PharmaTimes. *Abbott withdraws briakinumab applications in USA, Europe*. 2011 [cited 2018 Dec]; Available from: http://www.pharmatimes.com/news/abbott_withdraws_briakinumab_applications_in_usa,_europe_979765.
126. Ryan, C., et al., *Association between biologic therapies for chronic plaque psoriasis and cardiovascular events: a meta-analysis of randomized controlled trials*. JAMA, 2011. **306**(8): p. 864-71.
127. Papp, K.A., et al., *Efficacy and safety of ustekinumab, a human interleukin-12/23 monoclonal antibody, in patients with psoriasis: 52-week results from a randomised, double-blind, placebo-controlled trial (PHOENIX 2)*. Lancet, 2008. **371**(9625): p. 1675-84.
128. Griffiths, C.E., et al., *Comparison of ustekinumab and etanercept for moderate-to-severe psoriasis*. N Engl J Med, 2010. **362**(2): p. 118-28.
129. Hueber, W., et al., *Effects of AIN457, a fully human antibody to interleukin-17A, on psoriasis, rheumatoid arthritis, and uveitis*. Sci Transl Med, 2010. **2**(52): p. 52ra72.
130. Leonardi, C., et al., *Anti-interleukin-17 monoclonal antibody ixekizumab in chronic plaque psoriasis*. N Engl J Med, 2012. **366**(13): p. 1190-9.
131. Papp, K.A., et al., *Brodalumab, an anti-interleukin-17-receptor antibody for psoriasis*. N Engl J Med, 2012. **366**(13): p. 1181-9.

132. Thaci, D., et al., *Secukinumab is superior to ustekinumab in clearing skin of subjects with moderate to severe plaque psoriasis: CLEAR, a randomized controlled trial*. J Am Acad Dermatol, 2015. **73**(3): p. 400-9.
133. Lebwohl, M., et al., *Phase 3 Studies Comparing Brodalumab with Ustekinumab in Psoriasis*. N Engl J Med, 2015. **373**(14): p. 1318-28.
134. Paul, C., et al., *Ixekizumab provides superior efficacy compared with ustekinumab over 52 weeks of treatment: Results from IXORA-S, a phase 3 study*. J Am Acad Dermatol, 2019. **80**(1): p. 70-79 e3.
135. U.S. Food and Drug Administration (FDA). *Medical Review [Brodalumab]*. 2016 [cited 2019 May]; Available from: https://www.accessdata.fda.gov/drugsatfda_docs/nda/2017/761032Orig1s000MedR.pdf.
136. Van Belle, A.B., et al., *IL-22 is required for imiquimod-induced psoriasiform skin inflammation in mice*. J Immunol, 2012. **188**(1): p. 462-9.
137. Papp, K., et al., *Tildrakizumab (MK-3222), an anti-interleukin-23p19 monoclonal antibody, improves psoriasis in a phase IIb randomized placebo-controlled trial*. Br J Dermatol, 2015. **173**(4): p. 930-9.
138. Sofen, H., et al., *Guselkumab (an IL-23-specific mAb) demonstrates clinical and molecular response in patients with moderate-to-severe psoriasis*. J Allergy Clin Immunol, 2014. **133**(4): p. 1032-40.
139. Krueger, J.G., et al., *Anti-IL-23A mAb BI 655066 for treatment of moderate-to-severe psoriasis: Safety, efficacy, pharmacokinetics, and biomarker results of a single-rising-dose, randomized, double-blind, placebo-controlled trial*. J Allergy Clin Immunol, 2015. **136**(1): p. 116-124 e7.
140. Papp, K.A., et al., *Risankizumab versus Ustekinumab for Moderate-to-Severe Plaque Psoriasis*. N Engl J Med, 2017. **376**(16): p. 1551-1560.
141. Langley, R.G., et al., *Efficacy and safety of guselkumab in patients with psoriasis who have an inadequate response to ustekinumab: results of the randomized, double-blind, phase III NAVIGATE trial*. Br J Dermatol, 2018. **178**(1): p. 114-123.
142. Gaffen, S.L., et al., *The IL-23-IL-17 immune axis: from mechanisms to therapeutic testing*. Nat Rev Immunol, 2014. **14**(9): p. 585-600.
143. Lerner, A., P. Jeremias, and T. Matthias, *The World Incidence and Prevalence of Autoimmune Diseases is Increasing*. International Journal of Celiac Disease, 2015. **3**(4): p. 151-155.
144. Manzel, A., et al., *Role of "Western diet" in inflammatory autoimmune diseases*. Curr Allergy Asthma Rep, 2014. **14**(1): p. 404.
145. Amre, D.K., et al., *Imbalances in dietary consumption of fatty acids, vegetables, and fruits are associated with risk for Crohn's disease in children*. Am J Gastroenterol, 2007. **102**(9): p. 2016-25.
146. Brown, I.J., et al., *Salt intakes around the world: implications for public health*. Int J Epidemiol, 2009. **38**(3): p. 791-813.

147. World Health Organization (WHO). *Salt reduction*. 2016 [cited 2019 May]; Available from: <https://www.who.int/news-room/fact-sheets/detail/salt-reduction>.
148. Jantsch, J., et al., *Cutaneous Na⁺ storage strengthens the antimicrobial barrier function of the skin and boosts macrophage-driven host defense*. *Cell Metab*, 2015. **21**(3): p. 493-501.
149. Heer, M., *Nutritional interventions related to bone turnover in European space missions and simulation models*. *Nutrition*, 2002. **18**(10): p. 853-6.
150. Titze, J., et al., *Long-term sodium balance in humans in a terrestrial space station simulation study*. *Am J Kidney Dis*, 2002. **40**(3): p. 508-16.
151. Titze, J., et al., *Extrarenal Na⁺ balance, volume, and blood pressure homeostasis in intact and ovariectomized deoxycorticosterone-acetate salt rats*. *Hypertension*, 2006. **47**(6): p. 1101-7.
152. Nikpey, E., et al., *High-Salt Diet Causes Osmotic Gradients and Hyperosmolality in Skin Without Affecting Interstitial Fluid and Lymph*. *Hypertension*, 2017. **69**(4): p. 660-668.
153. Titze, J., et al., *Osmotically inactive skin Na⁺ storage in rats*. *Am J Physiol Renal Physiol*, 2003. **285**(6): p. F1108-17.
154. Titze, J., et al., *Glycosaminoglycan polymerization may enable osmotically inactive Na⁺ storage in the skin*. *Am J Physiol Heart Circ Physiol*, 2004. **287**(1): p. H203-8.
155. Schafflhuber, M., et al., *Mobilization of osmotically inactive Na⁺ by growth and by dietary salt restriction in rats*. *Am J Physiol Renal Physiol*, 2007. **292**(5): p. F1490-500.
156. Edelman, I.S., et al., *Interrelations between serum sodium concentration, serum osmolarity and total exchangeable sodium, total exchangeable potassium and total body water*. *J Clin Invest*, 1958. **37**(9): p. 1236-56.
157. Xu, W., et al., *Sodium channel Nax is a regulator in epithelial sodium homeostasis*. *Sci Transl Med*, 2015. **7**(312): p. 312ra177.
158. Machnik, A., et al., *Macrophages regulate salt-dependent volume and blood pressure by a vascular endothelial growth factor-C-dependent buffering mechanism*. *Nat Med*, 2009. **15**(5): p. 545-52.
159. Wiig, H., et al., *Immune cells control skin lymphatic electrolyte homeostasis and blood pressure*. *J Clin Invest*, 2013. **123**(7): p. 2803-15.
160. Mente, A., et al., *Urinary sodium excretion, blood pressure, cardiovascular disease, and mortality: a community-level prospective epidemiological cohort study*. *Lancet*, 2018. **392**(10146): p. 496-506.
161. Zhang, W.C., et al., *High salt primes a specific activation state of macrophages, M(Na)*. *Cell Res*, 2015. **25**(8): p. 893-910.
162. Hucke, S., et al., *Sodium chloride promotes pro-inflammatory macrophage polarization thereby aggravating CNS autoimmunity*. *J Autoimmun*, 2016. **67**: p. 90-101.

163. Kleinewietfeld, M., et al., *Sodium chloride drives autoimmune disease by the induction of pathogenic TH17 cells*. Nature, 2013. **496**(7446): p. 518-22.
164. Wu, C., et al., *Induction of pathogenic TH17 cells by inducible salt-sensing kinase SGK1*. Nature, 2013. **496**(7446): p. 513-7.
165. Wu, H., et al., *High salt promotes autoimmunity by TET2-induced DNA demethylation and driving the differentiation of Tfh cells*. Sci Rep, 2016. **6**: p. 28065.
166. Hernandez, A.L., et al., *Sodium chloride inhibits the suppressive function of FOXP3+ regulatory T cells*. J Clin Invest, 2015. **125**(11): p. 4212-22.
167. Yang, X., et al., *Exacerbation of lupus nephritis by high sodium chloride related to activation of SGK1 pathway*. Int Immunopharmacol, 2015. **29**(2): p. 568-573.
168. Monteleone, I., et al., *Sodium chloride-enriched Diet Enhanced Inflammatory Cytokine Production and Exacerbated Experimental Colitis in Mice*. J Crohns Colitis, 2017. **11**(2): p. 237-245.
169. Farez, M.F., et al., *Sodium intake is associated with increased disease activity in multiple sclerosis*. J Neurol Neurosurg Psychiatry, 2015. **86**(1): p. 26-31.
170. Sundstrom, B., I. Johansson, and S. Rantapaa-Dahlqvist, *Interaction between dietary sodium and smoking increases the risk for rheumatoid arthritis: results from a nested case-control study*. Rheumatology (Oxford), 2015. **54**(3): p. 487-93.
171. Vom Berg, J., et al., *Intratumoral IL-12 combined with CTLA-4 blockade elicits T cell-mediated glioma rejection*. J Exp Med, 2013. **210**(13): p. 2803-11.
172. Sawant, D.V., K. Hamilton, and D.A. Vignali, *Interleukin-35: Expanding Its Job Profile*. J Interferon Cytokine Res, 2015. **35**(7): p. 499-512.
173. Kulig, P., et al., *IL-12 protects from psoriasiform skin inflammation*. Nat Commun, 2016. **7**: p. 13466.
174. Hara, H., et al., *Development of dendritic epidermal T cells with a skewed diversity of gamma delta TCRs in V delta 1-deficient mice*. J Immunol, 2000. **165**(7): p. 3695-705.
175. Trinchieri, G., *Interleukin-12 and the regulation of innate resistance and adaptive immunity*. Nat Rev Immunol, 2003. **3**(2): p. 133-46.
176. Sugaya, M., K. Nakamura, and K. Tamaki, *Interleukins 18 and 12 synergistically upregulate interferon-gamma production by murine dendritic epidermal T cells*. J Invest Dermatol, 1999. **113**(3): p. 350-4.
177. Jacob, S.E., et al., *Simultaneous measurement of multiple Th1 and Th2 serum cytokines in psoriasis and correlation with disease severity*. Mediators Inflamm, 2003. **12**(5): p. 309-13.
178. Schmitt, D.A., J.P. Walterscheid, and S.E. Ullrich, *Reversal of ultraviolet radiation-induced immune suppression by recombinant interleukin-12: suppression of cytokine production*. Immunology, 2000. **101**(1): p. 90-6.
179. Schwarz, A., et al., *Interleukin-12 suppresses ultraviolet radiation-induced apoptosis by inducing DNA repair*. Nat Cell Biol, 2002. **4**(1): p. 26-31.

180. Schwarz, A., et al., *Prevention of UV radiation-induced immunosuppression by IL-12 is dependent on DNA repair*. J Exp Med, 2005. **201**(2): p. 173-9.
181. Meeran, S.M., T. Punathil, and S.K. Katiyar, *IL-12 deficiency exacerbates inflammatory responses in UV-irradiated skin and skin tumors*. J Invest Dermatol, 2008. **128**(11): p. 2716-27.
182. Becher, B., B.G. Durell, and R.J. Noelle, *Experimental autoimmune encephalitis and inflammation in the absence of interleukin-12*. J Clin Invest, 2002. **110**(4): p. 493-7.
183. Brunda, M.J., et al., *Antitumor and antimetastatic activity of interleukin 12 against murine tumors*. J Exp Med, 1993. **178**(4): p. 1223-30.
184. Nastala, C.L., et al., *Recombinant IL-12 administration induces tumor regression in association with IFN-gamma production*. J Immunol, 1994. **153**(4): p. 1697-706.
185. Cao, X., et al., *Interleukin 12 stimulates IFN-gamma-mediated inhibition of tumor-induced regulatory T-cell proliferation and enhances tumor clearance*. Cancer Res, 2009. **69**(22): p. 8700-9.
186. Colombo, M.P., et al., *Amount of interleukin 12 available at the tumor site is critical for tumor regression*. Cancer Res, 1996. **56**(11): p. 2531-4.
187. Young, L. and D. Czarnecki, *The rapid onset of multiple squamous cell carcinomas in two patients commenced on ustekinumab as treatment of psoriasis*. Australas J Dermatol, 2012. **53**(1): p. 57-60.
188. Langley, R.G., et al., *Safety results from a pooled analysis of randomized, controlled phase II and III clinical trials and interim data from an open-label extension trial of the interleukin-12/23 monoclonal antibody, briakinumab, in moderate to severe psoriasis*. J Eur Acad Dermatol Venereol, 2013. **27**(10): p. 1252-61.
189. Hue, S., et al., *Interleukin-23 drives innate and T cell-mediated intestinal inflammation*. J Exp Med, 2006. **203**(11): p. 2473-83.
190. Matsuoka, K., et al., *T-bet upregulation and subsequent interleukin 12 stimulation are essential for induction of Th1 mediated immunopathology in Crohn's disease*. Gut, 2004. **53**(9): p. 1303-8.
191. Sandborn, W.J., et al., *A randomized trial of Ustekinumab, a human interleukin-12/23 monoclonal antibody, in patients with moderate-to-severe Crohn's disease*. Gastroenterology, 2008. **135**(4): p. 1130-41.
192. Sandborn, W.J., et al., *Ustekinumab induction and maintenance therapy in refractory Crohn's disease*. N Engl J Med, 2012. **367**(16): p. 1519-28.
193. Ogawa, A., et al., *Neutralization of interleukin-17 aggravates dextran sulfate sodium-induced colitis in mice*. Clin Immunol, 2004. **110**(1): p. 55-62.
194. O'Connor, W., Jr., et al., *A protective function for interleukin 17A in T cell-mediated intestinal inflammation*. Nat Immunol, 2009. **10**(6): p. 603-9.
195. Hueber, W., et al., *Secukinumab, a human anti-IL-17A monoclonal antibody, for moderate to severe Crohn's disease: unexpected results of a randomised, double-blind placebo-controlled trial*. Gut, 2012. **61**(12): p. 1693-700.

196. Targan, S.R., et al., *A Randomized, Double-Blind, Placebo-Controlled Phase 2 Study of Brodalumab in Patients With Moderate-to-Severe Crohn's Disease*. *Am J Gastroenterol*, 2016. **111**(11): p. 1599-1607.
197. Feagan, B.G., et al., *Induction therapy with the selective interleukin-23 inhibitor risankizumab in patients with moderate-to-severe Crohn's disease: a randomised, double-blind, placebo-controlled phase 2 study*. *Lancet*, 2017. **389**(10080): p. 1699-1709.
198. Lee, J.S., et al., *Interleukin-23-Independent IL-17 Production Regulates Intestinal Epithelial Permeability*. *Immunity*, 2015. **43**(4): p. 727-38.
199. Zuniga, L.A., et al., *IL-17 regulates adipogenesis, glucose homeostasis, and obesity*. *J Immunol*, 2010. **185**(11): p. 6947-59.
200. Kohlgruber, A.C., et al., *gammadelta T cells producing interleukin-17A regulate adipose regulatory T cell homeostasis and thermogenesis*. *Nat Immunol*, 2018. **19**(5): p. 464-474.
201. Dimova, T., et al., *Effector Vgamma9Vdelta2 T cells dominate the human fetal gammadelta T-cell repertoire*. *Proc Natl Acad Sci U S A*, 2015. **112**(6): p. E556-65.
202. Parker, C.M., et al., *Evidence for extrathymic changes in the T cell receptor gamma/delta repertoire*. *J Exp Med*, 1990. **171**(5): p. 1597-612.
203. Davey, M.S., et al., *The human Vdelta2(+) T-cell compartment comprises distinct innate-like Vgamma9(+) and adaptive Vgamma9(-) subsets*. *Nat Commun*, 2018. **9**(1): p. 1760.
204. McKenzie, D.R., et al., *The Emerging Complexity of gammadeltaT17 Cells*. *Front Immunol*, 2018. **9**: p. 796.
205. Schenkel, J.M., et al., *T cell memory. Resident memory CD8 T cells trigger protective innate and adaptive immune responses*. *Science*, 2014. **346**(6205): p. 98-101.
206. Gebhardt, T., et al., *Different patterns of peripheral migration by memory CD4+ and CD8+ T cells*. *Nature*, 2011. **477**(7363): p. 216-9.
207. Ariotti, S., et al., *T cell memory. Skin-resident memory CD8(+) T cells trigger a state of tissue-wide pathogen alert*. *Science*, 2014. **346**(6205): p. 101-5.
208. Zaid, A., et al., *Persistence of skin-resident memory T cells within an epidermal niche*. *Proc Natl Acad Sci U S A*, 2014. **111**(14): p. 5307-12.
209. Lowes, M.A., et al., *The IL-23/T17 pathogenic axis in psoriasis is amplified by keratinocyte responses*. *Trends Immunol*, 2013. **34**(4): p. 174-81.
210. Bouchaud, G., et al., *Epidermal IL-15Ralpha acts as an endogenous antagonist of psoriasiform inflammation in mouse and man*. *J Exp Med*, 2013. **210**(10): p. 2105-17.
211. Parsonage, G., et al., *Global gene expression profiles in fibroblasts from synovial, skin and lymphoid tissue reveals distinct cytokine and chemokine expression patterns*. *Thromb Haemost*, 2003. **90**(4): p. 688-97.
212. Banno, T., A. Gazel, and M. Blumenberg, *Effects of tumor necrosis factor-alpha (TNF alpha) in epidermal keratinocytes revealed using global transcriptional profiling*. *J Biol Chem*, 2004. **279**(31): p. 32633-42.

213. Gudjonsson, J.E., et al., *Assessment of the psoriatic transcriptome in a large sample: additional regulated genes and comparisons with in vitro models*. J Invest Dermatol, 2010. **130**(7): p. 1829-40.
214. Molenda, M., L. Mukkamala, and M. Blumenberg, *Interleukin IL-12 blocks a specific subset of the transcriptional profile responsive to UVB in epidermal keratinocytes*. Mol Immunol, 2006. **43**(12): p. 1933-40.
215. Danielsen, K., et al., *Is the prevalence of psoriasis increasing? A 30-year follow-up of a population-based cohort*. Br J Dermatol, 2013. **168**(6): p. 1303-10.
216. Inglese, M., et al., *Brain tissue sodium concentration in multiple sclerosis: a sodium imaging study at 3 tesla*. Brain, 2010. **133**(Pt 3): p. 847-57.
217. Paling, D., et al., *Sodium accumulation is associated with disability and a progressive course in multiple sclerosis*. Brain, 2013. **136**(Pt 7): p. 2305-17.
218. Aguiar, S.L.F., et al., *High-Salt Diet Induces IL-17-Dependent Gut Inflammation and Exacerbates Colitis in Mice*. Front Immunol, 2017. **8**: p. 1969.
219. Chen, S., et al., *Tonicity-dependent induction of Sgk1 expression has a potential role in dehydration-induced natriuresis in rodents*. J Clin Invest, 2009. **119**(6): p. 1647-58.
220. Trama, J., W.Y. Go, and S.N. Ho, *The osmoprotective function of the NFAT5 transcription factor in T cell development and activation*. J Immunol, 2002. **169**(10): p. 5477-88.
221. Go, W.Y., et al., *NFAT5/TonEBP mutant mice define osmotic stress as a critical feature of the lymphoid microenvironment*. Proc Natl Acad Sci U S A, 2004. **101**(29): p. 10673-8.
222. Brouard, M., et al., *Epithelial sodium channel in human epidermal keratinocytes: expression of its subunits and relation to sodium transport and differentiation*. J Cell Sci, 1999. **112** (Pt 19): p. 3343-52.
223. Naik, S., et al., *Compartmentalized control of skin immunity by resident commensals*. Science, 2012. **337**(6098): p. 1115-9.
224. Wilck, N., et al., *Salt-responsive gut commensal modulates TH17 axis and disease*. Nature, 2017. **551**(7682): p. 585-589.
225. Chang, H.W., et al., *Alteration of the cutaneous microbiome in psoriasis and potential role in Th17 polarization*. Microbiome, 2018. **6**(1): p. 154.

Publications

Rothe M, Alpert C, Engst W, **Musiol S**, Loh G, Blaut M. *Impact of nutritional factors on the proteome of intestinal Escherichia coli: induction of OxyR-dependent proteins AhpF and Dps by a lactose-rich diet.* Appl Environ Microbiol. 2012 May;78(10):3580-91.

Winter O, **Musiol S**, Schablowsky M, Chen Q, Khodadadi L, Hiepe F. *Analyzing pathogenic (double-stranded (ds) DNA-specific) plasma cells via immunofluorescence microscopy.* Arthritis Res Ther. 2015 Oct 21;17:293.

Kulig P, **Musiol S**, Freiberger SN, Schreiner B, Gyülveszi G, Russo G, Pantelyushin S, Kishihara K, Alessandrini F, Kündig T, Sallusto F, Hofbauer GF, Haak S, Becher B. *IL-12 protects from psoriasiform skin inflammation.* Nat Commun. 2016 Nov 28;7:13466.

Musiol S, Alessandrini F, Schneider E, Jakwerth CA, Chaker AM, Guerth F, Ghiordanescu I, Schilling JT, Kau J, Plaschke M, Haak S, Schmidt-Weber CB, Buch T, Zissler UM. *TGF- β 1 drives TH9 but not Treg cells in allergy and immunotherapy.*

Paper submitted

Acknowledgement

The long journey of my thesis has finally come to an end. It has been a period of intense learning, not only on the scientific, but also on the personal level. Therefore, I would like to thank the people who have supported and helped me so much throughout this period.

First of all, I owe my gratitude to my supervisor Prof. Carsten Schmidt-Weber for giving me the opportunity to perform my doctoral thesis at the Center for Allergy and Environment and for his scientific advices and continuous support of my study. I really enjoyed the conversations we had in our meetings and during congresses.

I would also like to express my gratitude to Prof. Bernhard Kuester, for accepting me as a PhD student. Thanks for the supervision, the insightful comments and the scientific discussions during the Thesis Committee meetings.

Further, I also want to thank Prof. Esther von Stebut-Borschitz, Dr. Kirsten Dietze-Schwonberg (Universitäts-Hautklinik Mainz, Germany) as well as Kenji Kishihara (Nagasaki International University, Japan) for providing the *Il12b^{-/-}* and *Vd1^{-/-}* mice. My sincere thanks also go to Prof. Burkhard Becher and Dr. Paulina Kulig (University of Zurich, Switzerland) for their wonderful collaboration and for the opportunity to frequently join their team.

Special appreciation and thanks goes to my two advisors Prof. Francesca Alessandrini and Dr. Stefan Haak. You supported me with brilliant comments and suggestions, encouraged my research and allowed me to grow as a research scientist. Under your guidance I successfully overcame many difficulties and learnt a lot.

Stefan, thank you for your guidance during the last years and for teaching me how to deal with defeats. Thanks for giving me your knowledge and putting in effort at all times for the benefit of this thesis.

Francesca, I want to deeply thank you for picking me up and giving me the possibility to be a part of your group. I highly appreciate that you always had confidence in my work. Thank you for your patience, motivation and support during tough times.

Special thanks to our “top team” of technicians for the excellent assistance and for always having the willingness to help: Benjamin and Johanna, all the extensive experiments and working hours would have been impossible without your help. Thank you for all the emotional support during these years and the fun we had together.

I would also like to take the opportunity to thank Simon, Caspar and Uli for all the stimulating discussions during morning seminars, paper writing or in between and for the feedback you offered me. You always had an open ear for my scientific problems and questions. Thanks a lot Simon for taking the time to read my thesis.

In addition, I want to deeply thank my working colleagues. Dennis, Max and Mary together we were the first who start the exciting time of being a PhD student and shared a lot of ups and downs. My gratitude goes also to the Blank's: Alex, Sonja, Johannes and Michael. Thank you for the funny times we had in our room and for always having someone to talk to if it was about work or private stuff.

I especially want to highlight one person, Evelyn Schneider. In the last years you have not only become a good colleague, but one of my best friends. Thanks a lot for your constant encouragement, for helping me to fight against the daily grind in the lab and for reading my thesis, but most importantly for being always there for me.

I want to gratefully thank my best friend, Lars Holdinghausen, for his friendship and generous care. You are always beside me during happy and hard times, to push and to motivate me.

My deepest gratitude goes to a very special person. Christoph, you have become a fundamental part in my life. Thank you for your unconditional love, support and understanding. You always gave me the strength to move forward when I thought it was impossible to continue.

Finally, I would like to acknowledge the immense impact and support that my mother and father give me. Words cannot express how grateful I am to both of you for all of the sacrifices that you've made on my behalf. Thank you for your selfless love throughout my years of study and through the process of researching and writing this thesis.